
Article:
Hall, A.R. and Geoghegan, M. (2018) Polymers and biopolymers at interfaces. Reports on Progress in Physics, 81 (3). 036601. ISSN 0034-4885

https://doi.org/10.1088/1361-6633/aa9e9c

Polymers and biopolymers at interfaces

A R Hall[1,2] and M Geoghegan[1]

1 Department of Physics and Astronomy, University of Sheffield, Hounsfield Road, Sheffield S3 7RH, UK

2 Biomedical Diagnostics Institute, Dublin City University, Glasnevin, Dublin 9, Ireland

Abstract.

This review updates recent progress in the understanding of the behaviour of polymers at surfaces and interfaces, highlighting examples in the areas of wetting, dewetting, crystallization, and "smart" materials. Recent developments in analysis tools have yielded a large increase in the study of biological systems, and some of these will also be discussed, focussing on areas where surfaces are important. These areas include molecular binding events and protein adsorption as well as the mapping of the surfaces of cells. Important techniques commonly used for the analysis of surfaces and interfaces are discussed separately to aid the understanding of their application.

1. Introduction

The physics underlying polymers at surfaces, like much in science, has a simple core wrapped in a detail that masks the underlying principles. However, it is an understanding and a recognition of these principles that allows researchers to make progress in developing the field. In this spirit, consider a polymer in solution close to a surface. Does the polymer adsorb on the surface? If so, does it sit there, as flat as a pancake, or does it have only a few contact points, with the rest of the molecule fully solvated (Figure 1)? The answer lies — like so much of physics — in a consideration of energetics. Polymers in contact with solvents do so because such contact reduces their energy, through the formation of temporary and favourable polymer-solvent links. Hydrogen bonding may occur, especially if an aqueous solution is being considered, and van der Waals interactions will also take place; electrostatics is generally important because polar molecules tend to prefer polar solvents and non-polar molecules require non-polar solvents. Polystyrene (non-polar) will dissolve extremely well in non-polar toluene, but is insoluble in (polar) water. Poly(acrylic acid) will, however, dissolve in water because it has a polar carboxylic acid group which facilitates a network of hydrogen bonds. A polymer will thus lower its energy in contact with a good solvent. Similarly, a polymer will also lower its energy in contact with a compatible surface. Complexity arises when it is considered that the solvent itself will also lower its energy when in contact with a compatible surface, and surfaces compatible with the polymer

List of abbreviations

AFM	atomic-force microscopy	DLVO	Derjaguin, Landau, Verwey, and Overbeek
F8	poly(9,9-dioctylfluorene)	F8BT	poly(9,9-dioctylfluorene-*alt*-benzothiadiazole)
FCS	fluorescence correlation spectroscopy	FFM	friction force microscopy
FJC	freely-jointed chain	FPE	fish protein extract
FReS	forward recoil spectrometry	HSA	human serum albumin
LCST	lower critical solution temperature	LED	light-emitting diode
NRA	nuclear reaction analysis	PDMAc	poly(*N*,*N*-dimethylacrylamide)
PDMS	polydimethylsiloxane	PEDOT	poly(3,4-ethylene dioxythiophene)
PEG	poly(ethylene glycol)	PET	poly(ethylene terepthalate)
PFB	poly(9,9-dioctylfluorene-*alt*-bis-*N*,*N*′-(4-butylphenyl)-bis-*N*,*N*′-phenyl-1,4-phenylenediamine)	PLLA	poly(L-lactic acid)
PMAA	poly(methacrylic acid)	PNIPAm	poly(*N*-isopropyl acrylamide)
PSS	poly(styrene sulfonate)	PVME	polyvinylmethylether
PαMS	poly(α-methylstyrene)	P3HT	poly(3-hexylthiophene)
QCM-D	quartz crystal microbalance with dissipation	RBS	Rutherford backscattering
SBA	soybean agglutinin	SEM	scanning electron microscopy
SFM	scanning force microscopy	SIMS	secondary-ion mass spectrometry
SMFS	single molecule force spectroscopy	SNOM	scanning near-field optical microscopy
STM	scanning tunnelling microscopy	TCPS	tissue culture polystyrene
TIPS-pentacene	6,13-bis(triisopropylsilyl ethynyl) pentacene	TnPSM	modified porcine submaxillary mucin
UHV	ultra-high vacuum	UV	ultraviolet
UPS	ultraviolet photoelectron spectroscopy	WLC	worm-like chain
XPS	X-ray photoelectron spectroscopy		

tend to also be compatible with the solvent. Therefore the following interactions need to be considered in order to describe the energetics of adsorption: polymer-solvent, solvent-solvent, polymer-polymer, polymer-surface, and solvent-surface. The free energy of a polymer in solution is typically a few $k_{\mathrm{B}}T$. It is not possible to be too precise about this. After all, the energy of a gaseous atom is $3k_{\mathrm{B}}T/2$, but make it a diatomic molecule and that energy can rise to $7k_{\mathrm{B}}T/2$, if rotational and vibrational modes are excited. A polymer is solution contains many modes that may or may not be excited, so it is reasonable to note that individual interactions are of the order of $k_{\mathrm{B}}T$. This means that a polymer with N_{s} monomers in contact with a surface has an adsorption energy of the order of $N_{\mathrm{s}}k_{\mathrm{B}}T$. Fundamentally, this is why polymers stick to surfaces. They stick to surfaces because out of the many competing interactions, the adsorption of a polymer at a surface is so much stronger than the adsorption of solvent molecules to that surface.

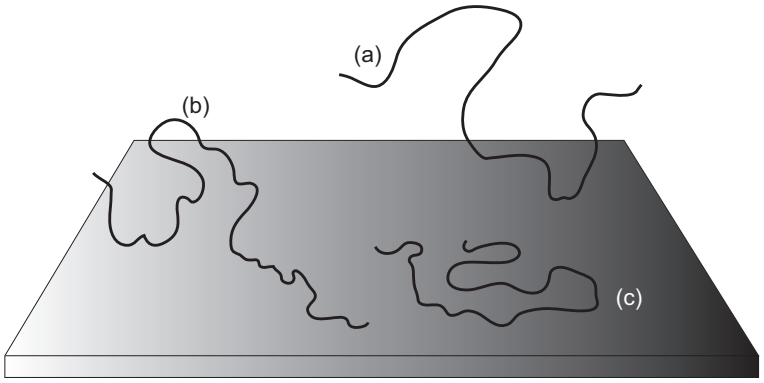

Figure 1. A polymer may have only one anchor point (a) on the surface, with the rest of the molecule spreading out into the solution. Other polymers may make more contact, with *trains* of many monomers in contact with the surface, *loops* into the solution, and solvated ends known as *tails* (b). The "pancake" conformation refers to polymers that are almost wholly attached to the substrate (c)

This review is an update to an earlier review by Geoghegan and Krausch [1], which, in turn is an update to an earlier review by Krausch [2]. Some perspective is obtained by considering the first of these. Back in 1995, the concept of studying single — or even individual — molecules was not incredible, but the lack of techniques available was an impediment. The idea that surfaces would play a significant role in films of functional materials was known to be important, but there was something of a disconnect between the chemists who could produce the functional polymers and the experts in the behaviour of polymers in thin films. The knowledge gap between those working on biomaterials or polymer electronics and those working on polymer films was quickly overcome and the second review discussed the ways in which surfaces and interfaces could affect the behaviour of polymer electronics devices. This review updates research in these areas, as well as adding selected research into biomacromolecules at surfaces. (Research considering biomacromolecules and surfaces is as old as that with synthetic polymers [3, 4].) Research into single molecules at surfaces had begun by the turn of the millennium, a field largely driven by biophysics and the growth of atomic-force

microscopy (AFM) and other techniques such as optical tweezers that were capable of manipulating single macromolecules.

The review by Krausch [2] took as a starting point the idea that differences in surface energy between different components of a polymer blend thin film or a block copolymer-induced structure gave surfaces their individual properties. The first experiments in this area were speculative and of value largely for the interesting results they presented. Reich and Cohen [5] presented optical microscopy results that showed phase separation in films of blends of polystyrene and polyvinylmethylether (PVME). It was some years later that a different team showed that the PVME in this blend was found at the surface in greater concentrations than in the bulk of the film [6], solely due to the differences in surface energy between the two components. The increasing access of good technology to different research groups ensured that such important results could be made. Here X-ray photoelectron spectroscopy (XPS) was used to identify PVME at the surface, and the simpler pendant drop experiment to contrast the surface energies of the two components. Theoretically, it was realized that polymers at surfaces could be treated adequately by mean-field theory. Here the lattice model of polymer physics, pioneered by Paul Flory and others over 60 years ago [7, 8, 9], was married to the mean-field theory of wetting by John Cahn [10] to provide a theoretical foundation for the study of surface structure in polymer films [11]. Experimentally, the work of Richard Jones and Ed Kramer at Cornell University provided an application of the new theory to thin films of mixtures of polystyrene and its deuterated counterpart [12]. This work continued at pace, and some of the developments are considered later in this review. It has to be conceded nevertheless, that the structure of polymer films, as applied to homopolymer mixtures, is a subject considered "done" by many. Of course there are always new and interesting results, such as the study of polymer film formation *in situ* during spin-coating [13, 14, 15, 16, 17, 18], which is a popular method of producing uniform films by rotating a drop of solution on a substrate at a few thousand rpm.

The study of single molecules on surfaces or at interfaces can be split into two categories. Some experiments manipulate individual molecules and others describe dilute mixtures whereby the behaviour of single molecules is observed, but only as an ensemble average [19]; many molecules are measured, but it is only by virtue of these molecules being very dilute that the study can be considered a single molecule experiment. The advantage of this latter scenario is that the experiments identify general behaviour, whereas in the former case there is the risk that an experiment may be performed on outlying samples. Thus reliable data for *individual* molecules can only be obtained by performing numerous experiments, which can be rather time consuming. However, it is often the outlying results that offer new and interesting insights into behaviour which would otherwise would be subsumed within the other data for experiments on dilute systems. Data that can be obtained by aggregate experiments on single molecules at surfaces include techniques such as fluorescence correlation spectroscopy (FCS) and surface-enhanced Raman spectroscopy, where dilute concentrations are needed to ensure that experiments are performed at the single

molecules level. FCS in particular has the ready capability of determining the number of molecules per unit volume, which is particularly useful given that what might be dilute (at the single molecule level) in the medium to which it is introduced, may not be so dilute at the surface. Experiments capable of studying individual molecules include optical tweezers, AFM, and high-resolution fluorescence microscopy experiments.

The study of ensemble behaviour of single molecules at surfaces is certainly a minority interest. Its headline experiments have involved the diffusion of polymers at surfaces using FCS [19, 20, 21, 22]. Molecular tracking has had considerable success in different areas, and particularly in cell biology [19]. High-resolution fluorescence microscopy has a role to play, and single polymer imaging has been demonstrated [23], but with further developments underway, such as stochastic optical reconstruction microscopy [24], again inspired by the needs of cell biology research, the *in situ* imaging of the behaviour of single molecules is one that promises to yield important results in the coming years. Of course, AFM-based techniques do provide single molecule resolution, either by AFM itself [25] or through scanning tunnelling microscopy (STM) [26]. STM has long been known for its atomic resolution, but with its restriction on substrates often inconvenient, it is worth noting the progress of AFM in this respect [27]. The resolution of torsional mode AFM [25] is better than 0.4 nm, so there is good reason to expect routine atomic resolution in polymers in the future. Nevertheless, scanning probe techniques (AFM and STM) are techniques used to study static phenomena and their insight into the behaviour of polymers at interfaces is less likely to reveal new physics than dynamic techniques such as those that are fluorescence-based, despite the better resolution of the scanning probe microscopy experiments. (Scanning probe microscopy will have certainly a large impact in solving different kinetic problems, for example, self-assembly problems such as crystallization, where video rate scanning probe techniques have already been shown to be useful [28]. In fact more recent developments have imaged biological action at work, with video imaging of the myosin molecular motor [29].) The high resolution of electron microscopy would be expected to make some impact in the study of single molecules at surfaces, but sample preparation and contrast limitations have minimized its effectiveness, although cryo-techniques can be effective at considering surface-bound molecules [30]. Single molecule microscopy studies are considered in reviews elsewhere [19, 31].

Molecular force probe techniques are a class of AFM in which a molecule, attached to an AFM tip, is brought to, and pulled away from a surface. In some cases the polymer rests on the surface, and the AFM probe is used to study the forces involved in its removal from the surface. This is known as single molecule force spectroscopy (SMFS) and these experiments provide significant insight into the structural properties of the individual molecules at surfaces. An important contribution of experiments of this type has been to the understanding of the folding behaviour for proteins [32, 33] and the study of microbial surfaces [34]. We consider the impact of these techniques in some detail in this review.

Polymer electronics is a high-profile research theme where interfaces play a key role

[35]. Polymer electronic devices are prepared in film form; displays consist of a series of films, containing layers of pixels, electrodes, transistors, or transparent protecting films. The polymeric components have to be prepared in a way so as to be compatible with the layer with which it is in contact. At one level this is a matter of macroscopic physics. There is no point in putting a low work function polymer in contact with an anode because low work function polymers are not generally very good for hole transport [36, 37, 38]. However, even in pure semiconductor physics, interfaces play an important role in devices [37]. The interfaces between dissimilar materials cause traps, and equalization of Fermi levels cause internal charge flow and *band-bending*, which, in turn, affects device performance. However, from the perspective of this review, the way in which the morphological evolution of structure affects the performance of devices is of some interest. Certainly, charge transport is affected by the morphology of the film. Isolated domains are effective traps for different components, so continuous structures are to be preferred. However, in some cases, such as photovoltaic devices, interfaces are required because it is at *heterojunctions* where the excited state (*exciton*) caused by the absorption of a photon is converted into charge and thus, by the application of a bias voltage, a current is generated.

1.1. Biopolymers

An understanding of the behaviour of biopolymers at interfaces is often considered important for negative reasons. Biopolymers *foul* interfaces, and the unfeasibly large technological subdomain of PEGylation is designed with the prevention of proteins reaching interfaces. PEGylation — the attachment of poly(ethylene glycol) (PEG) to surfaces or functional molecules such as drugs — is a standard technique to create biocompatibility. The *Oxford English Dictionary* defines compatible as meaning "mutually tolerant" or "congruous", yet biocompatibilization is the art of making a material inert in a biological environment. The host environment is not to interfere with, or affect, the biocompatibilized foreign object. Creating biocompatibility involves chemistry, if PEGylation is the goal, but understanding polymers at surfaces is key. Proteins are interesting molecules because of the richness of their structure. In a native state, they are folded with large parts of the protein ordered into α-helices and β-sheets. Here they give biological function [39, 40], be it molecular transport, facilitating biochemical reactions, supporting the immune system, or whatever other role is required. In their unfolded (non-native) state, they can be the source of many problems. Once proteins are folded, they are stable, but when misfolded, or unfolded, they can be prone to aggregation, which is thought to be responsible in conditions such as Alzheimer's disease, or bovine spongiform encephalopathy (mad cow disease). Proteins can fold or unfold at surfaces, and so their role is important in understanding proteins themselves. Force spectroscopy studies [33] are a useful means of understanding the conformation of proteins in different environments and thus may play a key role in understanding what can cause misfolding.

The prokaryotic cell wall is a complex environment consisting of many proteins, biosurfactants, and polysaccharides. Their adhesion is controlled by *adhesin* molecules, and the process of adhesion involves the secretion of these molecules to test the viability of a surface. Adhesins are part of a broader class of molecule known to biologists as *virulence factors*, but for our purposes we can take them to be either proteins or polysaccharides. If these molecules are compatible with a surface, the cell will adhere to that surface, and a biofilm may form: the surface is not biocompatible. It is common practice for researchers to consider the cell as an inert colloidal particle and its adsorption to be controlled by electrostatic and van der Waals forces. The application of theory based on these ideas — Derjaguin, Landau, Verwey, and Overbeek (DLVO) theory [41] — is commonplace. However, cells are not static inert objects, but adapt to their environment. Their behaviour, and thus their physics is environmentally dependent. This is as true in the bulk as it is on surfaces. In the bulk, chemotaxis depends on the availability of nutrients or presence of toxins and the cell's response to these informs different dynamical properties. On surfaces a dispassionate consideration of cell walls is not in itself enough for a determination of whether or not a cell will adhere to a given surface; for example, bacteria can express many different adhesins and adhesin expression is dependent upon environmental factors [42].

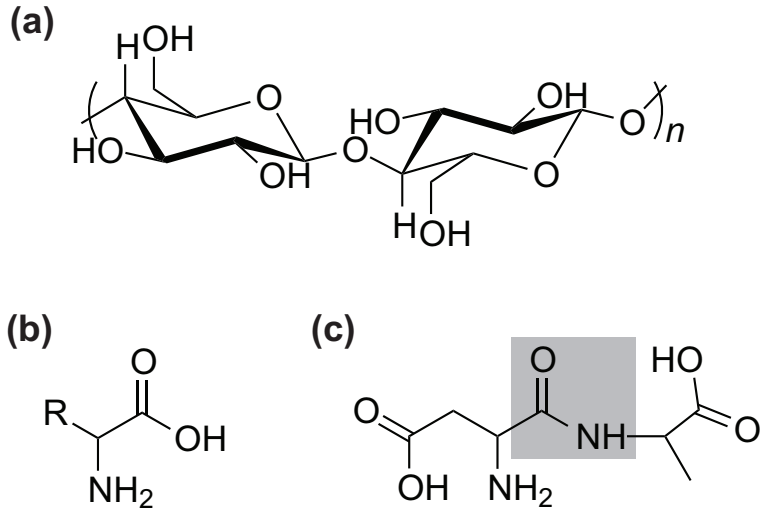

Figure 2. (a) Cellulose is a well-known example of a polysaccharide. It consists of glucose chains joined by the glycosidic (here –O–) bond. (Cellulose is hydrophilic, but insoluble in water.) (b) An amino acid consists of amine and carboxylic acid groups, with the functional unit (R) differentiating the different kinds. A protein is a series of amino acids joined by peptide bonds. The shading in (c) shows a peptide bond used to join two amino acids, aspartine (left) and alanine (right). Further additions to the peptide would occur at the amine for aspartine, and carboxylic acid for the alanine. The carboxylic group in the aspartine part of the dipeptide is part of the functional group, R

That proteins and polysaccharides are biologically important is clear, but it would be worthwhile to identify whether their function within biological systems is completely

driven by their chemistry, or whether the underlying physics inherent in large molecules also affects their behaviour. A protein is a series of amino acids joined by peptide bonds, and a polysaccharide is a series of sugar molecules joined together by glycosidic bonds. These are shown in Figure 2. In both cases there are plenty of hydroxyl groups that give rise to the hydrophilicity of the components, as they are sources of hydrogen bonding. Whilst the specific combination of chemical groups or amino acids will interact individually with their environment, the ability of the chain to work as a single entity, as required for its biological function, is driven by the form of the molecule. This is particularly pertinent in the case of proteins, with their naturally folded peptide chains. This type of conformation arises from an energy landscape where one of the most stable low-energy forms is a "marginally compact tube" [43], which has a propensity for generating α-helices and β-sheets, the most important secondary structures in proteins [44]. Furthermore, proteins have been shown to maintain their native folded structure despite amino acid replacement, suggesting that the overall shape and associated crystalline behaviour is at least partially independent of the chemistry of these large biomolecules [45].

Eukaryotes do not have a cell wall, but rather have a membrane. (Plants, however, can have cellulose-based cell walls surrounding the outer membrane.) Their adhesion to surfaces is based on a wider array of adhesion molecules, and these are largely proteins. Their purpose is to ensure that tissue binding is complete, and are not optimized to bind to inorganic surfaces. Since their binding is expected to be to biological tissue, eukaryotic cells are best grown on hydrophilic surfaces in contrast to many prokaryotes, which are best cultured on hydrophobic surfaces.

2. Techniques for the structural investigation of surfaces and interfaces

There are numerous experiments that can be performed to understand the nature of a surface or interface. The questions that arise are based loosely around the information that is needed. An experiment designed to provide morphological information is not likely to be useful if the requirements are chemical information. Furthermore, if the interface is buried, it will be harder to access. It may be necessary to destroy the sample to access that interface, but there are also techniques that can access covered interfaces *in situ*, for example by using neutrons. Techniques involving neutrons have their own limitations, such as a large associated cost and the requirement for access to facilities for which instrument time may take many months to obtain. Selective deuteration to provide contrast is often necessary. Most techniques have some requirements on samples; at the very least samples must be very clean for most experiments. Other means of differentiating experimental techniques are those that provide real-space information, and the scattering techniques, which provide data in reciprocal space where detailed unambiguous analysis becomes challenging. Here we shall split our consideration of techniques for the study of interfaces into those that provide information primarily about surfaces, and those that provide information about buried interfaces. The choice

of techniques is subjective, but those considered here have been demonstrated to be important over a number of years.

2.1. Surface analysis techniques

Surface analysis is a phrase often used by veterans of the field specifically to mean photoelectron spectroscopy and secondary-ion mass spectrometry (SIMS). These two techniques would provide chemical information about the surface. Initially, routine high-resolution surface imaging could only be provided by scanning electron microscopy (SEM). Now there is much more choice; photoelectron spectroscopy, SIMS, and SEM are high vacuum techniques and so newer techniques were designed to be somewhat more flexible. The suite of scanning probe techniques allows much greater choice in how samples can be measured, and provides a wide variety of data. Neverthless, if chemical information is needed, photoelectron spectroscopy and SIMS are hard to beat. Infrared techniques, however, can also provide much useful chemical information. There are many reviews concerning surface analysis, but if the reader wishes to see a complete overview, the book edited by Vickerman is to be strongly recommended [46]. Here, with due deference to its position in the history of polymer surfaces, X-ray photoelectron spectroscopy, which is sometimes called electron spectroscopy for chemical analysis, is discussed.

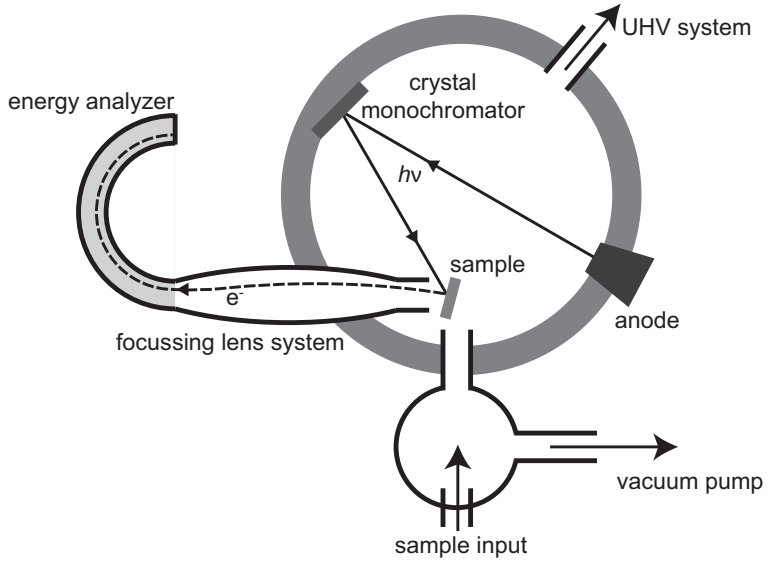

Figure 3. Schematic diagram of a typical XPS set-up. X-rays generated from an appropriate anode are made monochromatic by a crystal grating and then incident on the sample. Ejected electrons are collected by a focussing system to maximize the count-rate, before being energy selected by the use of electrostatic fields in an energy analyser. The voltage across the analyser is scanned and each potential across the analyser corresponds to a given electron energy

2.1.1. X-ray photoelectron spectroscopy. The two photoelectron techniques, XPS and its longer wavelength sibling, ultraviolet (UV) photoelectron spectroscopy (UPS), offer the same operating principle although their uses are slightly different. X-rays or UV are used to eject electrons from the sample. The high-energy X-rays are capable of ejecting core electrons and the resultant information (the energy of these electrons) provides information on the chemical composition and bonding in the material under illumination. UV radiation ejects outermost (valence) electrons form the material under study, and this can enable a better understanding of the electronic structure of the material. UPS is often used for measuring density of states in materials. UPS therefore is mostly (but not exclusively) used for understanding general (bulk) properties and so is of less interest than XPS to those whose primary concern is the surface.

Monochromatic X-rays are generated in a metal source, such as a K_α source of magnesium or aluminium, in an ultra-high vacuum (UHV) chamber (Figure 3). These X-rays, of energy 1254 eV (Mg K_α) or 1487 eV (Al K_α) are generated in an anode, which is usually a heated filament. The anode also generates other emission lines as well as the K_α lines that are often used, and so a crystal monochromator can be employed to remove unwanted lines. (Recent developments include the use of synchrotron radiation in XPS measurements which dispose with the need for a metal source. Furthermore these are tuneable in energy, and here crystal monochromators are particularly helpful.) X-rays are then incident on the sample and they will eject core electrons. X-rays, being uncharged and highly energetic, have a very strong penetration of most samples, but the photoelectrons ejected in the analysis do not travel far. Indeed, it is only the photoelectrons generated very near the surface that can escape the sample and this limits the depth of available information from XPS to no more than 10 nm from the surface, although in most cases it will be less than this.

The energy of the core electrons is different from one element to another, and furthermore bonding changes this energy slightly. The photoelectron energy is measured, and the count rate plotted accordingly. The greater the photoelectron (kinetic) energy is, the less the electron binding energy must be. Alternatively, the count rate can be plotted as a function of binding energy, and an example of this is shown in Figure 4. The binding energy is often plotted in a decreasing energy scale for easy comparison to the kinetic energy. Either way, the binding energy plots are more useful because it is these rather than the kinetic energy plots that can be compared between different X-ray sources. The binding energy is calculated using the simple Einstein energy relation,

$$E_\mathrm{b} = h\nu - E_\mathrm{KE}, \tag{1}$$

where E_KE is the kinetic energy of the ejected photoelectron. This relation needs to be modified to account for the chemical shift due to different bonds (Figure 4) or if the sample is conducting, but it nonetheless encompasses the basic physics.

The data shown in Figure 4 provide an example of the utility of XPS. Poly(3,4-ethylene dioxythiophene) (PEDOT) is often used as an anode or a hole-transport layer in contact with the anode. (It is used synthesized as a complex with poly(styrene

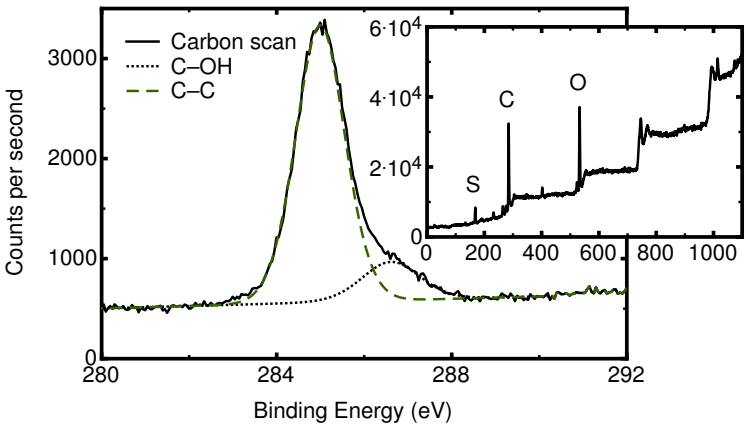

Figure 4. XPS data are first obtained with a wide scan to check the presence of the elements under study. An example *survey* scan is shown in the inset, along with the locations of the primary carbon, oxygen, and sulfur peaks under study. These scans are low resolution, but for a detailed study, high resolution scans are then performed. The data in the figure are of a C(1S) scan of film of the synthetic metal poly(3,4-ethylene dioxythiophene) (PEDOT) complexed with poly(styrene sulfonate) (PSS) after crosslinking with glycerol. The data are shown as a solid line, and the broken lines show fitting to the data. The fitting allows a clear differentiation between C–OH and C–C bonds. By comparing the relative areas of the peaks associated with the relevant elements and their bonds, the surface compositions of the film can be deduced. These data were used in a study of the water resistance of such films by Rodríguez *et al* [47]

sulfonate) (PSS), which acts as a dopant and allows processing of the PEDOT in aqueous solution because PEDOT is generally insoluble. It is known that adding high boiling point alcohols such as glycerol [48] or sorbitol [49] to PEDOT/PSS layers can improve performance of polymer devices, but optimizing performance is aided by a detailed knowledge of their structure. The XPS data in Figure 4 show that there is a strong contribution of C–OH bonds in the scan, which is commensurate with a significant amount of glycerol at the surface [47]. The glycerol is not conducting (or semiconducting) and so charge transport between this hole-transport layer (or anode) and the semiconducting layer of the device must be though an insulating layer. Whether this insulating layer improves the quality of the device is not clear, but it is difficult to remove it because thermodynamics (surface energy) control its presence at the surface. It is known from XPS [50] and neutron reflectometry [51] measurements that, without the alcohols, the PSS is located at the surface, so even then the PEDOT is not in contact with the semiconducting layer.

2.1.2. Secondary-ion mass spectroscopy. SIMS is a technique whereby medium-energy ions are incident on the surface and, on collision, send out fragments of the surface of the film which are detected in a mass spectrometer. SIMS complements XPS because, unlike XPS, it can provide molecular information. A SIMS spectrometer uses a beam of ions — argon (Ar^+) is typical, but other ions (which may be positive or negatively

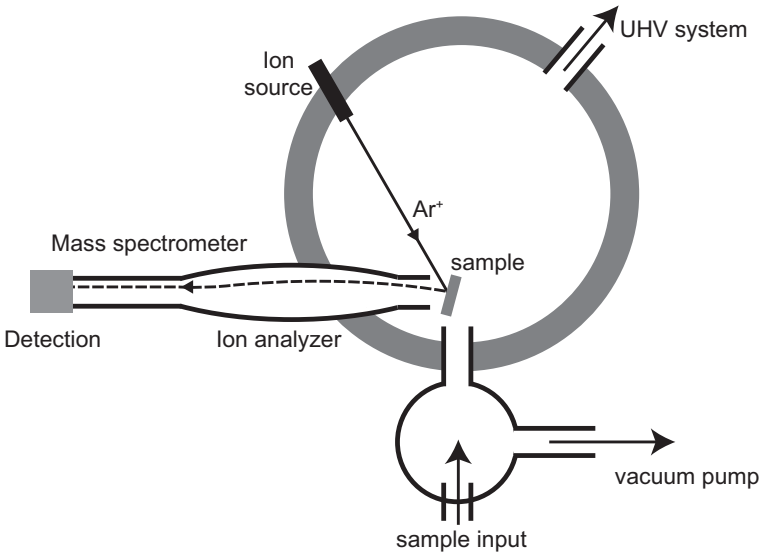

Figure 5. Schematic diagram of a typical SIMS set-up. Charged ions (here Ar^+) are incident on the sample, whereupon they create secondary ions (fragments) in the film, which are collected by a lens (ion analyser) and are magnetically selected in a mass spectrometer before detection

charged) such as caesium, oxygen, gallium, and xenon are common — accelerated to an energy of typically 40 keV. This energy is large enough to eject many ions from the film, but, because they are charged, only material in the near surface region can escape, as is also the case for XPS. The typical set-up (Figure 5) is in principle quite similar to an XPS system.

The fragments ejected from the surface are detected in a mass spectrometer, and are differentiated by their mass/charge ratio. Most fragments are singly charged and so the mass/charge ratio simply represents the molecular mass in g/mol of the fragment. Example SIMS data are shown in Figure 6 in which a mixture of poly(L-lactic acid) (PLLA) and polystyrene is compared with pure films of the two surfaces. (The PLLA is contaminated with polydimethylsiloxane (PDMS), which provides extraneous peaks.) Here, the phase separation of PLLA and polystyrene within the film disrupts the flatness of its surface, creating a film with a topographically structured surface [52]. It has long been known [53] that certain topographically structured surfaces can provide (for reasons not completely understood) a beneficial substrate on which eukaryotic cells can grow and proliferate better than they can on a flat surface [54]. In this work, osteoblast (bone-forming) cells do not grow particularly well on either the polystyrene or PLLA surfaces. PLLA is not particularly hydrophilic; despite its name, it is not an acid: L-lactic acid is polymerized and its carboxylic group is lost in the polymerization reaction. Nevertheless, the addition of structure by mixing the two polymers improves the surface for cell growth, and the SIMS data provide direct evidence showing that both components are at the film surface.

SIMS and XPS experiments are complementary, and one can be used in place of

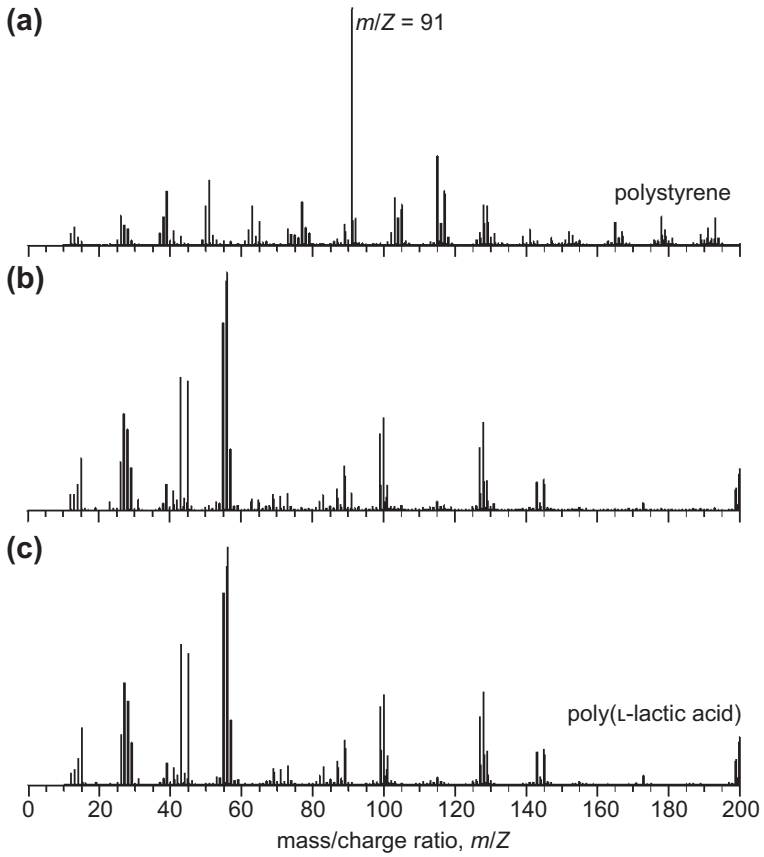

Figure 6. SIMS data for polystyrene (a) and PLLA (c) films. The plots in part (b) show a mixture of PLLA and polystyrene. The abscissae are in units of g mol^{-1} e^{-1}, where e is a unit of elementary charge. Using the line marked $m/Z = 91$, it is clear that the mixture contains little polystyrene at the surface. Adapted with permission from Lim *et al.* [52]. Copyright (2005) American Chemical Society

the other. In the study of PLLA and polystyrene described here [52], XPS was also performed and a slightly increased polystyrene fraction at the surface was determined than for the SIMS experiments, which helps to add limits to the accuracy of the experiments.

2.1.3. Scanning probe microscopy. The scanning probe microscopies are a suite of techniques in which a small probe scans across a surface, determining information about the surface topography, strength, chemical structure, or electrical or magnetic properties.

The most common form of scanning probe microscopy is scanning force microscopy (SFM) in which topographical information about a film surface is obtained by scanning the probe across that surface and measuring the probe deflection as it navigates nanoscale surface features. Alternatively the deflection is kept constant and the topography can be monitored from the vertical displacement of the probe [55]. Here the probe is a small cantilever with a tip of $\sim$ 30 nm in radius, typically made of

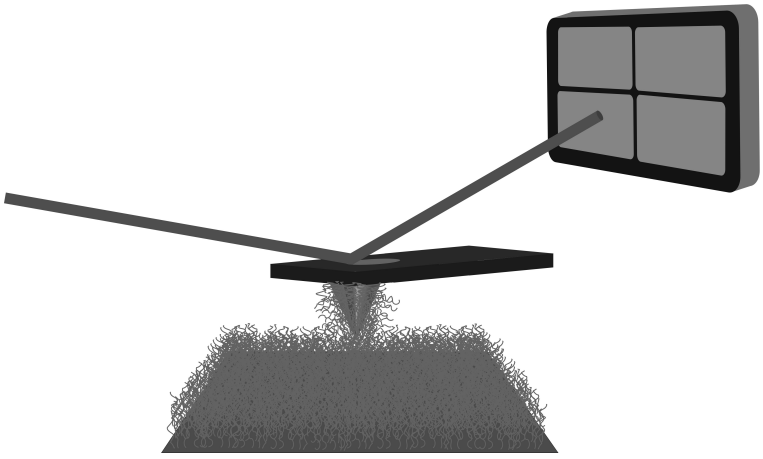

Figure 7. A scanning force microscope consists of a cantilever and tip which is moved across the surface determining relevant properties of that surface. As the topography changes, surface forces will change and the tip may move in response to these changes. The deflection or movement of the tip can be monitored by the reflection of a laser on the back of the cantilever. This laser beam is detected on a quadrant photodiode. The SFM tip can be modified as necessary. This schematic diagram shows a tip coated with polymer molecules, which is an example of how tribological interactions between different materials can be obtained. Such tip modification allows a control of the interactions with the surface, such as the adhesion, in order to gain a better understanding of surface and material properties

silicon or silicon nitride. (These materials allow for manufacturing accuracy coupled with durability during repeated measurements.) The key components of the SFM are shown in Figure 7. As the tip is moved across the surface, the forces that the surfaces exert on the tip will change. If necessary, a feedback loop can be maintained to keep these forces constant. As the tip rises and falls a map of the surface can be obtained with great (sub-nanometre) precision. For polymer surfaces, dragging a SFM tip across a surface can cause damage to the surface and so intermittent contact is often desirable. In this 'tapping' mode the cantilever is driven to a frequency near its resonance and makes contact with the surface only during part of the oscillation. How much of the oscillation is spent in contact with the surface can be controlled. The key requirement is to tap hard enough so that the tip can detect the contours of the surface, but not so hard that it actually indents into soft materials [56].

There are many other variants of the technique. Friction (or lateral) force microscopy (FFM) is a contact mode experiment, whereby the tip is dragged along the surface. An increase in friction results in an increase in lateral force on the cantilever, which will cause it to bend. The lateral force on the cantilever is directly proportional to the load, according to Amontons' law [57]. Here the load is the force on the cantilever driven by the electronics of the instrument. FFM is a particularly useful technique for determining interactions with the tip that might not be clear from measurements of topography. A flat surface with hydrophobic and hydrophilic components can be readily studied using FFM [58]. In the case of polymer surfaces, friction force microscopy can

provide valuable information about the viscoelastic properties of a polymer surface [59] or material interactions, as schematized in Figure 7, through grafting polymers to the tip surface [60].

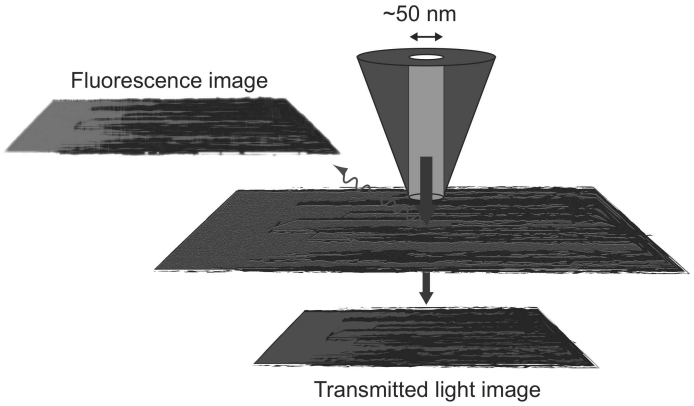

Figure 8. A scanning near-field optical microscope requires a tapered optical fibre through which light is directed. The thickness of the fibre is generally between 30 and 100 nm, and the wavelength of the light depends on the information required. If fluorescence imaging is required, then a wavelength appropriate for the fluorescence is required. A map may be taken of the fluorescence (or sometimes simply reflected) light or an image may be taken after absorption through the film, assuming the film is thin enough and the substrate transparent

The resolution of optical microscopy is generally restricted by the Abbe limit of approximately $\lambda/2$. This diffraction limit can be circumvented by the use of scanning near-field optical microscopy (SNOM), which is a scanning probe technique in which the probe is an optical fibre brought very close to the sample surface as schematized in Figure 8. The use of SNOM to interrogate polymer surfaces is much less commonly used than SFM, but is nevertheless important, especially in areas such as polymer optoelectronics. Here UV light is passed through the optical fibre and it illuminates the surface. The light may pass through the film as the probe scans across the sample, allowing a transmission image to be built up. Alternatively, scattered light may be detected, in which case a reflection image would be obtained. SNOM, however, is at its most powerful when the incident light from the fibre is used to excite optoelectronic molecules in the film. Through a judicious choice of illuminating light, the molecules in the material fluoresce. Here, an image may be taken locating chemical species in the film by their optical behaviour. This information may be obtained simultaneously with a topography image. The SNOM tip is small enough to be used in the same manner as an SFM tip. It is not ideal, but it is good enough for correlating optical and morphological properties of the film.

Data that exemplify how well SNOM can be used to reveal information about a film are shown in Figure 9. Here, a blend of the opto-electronic polymers poly(9,9-dioctylfluorene-*alt*-benzothiadiazole) (commonly denoted F8BT) and poly(9,9-dioctylfluorene-*alt*-bis-*N*,*N*′-(4-butylphenyl)-bis-*N*,*N*′-phenyl-1,4-

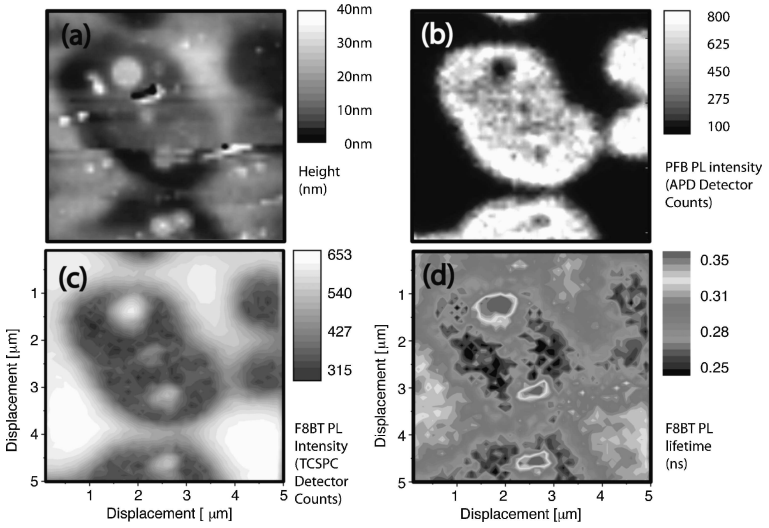

Figure 9. SNOM can be used to obtain topographical information, and this is shown (a) for a blend of F8BT and PFB. (b) The light is transmitted through the film and collected using an avalanche photodiode (APD). (c) Photoluminescence data from F8BT (obtained in transmission). The use of time-correlated photon counting (TCSPC) allows a determination of the lifetime of the excitation as a function of position, and a map of the photoluminescence lifetime is also shown (d). Reprinted from Cadby *et al.* [61], with the permission of AIP Publishing

phenylenediamine) (PFB) is imaged using SNOM [61]. The fluorescence is obtained in transmission in this case after being irradiated with 440 nm light from the SNOM. When mixed with F8BT, PFB emission is suppressed at long wavelengths, allowing a mapping of the the F8BT lifetime as a function of its environment. Here, it is likely that the exciting radiation generates excitons (Coulombically-bound electron–hole pairs) which affect the speed of fluorescence. The more PFB that is present, the slower the luminescence.

Of course, there are many other examples of scanning probe methods. STM, for example has an extremely good resolution, but it is seldom used to study polymer surfaces because it requires conducting and flat substrates in order to function. Further developments have revealed the possibility of parallel processing of polymer surfaces using AFM [62] and SNOM [63, 64]. These techniques have been developed with an eye on memory storage and lithography, and are beyond the scope of this review.

2.1.4. Force spectroscopy Molecular force spectroscopy and single molecule force spectroscopy are AFM-based techniques used to measure the interaction of an object with a surface, and may or may not be linked to a scanning probe. The object in question may be a polymer, a bacterium or eukaryote, a microparticle, or any other suitably small material [31, 34, 66, 67, 68, 69, 70] that can be attached to an AFM cantilever. The cantilever is brought towards the surface and allowed to adhere, if indeed it does adhere, with its deflection monitored at all points along the approach. The cantilever is then removed, and again its deflection is monitored. As a material

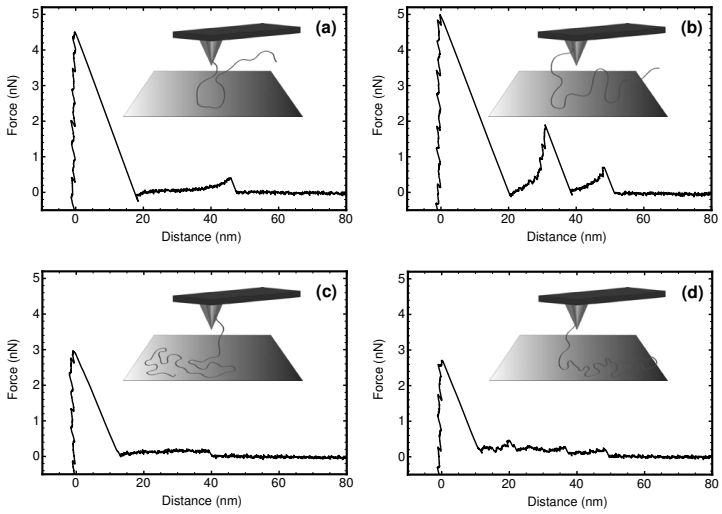

Figure 10. Single molecule force spectroscopy can be used to measure the adsorption of polymers in different environments. The adsorption of poly(*N*,*N*-dimethylacrylamide) (PDMAc) to a silicon substrate depends strongly on its environment. In the case of some environments different conformations are also possible. Here data for PDMAc are shown in water at pH 3. In (a) the polymer has only one contact point with the substrate (as in Figure 1a), but in (b), there are two as noted by the multiple peaks in the retraction curve data shown. (c) A 'plateau' in the retraction data shows that the polymer undertakes a 'pancake' conformation on the surface, as is also schematized in Figure 1c. (d) A mixture of 'loops' into the solution and 'trains' on the surface are also possible (Figure 1b). The schematic diagram in each inset indicates the possible conformation of the polymer matching the retraction data; the polymer in the schematic diagram is not to scale with the tip. This figure incorporates previously published data [65]

approaches the surface there is initially no measurable interaction, but very often an accelerated adhesion is observed as the material 'snaps to' the surface. At this point any further approach is repulsive because there is a compressive effect on the cantilever and material. Retraction of the cantilever will be affected by the adhesion of the material to the surface, so the probe will need to be pulled off the surface. For many particulate probes, this is the end of the process. The probe is retracted, and there is no further interaction. However, for polymer-coated probes or single polymer chains, mechanical work is done on the polymers after the initial detachment, assuming that some polymer is left on the surface. Here polymers are straightened as they are stretched away from the surface, with an associated entropic cost. This is reflected as an increasing force on the polymer as the tip is retracted from the surface. Results for different conformations of a polymer are indicated in Figure 10. More complicated polymers include proteins, which can be denatured as they are pulled away from the surface, with associated information about the length scale of the folding. In the case where there are multiple points of attachment between the polymer and the surface, mathematical models can be used to extract information from the multiple binding events.

Although DLVO theory can be used to describe the interactions measured by force spectroscopy [71, 72, 73], in its basic form it does not account for the interplay between all of the different types of force [74], being solely based on a combination of attractive van der Waals interactions and repulsive double-layer forces [41], and discretion must be used when selecting it for analysis [75, 76]. The extended form of DLVO theory includes some extra features, and can be a better model for forces in a more complex system [77]. However, there is currently no comprehensive theory for bacterial or cellular interactions at a colloidal level, as adhesion in these systems involves a wide range of surface molecules and polymers with different physio-chemical natures as well as contributions from cell elasticity and hydrodynamics [78].

Beyond DLVO theory, there are two alternative models that have been extensively used in the interpretation of force spectroscopy data, and model selection is typically based upon the predicted physical properties of the molecules involved in the interaction. In biological systems, data from flexible polysaccharides are more likely to be fitted using the "freely-jointed chain" (FJC) model, whereas the "worm-like chain" (WLC) model is generally considered more appropriate for DNA and proteins, which are more rigid [79].

The FJC model considers the polymer as comprising n rigid elements with a length l_{K} (the Kuhn length) that are connected through flexible joints which can rotate freely in any direction. At low forces, the polymer formation is that of a Gaussian chain, but as force is increased, orientation becomes less random, with preferential alignment oriented along the direction of the external force. Smaller Kuhn lengths correspond to a more flexible polymer [73, 80]. In the FJC model, the force required to stretch a polymer to a length x is given by

$$F_{\mathrm{chain}} = \frac{-k_{\mathrm{B}}T}{l_{\mathrm{K}}}\mathbf{L}^{-1}\left(\frac{x}{l_{\mathrm{c}}}\right), \tag{2}$$

where k_{B} is the Boltzmann constant, T is the absolute temperature, l_{c} is the contour length of the portion of the chain that was stretched, and $\mathbf{L}^{-1}$ is the inverse Langevin function, approximated by the first four terms of its series,

$$\mathbf{L}^{-1}\left(\frac{x}{l_{\mathrm{c}}}\right) = 3\left(\frac{x}{l_{\mathrm{c}}}\right) + \frac{9}{5}\left(\frac{x}{l_{\mathrm{c}}}\right)^{3} + \frac{297}{175}\left(\frac{x}{l_{\mathrm{c}}}\right)^{5} + \frac{1539}{875}\left(\frac{x}{l_{\mathrm{c}}}\right)^{7}. \tag{3}$$

An example of the application of the FJC model in a biological context is the investigation of bacterial surface macromolecules on *Pseudomonas putida* using SMFS. It was found that the biopolymers had segment lengths in the range 0.154 – 0.45 nm, but that 65 % of measurements gave a segment length of $0.154 - 0.20$ nm, suggesting that many of the polymers present on the cell surface were highly flexible [80].

In the WLC model, the polymer is considered as a continuous flexible chain of length L_{c} with a bending stiffness, κ, that can be used to evaluate the persistence length, L_{p} by [81]

$$L_{\mathrm{p}} = \frac{\kappa}{k_{\mathrm{B}}T}. \tag{4}$$

There is no analytical solution to the WLC model, but the most common approximation is the interpolated WLC [82], given by

$$F = \frac{k_{\mathrm{B}}T}{L_{\mathrm{p}}}\left[\frac{1}{4}\left(1-\frac{x}{L_{\mathrm{c}}}\right)^{-2} - \frac{1}{4} + \frac{x}{L_{\mathrm{c}}}\right], \tag{5}$$

where F is the elastic restoring force of the chain and x is the end-to-end separation distance. In some cases, the persistence length can be obtained from techniques such as small angle X-ray scattering [83]. The suitability of fixing persistence length can be evaluated by comparing experimental data and the WLC model in a force versus normalized distance plot. Such fixing was appropriate in a study of the swelling of grafted poly(methacrylic acid) (PMAA) layers [84], where L_{p} was taken as 0.5 nm (it had been previously determined using small angle X-ray scattering for bulk PMAA [83]), which gave a good fit up to high extension levels, and resulted in greater data fitting accuracy for the contour length, since only one parameter was fitted to the WLC model. This model has also been applied to data obtained when performing force spectroscopy on different bacteria [85, 86, 87]. (Hydrophilic silicon nitride tips do not always give the required peaks and on occasion hydrophobic tips were required to obtain data that could be fitted to the WLC model [88].)

Force spectroscopy is usually performed with an uncoated AFM tip, or an AFM tip coated with gold or a suitable self-assembled monolayer. With such tips, the polymers to be investigated may be in contact with the surface, in which case the process is known colloquially as '*fishing*'. Molecules that cannot be functionalized, for example by thiolation to react with a gold-coated tip, are generally studied after being picked up on an AFM tip. (It is by no means always necessary to functionalize a molecule in order for it to attach to an AFM tip.) For this to work as a single molecule technique, the polymers must be dilute on the surface, and not entangled with other polymers. The tip can then pick up these molecules and thus measure the interaction with the surface through a retraction curve. This method can be very frustrating as most experiments will not yield a result, because the probe simply makes contact with the substrate. Automation allows for easier experiments, and is becoming increasingly sophisticated [89]. Generally, these fishing expeditions are for biomolecules, which are often very large, making the experiment a little easier. An uncoated AFM tip can be used to characterize dense layers of grafted polymers (brushes), which are tethered by one end to the substrate [90, 91, 92, 93, 94, 95, 96, 97]. By retracting the tip, physisorbed polymers are extended and their length and dispersity in lengths can be assessed.

2.1.5. Quartz crystal microbalance with dissipation A key part of understanding the interaction of polymers and biopolymers at surfaces relates to adsorption, be it either favourable or unwanted. One method to measure this in both gaseous and liquid environments is to use a quartz crystal microbalance with dissipation (QCM-D). The QCM-D relies on a freely oscillating piezoelectric sensor formed of a thin single crystal quartz (SiO_2) disc with electrodes on the upper and lower face (see Figure 11) [98]. Direct piezoelectric materials are well suited to use as sensors because mechanical

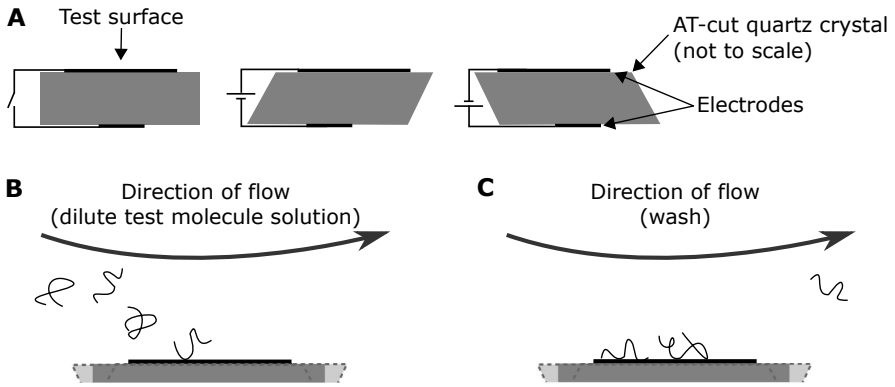

Figure 11. Schematic diagram of aspects of QCM-D operation. A: when no electric field is applied, the crystal is under no mechanical stress and the lattice is in a 'neutral' position (left). If an electric field of a given direction is applied (middle and right), the crystal is subjected to mechanical stress and deforms, resulting in a lateral shift of the test surface, therefore, the application of an alternating voltage gives rise to sinusoidal oscillations in the crystal. B: during a measurement, the oscillation frequency of the crystal is monitored as test molecules flow across the surface. The amount of adsorbed test molecules is determined using the shift in frequency of crystal oscillation. C: once a layer has adsorbed, the dilute test molecule solution is replaced with a clean solution (a wash, typically a buffer) so that any loosely bound material is removed. The viscoelastic properties of the adsorbed layer can be evaluated from the damping (or dissipation) of the measured crystal oscillations

deformation induces a proportional change in the electric polarization of the material [99]. In the reciprocal effect, application of an external electric field to the piezoelectric material induces mechanical stress in the crystal lattice, resulting in deformation of the crystal. When this crystal is oscillated using a sinusoidal electric field (i.e. an alternating voltage), the fundamental crystal resonance, f_0, is dictated by the thickness of the quartz in the sensor, t_q, the shear modulus of the quartz, μ_q, and its density, ρ_q, such that

$$f_0 = \frac{1}{2t_\mathrm{q}}\sqrt{\frac{\mu_\mathrm{q}}{\rho_\mathrm{q}}}. \tag{6}$$

For use in the QCM-D, quartz crystals are typically cut in the AT form, which generates motion lateral to the sensor surface and is relatively immune to temperature-induced fluctuations at room temperature [100]. This mode of operation is referred to as *thickness shear mode*.

In its simplest form, prior to a dissipation measurement, the quartz crystal is driven at a selected frequency close to its fundamental mode, setting up oscillations with a constant amplitude. At the start of the measurement the driving voltage is withdrawn, allowing the oscillations to decay naturally to zero. As additional viscoelastic material is adsorbed the rate of decay of oscillations will be 'damped' (*dissipation*) and the resonance frequency of the oscillations is associated not just with the quartz sensor, but with any adsorbed material [101, 102, 103]. More commonly, and to allow for much longer measurements to understand the binding of multiple molecule types by

sequentially flowing them across the sensor (generally interspersed with flow of a wash buffer to remove any non-adherent molecules in between tests, see Figure 11), a *continuous resonance mode* can be used, where the driving electric field is maintained throughout and relative shifts in the crystal frequency (Δf) are measured [100]. The QCM-D can therefore be used to track adsorption of molecules and biomolecules to the sensor surface [104]. In addition to monitoring the amount of adsorbed material, it can also provide information about the viscoelasticity of the adsorbed molecules, and is therefore useful for testing for adsorption barriers [105].

The mass of adsorbed material can be evaluated using the Sauerbrey model, which neglects viscoelastic effects, and assumes a rigid adsorbed layer. According to the Sauerbrey equation [106], the frequency change Δf in the piezoelectric crystal due to the adsorbed mass Δm is given by

$$\Delta f = -f_0^{3/2} \sqrt{\frac{\eta_\mathrm{l} \rho_\mathrm{l}}{\pi \rho_\mathrm{q} \mu_\mathrm{q}}}, \tag{7}$$

where ρ_l and η_l are the density and viscosity of the fluid, respectively. The adsorbed mass is determined from the changes in viscosity. Masses given include that of any water that is bound or coupled to the surface. This model is appropriate if changes in energy dissipation are small and the adsorbed layer is relatively rigid. The use of an unmodified Sauerbrey equation for soft or viscoelastic films can lead to an underestimate of adsorbed mass [102].

Dissipation data may also be obtained to allow analysis of viscoelastic effects; if the material is tightly-bound and rigid, then minimal dissipation modification would be expected, so the greater the dissipation change for a unit change in gained mass, the more viscoelastic the adsorbed material is [107]. This increase in dissipation can be caused by two things: a more viscoelastic molecule or a poorly attached layer causing dissipation due to friction associated with moving out of synchronization with the resonating crystal. If there is doubt, the origin of the dissipation can be established from thickness data obtained by methods such as ellipsometry; if the change is related to molecule properties, the layer should be thicker, whereas if it is due to loosely bound material there should be a thinner layer. One might argue that ellipsometry is as versatile a method, but QCM-D offers much higher sensitivity and has been shown to detect single molecule binding events, which is beyond the capability of any ellipsometer. However, the benefits of combining QCM-D with other surface analysis techniques within a single system (such as ellipsometry [105] or localized surface plasmon resonance [108]) is not without merit, as this enables additional information to be obtained simultaneously through the same sample and measurement platform.

2.2. Depth profiling and buried interfaces

Techniques that allow us to understand the variation of a particular quantity as a function of distance from an interface are known as *depth-profiling* experiments. The ability to provide information away from the exposed surface of a film is very important,

and particularly so in the case of buried interfaces. Experiments in aqueous solution are important for biological samples; these are often not of interest in a dry state. To image buried interfaces is not easy. If the interfaces are in a low viscosity liquid environment then scanning probe techniques can be used, assuming the liquid will not damage the apparatus, but other techniques described above such as SIMS and XPS are inappropriate due to their vacuum requirements. For these reasons most buried interfaces can only be effectively studied in one dimension by depth profiling.

2.2.1. Reflectometry. Perhaps the most powerful depth profiling technique is that of neutron reflectometry [110, 111, 112, 113]. Here, a beam of neutrons is incident on the sample to be studied. The neutrons may be monochromatic, or as is more often the case, pulsed with a spectrum of wavelengths in the Ångstrom range. The very short wavelength of the neutrons, and for X-rays when considering the similar technique of X-ray reflectometry [111], allows for an extremely good depth resolution. Neutrons are versatile because they are only weakly scattered by many materials, which means that they can traverse large distances before reaching the interface in question. Water, unfortunately, does scatter neutrons, but it is not necessary to send neutrons through a bath of water in order to reach the interface to be studied; neutrons can interrogate the interface in question by passing through many substrates with little loss of intensity (e.g. silicon). Contrast in neutron reflectometry experiments is most often achieved by selective deuteration of one of the components in the film. If two polymers are mixed, then one of them would normally be deuterated. In aqueous environments it is generally advantageous to use heavy water, because of the extensive scattering of neutrons by normal water (H_2O). Although it is possible to account for this scattering by careful analysis, it detracts from the quality of the data. The use of heavy water does make some biopolymer experiments difficult to consider, because often H/D exchange occurs in biopolymer solutions, particularly in the case of certain proteins [114]. Nevertheless, neutron reflection has been used in many experiments to study biomacromolecules, and an example is shown in Figure 12 for the rather shorter chain molecule, mycolic acid [109]. Many of the advantages of neutron reflectometry also apply to X-ray reflectometry. X-ray scattering techniques work best when there is a heavy element present in the sample, as these provide contrast. This restriction is not prohibitive, however, and X-rays are also useful for the characterization of the surface of thin films. X-ray reflection is, however, not viable for the study of buried liquid interfaces. Nevertheless X-rays are less expensive than neutrons and are available in laboratory apparatuses. Which technique is used depends therefore on a variety of different parameters but the information obtained is broadly similar. By way of example, the use of X-ray reflectometry to study the structure of films to explain adhesive behaviour [115] provides information broadly comparable to studies used for similar purposes with neutrons [116, 117, 118, 119, 120].

2.2.2. Ion beam analysis. Other depth profiling techniques require the use of ions to penetrate the film, revealing chemical information as a function of depth. Dynamic

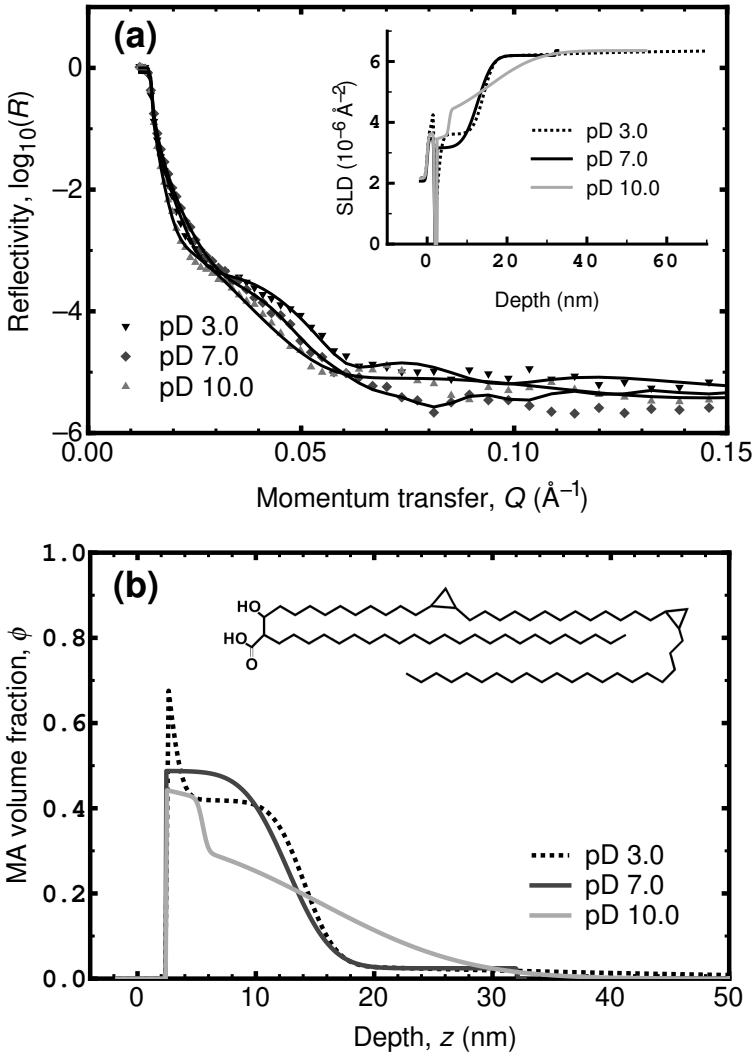

Figure 12. Mycolic acid is a biosurfactant associated with mycobacteria. Here, neutron reflectometry data are shown for an aqueous solution mycolic acid from the human tuberculosis bacterium with the carboxylic acid group exposed. The neutron reflectometry data are shown in (a), and in the inset, the scattering length density profile is displayed. This scattering length density profile is from a silicon substrate ($z = 0$), and attains a rather large value of 6.48 Å^{-2} at large depths; this scattering length density corresponds to heavy water. There is a clear extension of the acid at pD 10, but not much change between pD 3.0 and 7.0. (Note the use of pD, rather than pH.) The volume fraction profile of the mycolic acid is extracted and shown in (b). The inset in (b) shows the chemical structure of α-mycolic acid, which is one of a mixture of mycolic acids contained with the sample studied here. Reprinted from Zhang *et al.* [109]. Copyright (2010), with permission from Elsevier

SIMS, for example, involves the ion beam etching the sample [121, 122]. By knowing the etching rate, the chemical information yielded can be correlated with the depth. Dynamic SIMS is less often used, partly because of the difficulties in interpreting data when different components in the film have different etching rates. Contrast, such as H/D differentiation, although not always necessary, can help data interpretation.

Techniques falling under the umbrella of ion beam analysis do not include dynamic SIMS, which is more a mass spectrometry technique. Ion beam analysis generally requires a means of monitoring the energy of ions as they exit a film that was interrogated by a beam of ions, which may or may not be the same as those incident on the film. With ion beam analysis, different techniques allow for a very flexible approach. The best known ion beam technique is *Rutherford Backscattering* (RBS) [123, 124]. Here a beam of ions (usually α-particles) of energy of the order of 3 MeV is incident on the sample. These ions have a small collision cross section (recall the revelations about the interaction of α-particles with gold and other metals in the original experiments of Geiger and Marsden [125]) and so it takes a relatively thick film, up to 10 μm, to stop them all. By measuring the energy of the detected α-particles, one can determine the depth in the film at which the backscattering event took place. (The energy loss of α-particles in different materials is tabulated [126].) With these measurements, a depth-profile can be constructed. RBS is less commonly used in soft matter research, because there are relatively few polymeric systems that contain the heavy elements required for good RBS data, although some studies have been performed [127], and other studies have been concerned with the location and behaviour of heavy elements in polymer matrices [128, 129, 130]. Figure 13 shows an example of such data. Heavy elements can, however, also be added as markers to define the movement of polymers [131], or to stain an individual component of a mixture [132]. RBS, like SIMS and XPS, is restricted by a vacuum requirement because the α-particles will be scattered in air. Nevertheless, developments have been made to allow their use to study samples in different environments [133, 134], although their application is away from the areas concerned in this review.

Ion beam techniques more commonly used for the study of thin polymer films include *nuclear reaction analysis* (NRA) and *forward recoil spectrometry* (FReS) because they both allow a means of determining the profile of light elements in the sample, and as such are very often complementary to neutron reflectometry. (Neutron reflectometry provides excellent resolution, but because the information obtained is in Fourier space, it is often useful to start with depth profiling information which can provide the initial conditions for fitting the reflectivity data.) FReS, sometimes called elastic recoil detection analysis (ERDA) is a relative of RBS. In RBS the incident α-particle recoils from the nucleus. In FReS the energy of the deflected α-particle is not needed, but rather the energy of protons and deuterons ejected from the nucleus are measured. Their energy is obtained using kinematics, just as in RBS; here however the nucleons are *forward scattered*, as opposed to the backscattering in RBS. Backscattering means that the incident particles recoil on hitting the nucleus and forward scattering means that the ejected particles are sent away from the initial beam. The forward scattering is a consequence of the protons and deuterons being a lighter mass than the incident α-particles. An advantage of FReS is its ability to determine the volume fraction-depth profile of both deuterated and non-deuterated components of a film.

Nuclear reaction analysis is another ion beam analysis technique that can provide a

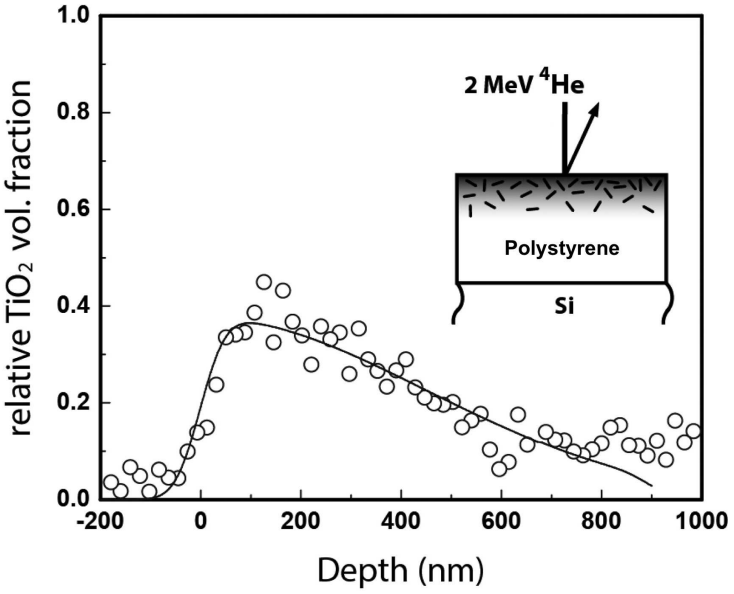

Figure 13. Rutherford Backscattering data from nanorods of titanium dioxide in a matrix of polystyrene. The TiO_2 nanorods are allowed to diffuse into the polystyrene at 190° and the diffusion can be modelled using Fick's second law, from which a diffusion coefficient may be obtained. These measurements in which a heavy element such as titanium is used are ideal for RBS because of the high scattering cross section. In such experiments the excellent resolution afforded by reflectometry is not needed and furthermore, the large length scales associated with interdiffusion of this nature are usually inaccessible with reflectometry techniques, which work better with sharper interfaces. Adapted with permission from Choi *et al.* [130]. Copyright (2015) American Chemical Society

volume fraction-depth profile of a given component in a film. There are many different variants of NRA, but the most popular for the determination of the structure of polymer films is ^{3}He NRA. Here a mono-energetic beam of $^3He^+$ ions is incident on the film. The energy of the ions is typically $\sim$ 1 MeV, and at about this energy $^3He^{++}$ (the other electron is immediately lost on impact with the film) reacts with deuterons to yield a lithium compound nucleus, which quickly decays to create an α-particle and a proton, as well as about 18.5 MeV of energy; the reaction is very exothermic. The ^{3}He nucleus loses energy as it penetrates the sample, and this changes the reaction kinetics, altering the energy of the proton and α-particle produced. Either the proton or α-particle can be detected, and their energy allows a calculation of the position in the sample at which the reaction took place. (How well ^{3}He is stopped by matter is tabulated [126], just as for α-particles, so one can work out the energy that these nuclei must have had at a certain depth in the sample.)

3. Physical phenomena at surfaces and interfaces

In a mixture of two incompatible polymers, the different polymers will seek to limit their area of contact. This will cause one phase to dissolve in another to create spherical

domains. These domains seek to merge with other, similar, domains to form bigger spheres, reducing their surface to volume ratio. However, even circular structures are not necessarily stable, because of the difference in pressure across a surface (the Laplace pressure) and the disjoining pressure caused by having different material phases in contact.

The interface between two polymer components tells us about the competition between entropy and enthalpy, and thus allows us to dissect the interfacial energetics of a particular set of materials. The structure of a blend or mixture of polymers at a free or fixed interface also will be different to that in the middle of the film. These interactions can lead to stratified or segregated structures, where polymers wet the surface. Sometimes the film will simply dewet its surface. Finally, polymer films can be controlled by chemically attaching them to the surface. These are known as polymer brushes, and have many applications in terms of controlling film stability, adhesion, colloidal stabilization, cell culture, and even in all-polymer electronic devices.

The structure and morphology of polymer blend films has been intensively studied over the past 25 years, and developments have been made with specific applications in mind, such as the use of blends in optoelectronic devices. From a more general perspective the study of the formation of films during drying is an area of research where experimental developments have allowed quantitative studies to take place. Although these subjects will be covered here; films of one homopolymer have been used as a vehicle for fundamental studies of basic phenomena, such as crystallization, and this will also be addressed. Finally, the use of films as actuators will be presented, highlighting the role of brushes in this new area of research.

Perhaps the area of polymer thin film research that has received the most attention is dewetting and related phenomena. The stability of films and coatings is important in many areas of technology, and so we consider developments in this area first.

3.1. Wetting and dewetting

The stability of most polymer films can be characterized by the use of contact angle experiments (Figure 14), which typically give a description of the free energy of a sample compared to that of water: hydrophilic surfaces are those where the interfacial energy of the water-solid contact is below the free surface energy of the solid, whereas hydrophobic surfaces exhibit the opposite relationship, with the solid having the smaller surface energy, or tension.

In systems where the contact angle does not vary with time and an equilibrium, *static contact angle* is attained, the surface energies in the system can be related to the contact angle θ, by

$$\gamma_{\mathrm{LV}} \cos\theta = \gamma_{\mathrm{SV}} - \gamma_{\mathrm{SL}}, \tag{8}$$

where γ_{LV}, γ_{SV}, and γ_{SL} are the liquid–vapour, surface–vapour and surface–liquid, interfacial energies respectively. This equation is only true for an ideal surface (flat,

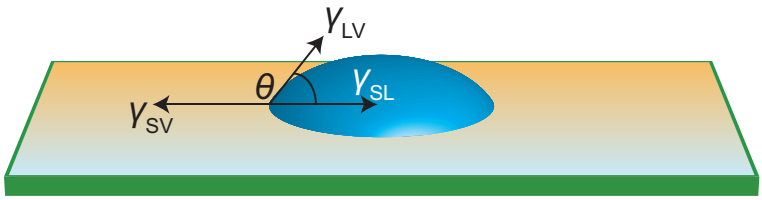

Figure 14. The contact angle of a liquid is a balance between the surface and interfacial energy of the different components: γ_{LV} for that between the liquid and its vapour; γ_{SV}, that between the solid and the liquid vapour; and γ_{SL} for the interface between the solid and liquid phases. For experiments in which the liquid is water, a contact angle, θ less than 90° denotes a hydrophilic surface; when $\theta > 90°$, the surface is hydrophobic; and for $\theta > 150°$, the surface is usually referred to as superhydrophobic

rigid, insoluble, chemically homogeneous, and unreactive) and it takes its name (the Young equation) from Young's work in the early 19$^{\text{th}}$ century [135].

The contact angle is particularly relevant for biomaterials, where very hydrophilic surfaces tend to be associated with good biocompatibility. The ability of a material to remain solvated in the presence of other macromolecules means that that surface is less likely to be fouled. Wettability of surfaces is also a strong indicator of adsorption, with profound consequences for cell growth and protein fouling [136]. This can be characterized through instability in the temporal behaviour of the contact angles, with changes in droplet volume (in conditions with minimal evaporation) either due to droplet absorption, spreading, or a mixture of the two [137]. In the case of such *dynamic contact angle* measurements, wetting of a hydrophilic surface is associated with an advancing water contact angle [138], and dewetting of a hydrophobic surface with a receding contact angle [139]. Absorption is not always relevant because it requires the surface to have some limited solubility in water but can be considered in terms of a decrease in droplet basal area along with a decrease in volume, whereas spreading results in an increase in basal area.

Both static and dynamic contact angle measurements play an important role in the characterization of polymer surfaces for use in various applications, ranging from the medical field, in terms of reducing harmful biofouling or encouraging native cell growth on implants [140, 141]; to optometry and contact lens anti-fouling properties [142, 143, 144], wetting agents [145] and in-built drug delivery [146, 147], to the replacement of petrolium-based polymers with biopolymers which are able to replicate their hydrophobic properties [148].

Although the water contact angle is an important characterization tool for biomaterial surfaces and for surfaces that may be placed in contact with water, it is less useful for understanding whether or not a film is stable. The Young equation (Equation 8) also allows prediction of film stability, and can be used to define stability through the spreading coefficient,

$$S = \gamma_{SV} - (\gamma_{SL} + \gamma_{LV})\,. \tag{9}$$

When $S > 0$, the solid-vapour interface is the high energy surface, and so the liquid will

preferentially coat that surface; i.e. the film will *wet* the surface. Similarly, when $S < 0$, the film will be unstable on the surface and will want to *dewet* the substrate.

The stability of thin polymer films depends predominantly on long-range interactions between the film and its environment, and these generally take the form [41]

$$W_j(x) = -\frac{A_{ijk}}{12\pi x^2}, \tag{10}$$

where W_j represents the interaction energy of two parallel and planar semi-infinite media (i and k) separated a distance x by a medium j. The parameter A_{ijk} is known as the Hamaker constant and depends on all three materials, although approximations can be made to calculate A_{ijk} from Hamaker constants of the component materials, A_{ii} where the two (identical) components are separated by vacuum. A more detailed (Lifshitz) treatment relies on the dielectric properties of the different layers [41].

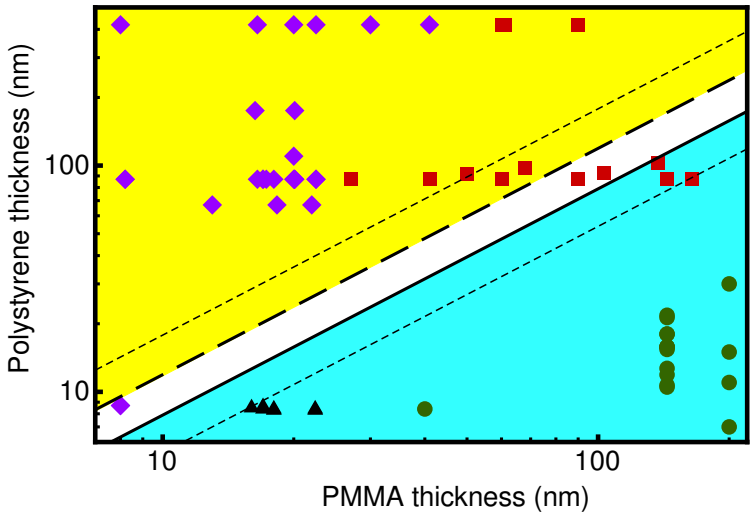

Figure 15. Phase diagram for the dewetting of a bilayer of PMMA on polystyrene on a silicon substrate. Filled diamonds represent the instability of the upper PMMA layer on a stable polystyrene film; circles the reverse situation, whereby the PMMA layer is stable, with a broken polystyrene film beneath it. Both layers can be destroyed through thermal nucleation (squares). Triangles represent data for films that could not be attributed to a particular structure. The upper left shading represents regions of the film for polystyrene, and the lower right triangular shaded region is for stable PMMA films. The thin dashed lines represent uncertainty in the limits on the stability of the PMMA films. Data used with permission from de Silva *et al.* [149]

The different Hamaker constants allow an interplay between the stability of different components in polymer films. In principle a film (B) on a substrate that may be stable in itself can be made unstable by placing a different film (A) on top of it. If the interaction of A with the substrate is stronger than B, even accounting for the fact that A is separated from the substrate by B, then B will dewet. Such a "phase" diagram for dewetting (Figure 15) has been demonstrated for bilayers of poly(methyl methacrylate) (PMMA) on polystyrene on silicon substrates [149].

Whilst varying the thickness of the layers allows the interaction between the films to be tailored to control stability, a film may create its own interface potential that can strongly affect film stability. Diblock copolymers with each block containing similar chain sizes will order to form a stacked (lamellar) structure, with the block that lowers the interfacial energy segregating to the substrate and the block that lowers the surface energy segregating to the surface. These blocks may be the same, or different blocks may segregate to the different interfaces. A lamellar structure will only form if the ratio of the chain lengths in each block is close to unity and the blocks are immiscible. A surface will perturb the structure, and even if the two blocks are miscible, they will order close to the surface, with the amount of order decaying with distance from the substrate. This creates an oscillating interface potential the minima and maxima of which become less pronounced with distance from the substrate, which permits a situation where the melt above a residual layer ordered at the substrate may dewet [150]. Here the dewetting of a diblock copolymer containing immiscible blocks (poly(2-vinylpyridine) and polystyrene) occurs to allow a disordered state to exist close to the substrate whilst retaining a lamellar structure at the air interface, and can proceed when the energy driving ordering is weak. However, the differing diblock copolymer film thicknesses at which this dewetting may occur result in discrete contact angles, even though the composition of the film is the same.

Other recent challenges in dewetting concern the effect of the preparation of thin films on their subsequent behaviour. The microscale morphology of films, and the conformation of polymers within the structures produced by common techniques such as spin coating, are not expected to be at equilibrium. Indeed, there are no methods currently available that routinely produce films at equilibrium. Part of the reason for the resultant out-of-equilibrium structures is the rapid quench in many drying processes, but also there will be a contribution due to the presence of solvent within the polymer film after casting. Later evaporation of the solvent leads to residual stresses within the film, which in many cases is already glassy. There is a clear effect on the distribution of holes in such films, as has been determined by simple optical microscopy experiments [151], where it was observed that the longer the films have to relax, the fewer the number of holes that appeared in the dewetted film (Figure 16).

Relaxation effects are categorized in terms of a response to "residual stresses" in polymer films. The nature of these residual stresses is open to some debate, and they are likely to be dependent on the method of film preparation. Nevertheless, there are other generic factors that may play a significant role across different preparation routes, albeit to different degrees. One of these is the role of entanglements. In confined films, entanglements are expected to remain in films at equilibrium [152], but it is accepted that this is unlikely to be observed in experiments and that polymers may have perturbed conformations [1, 153, 154, 155, 156]. Although a molar mass dependence of polystyrene film stability was observed on topographically structured surfaces [153] or surfaces with a gradient in surface energy [157], these experiments did not perturb stresses within the films. Other experiments have shown that long (polystyrene) chains were capable

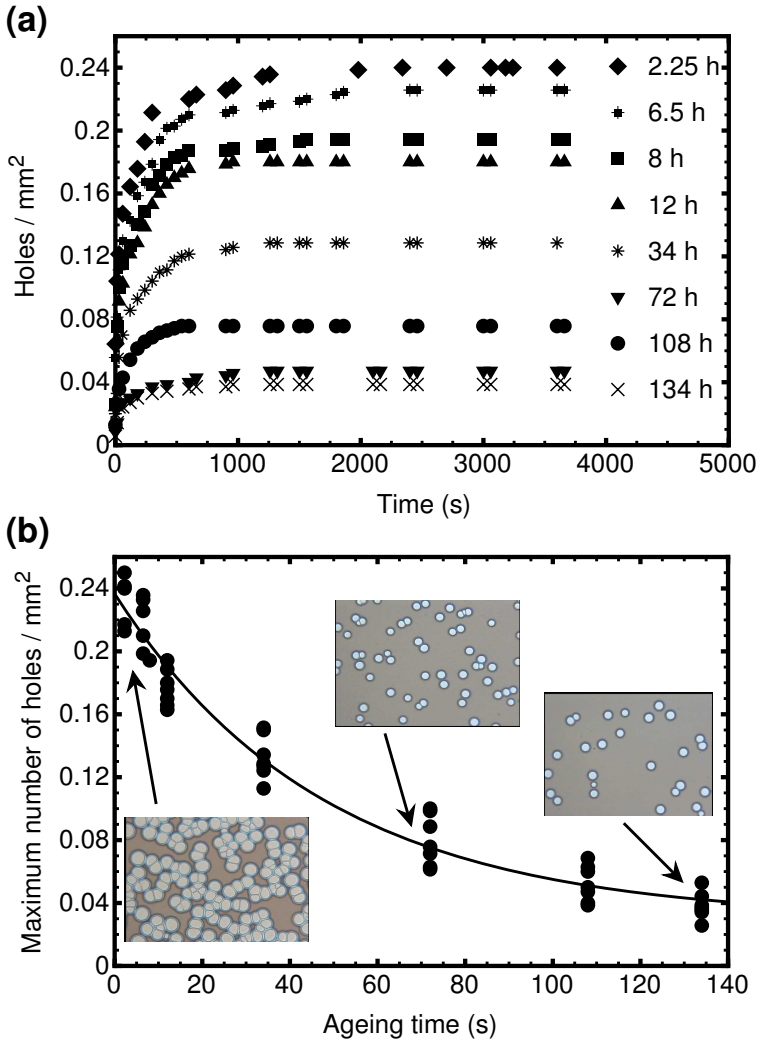

Figure 16. (a) The areal density of holes, N, as a function of time at 125°C for 40 nm thick polystyrene films after being aged at 50°C for different times. The maximum hole density (per 10^4 μm^2), $N_{\max}$ for each sample is reached in about 100 s. (b) $N_{\max}$ as a function of ageing time for similar polystyrene type of films stored at 50°C for various times. The insets show some typical corresponding optical micrographs (310×230 μm^2). The solid line is a fit to the data with a decaying exponential. Adapted with permission by Macmillan Publishers Ltd: *Nature Materials* from Reiter *et al.* [151], copyright 2005

of relaxing rather quickly, indicating that they were closer to equilibrium than shorter polymers of the same chemical structure [158].

A rather clever means of addressing stresses in thin films was to create them in a controlled manner during dewetting. This was achieved by spin coating polystyrene onto PDMS substrates [159]. Initiation of the dewetting perturbs and deforms the substrate, which arrests the dewetting. The process continues on time scales longer than the reptation time of the polymer, which is its longest viscoelastic relaxation time and is the time it takes to diffuse its own length, which is valid for polymers that are long enough to be considered entangled [8, 9]. On these longer time scales, the dewetting

was that of a viscous fluid, with a behaviour dominated by slippage. Slippage in itself has been of some considerable interest in dewetting since systematic SFM experiments were able to follow the shape of the rim during dewetting from a deformable polymer interface [160]. The shape of the rim is important, because it can reveal much about the viscoelastic behaviour of polymers. An initial simple approach to dewetting proposed that the gain in surface energy by the dewetting process is translated into the kinetic energy of the dewetting polymer [161], which is only valid for a low viscosity liquid on a non-deformable substrate. For deformable and liquid substrates, the dewetted polymer accretes into a rim, whose shape depends strongly on the viscosity of that polymer, as well as that of the substrate. Here friction can also be important, and this will increase with the size of the rim, which forces the dewetting speed to decrease. Of course, if friction is limited, then the dewetting polymer may well slip at the interface. Its tendency to slip depends on how much the chains of the two layers can interpenetrate; generally, interpenetration or interdigitation is limited, because otherwise the layers would be compatible and the films stable. Certainly, it has been clearly demonstrated that dewetting proceeds more rapidly on surfaces with less slippage, and hence less friction [162, 163].

Applications of dewetting in various nanotechnologies are still being developed but the basic science must be fully understood before real progress can be obtained. It is expected that dewetting can be advantageously used in a number of new areas, in particular those where patterning is important [164]. For example, the use of selective dewetting to align electrode materials has been developed, a route that may be easily applied using ink-jet printing [165, 166]. Microcontact printing and other patterning techniques can be used to control the structure of films [167, 168, 169, 170, 171]. Although the fundamental science of dewetting is still proceeding, the development of technologies based on dewetting probably has slowed somewhat in the past decade and it is perhaps likely that a new breakthrough is needed to reignite the field.

3.2. Blends in optoelectronic devices

Ever since the observation of electrical conductivity in excess of 10 kS/m in doped polyacetylene was reported in 1977 [172], there has been interest in developing polymers for electronics applications. Although conducting polymers, and PEDOT in particular, have applications in various areas from antistatic films [173], transparent electrodes [173, 174], and bioelectronics [175, 176], it is in the area of polymeric semiconductors where the greatest interest is to be found. Interfaces in polymer electronics are crucial for numerous reasons because they influence and direct morphological behaviour, and can also influence the electronic properties directly.

Blends are of primary interest in photovoltaic devices and light-emitting diode (LED) technology. In the case of LEDs, a current is driven through a forward-biased polymer blend, in which one component is a hole-transporting and the other an electron-transporting polymer. Electrons and holes meet, and form a bound state, called an

exciton [37]. This exciton may decay back to an electron and hole, or it may radiatively decay, giving off a visible photon. (The band gap is the primary determinant of the wavelength of the light emitted.) Clearly for an optimal LED, the amount of excitons giving off light must be maximized, and the number of holes and electrons making it to the opposite electrode without giving off light must be minimized. A parameter by which a device may be controlled is the ratio of the two components in the polymer layer. Other aspects, such as the contact between the layer and electrodes, and the benefits of injection layers will not be discussed here, but they are important considerations [177], and they also affect polymeric photovoltaic cells and transistors [37, 178].

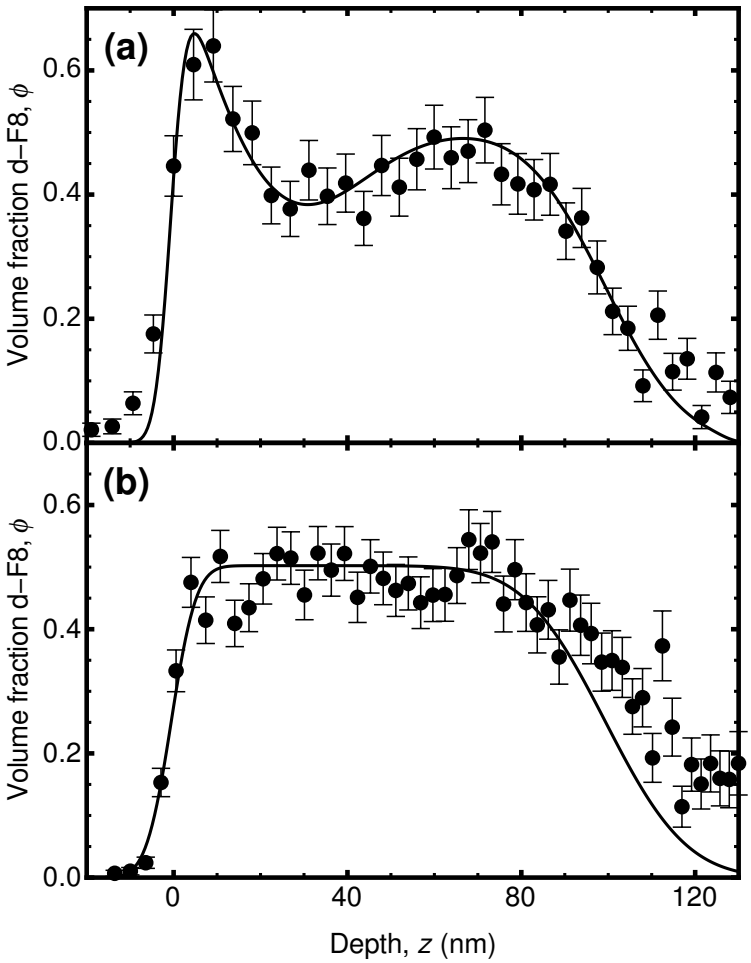

Figure 17. ^{3}He NRA data and simulations (volume fraction-depth profiles) for a blend of 50% F8 and 50% F8BT by volume cast from (a) toluene and (b) chloroform. The peak in the data at $z = 0$ for the toluene-cast film indicates that d-F8 (the d- indicates that the F8 is partially deuterated, for contrast in the ion beam experiment) preferentially segregates to the air interface, with an F8BT-rich region immediately behind it. There is much less structure visible in the chloroform-cast film. The non-sharp interfaces at $z = 0$ and $z \approx 100$ nm are due to the resolution of the experiment. Such resolution effects mask the volume fraction of d-F8 at the surface of the film in the data for the toluene-cast film, which could be close to unity. Taken from Higgins *et al.* [179]

Solar cells essentially work in the opposite sense to LEDs, with incoming light creating an exciton in the blend, which is required to dissociate at an interface between the two components. This dissociation will create electrons and holes, and these must dominate over the competing process of re-radiation. A small bias potential is placed over the cell in order to optimize current collection. The difference between the morphology of the active layer in photovoltaic devices and LEDs is that photovoltaic cells require sharp interfaces at which excitons can dissociate, whereas LEDs benefit from a greater degree of mixing because sharp interfaces can provide charge traps [1, 37], which are certainly not desired. In both cases, a clear path for the charges to the electrodes is necessary. These requirements for photovoltaics and LEDs are largely based on our understanding of the behaviour of charge transport and excitonic behaviour rather than systematic experimental studies linking morphology to optoelectronic behaviour.

Despite the difficulties in creating systematic studies, it is possible to link structure-property relationships, and this will be exemplified considering a blend of poly(9,9-dioctylfluorene) (F8) and F8BT which is commonly used as a model LED. Electroluminescent properties of blends of these two polymers are optimized when films are made with 5% F8BT [180]. Varying the composition of F8BT with respect to F8 changes device properties, but also enables a test of the effect of morphology. For example, casting this blend (F8/F8BT) from different solvents reveals different structures, as can be seen in Figure 17 for toluene and chloroform [179]. The thin layer of F8 attracted to the surface in the toluene-cast film has a profound effect on the photoluminescence properties of these blends. In photoluminescence experiments light is incident on the surface and the radiation emission from the surface is detected. When F8 is irradiated with 405 nm wavelength light, it fluoresces at around 430 nm. However, when mixed with F8BT, this fluorescence is quenched and a broad green emission at $\sim$ 500 nm is observed. Here, energy transfer between F8 and F8BT takes place. For blends cast from chloroform, where the F8 and F8BT are much better mixed, there is indeed energy transfer. However, when the film is cast from toluene, the blue emission from F8 is retained remarkably well even at concentrations as low as 50% F8. The F8 layer at the surface is pure enough to fluoresce. The results are shown as a function of composition in Figure 18 [181].

Photoluminescence is not usually an important factor in real devices, but the data shown in figures 17 and 18 illustrate important phenomena, namely how the role of the casting solvent for the blend can affect device properties. In real devices, other effects can be important, and the role of crystallinity is particularly important in polymer devices, because of the strong affect crystallinity has on charge transport. For example, in model solar cells, blends of poly(3-hexylthiophene) (P3HT) and the fullerene-based [6,6]-phenyl-C61-butyric acid methyl ester are particularly susceptible to the crystalline behaviour of P3HT [182, 183], which emphasizes the importance of understanding the crystalline structure of P3HT [184, 185]. Structure-property relationships in polymer electronics is an active and ongoing area of research. New materials are continuously being developed and optimized, so new understanding on how to prepare the optimal

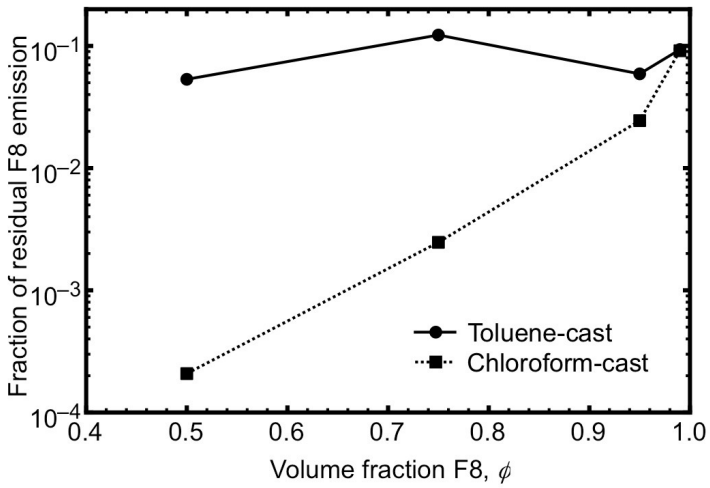

Figure 18. Residual F8 photoluminescence emission (integrated signal from 410 to 475 nm after irradiating with a 405 nm laser) from a blend with F8BT after casting from toluene and chloroform [181]

morphology is important. Isoindigo-based polymers [186, 187] are an example of a recent area of research and already their structure-property relationships have been the focus of different studies [188, 189].

3.3. Crystallization

The crystallization of polymer films remains a controversial subject because the origin of polymer crystallization is unclear. Polymers cannot form single crystals of the quality that is necessary in many industrial processes, such as the polysilicon used in solar cells. Routes to high purity crystals require chemical vapour deposition, which is incompatible with polymers, which have no vapour pressure at room temperature, and decompose at high temperature. Excepting those that are atactic, polymers are inherently semicrystalline. The crystallization starts with the formation of lamellae [190, 191, 192, 193], due to chain folding effects. These lamellae grow until spherulites are formed. However, an important question is whether there is an energy barrier to the formation of polymer crystals. Given that lamellae grow at different rates and that the fastest growing rate dominates the crystallization process, crystallization is accepted to be a kinetic phenomenon, and so it is perhaps more likely that an activation energy is required. (There has been some consideration of a spinodal process [194], which does not require an activation energy and would be spontaneous.)

The role of a surface in polymer crystallization is important, particularly if it is accepted that polymer crystallization proceeds by nucleation. Here the surface can act as a nucleating site for crystallization, which would mean that crystallization should occur at a higher temperature on cooling, or at a lower temperature on heating. Experimentally, this has been shown to be the case. Grazing incidence X-ray diffraction

has been used to show that poly(ethylene terephthalate) (PET) will start a process of surface crystallization at a temperature close to its glass transition temperature, and below that for which bulk crystallization occurs [195, 196]; SFM has also been used to confirm the lower temperature of surface crystallization in PET [197]. Similar results have also been shown for polymers confined within nanopores [198].

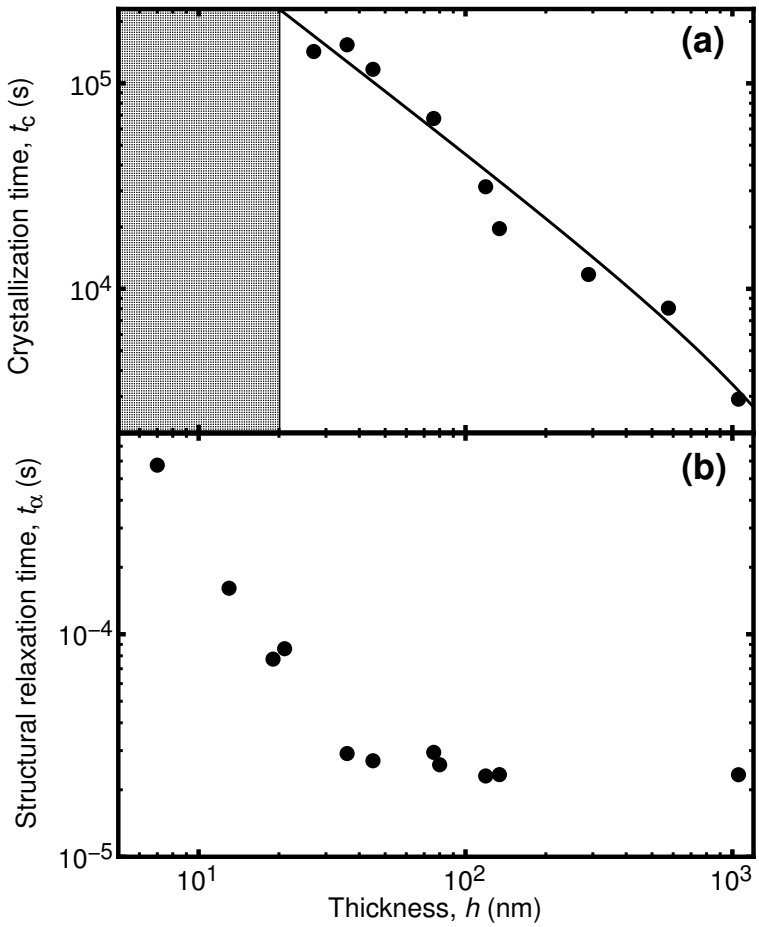

Figure 19. Dielectric spectroscopy results showing the crystallization (a) and structural relaxation (b) times of PET films as a function of thickness [199, 200]. Below 20 nm crystallization was not observed on the time scales of the experiment. This is the shaded region in (a). The solid line in (a) is a fit to $t_c \propto h^{-1}$, which is to be expected from crystallization controlled by finite-size effects [201]

Although the temperature is a significant parameter in polymer crystallization, film thickness also plays an important role, because confinement controls crystallization. This is apparent by the observation that crystallization is faster at the surface than in the bulk [196]. Although X-rays are an important means of observing crystallization phenomena in confined films, they are by no means unique. Dielectric spectroscopy has been used to observe PET crystallization as a function of film thickness [199]. Here the structural relaxation time is observed to increase for films thinner than 20 nm (Figure 19). This relaxation time is associated with the glass transition of the films (it is also known as the α-process), and its increase suggests a glassy film. In

this case, a layer of PET was observed to be irreversibly adsorbed onto the aluminium electrodes (substrate) required for the broadband relaxation spectroscopy experiment. This strong adsorption is responsible for the increased glass transition for these thinner films. For these very thin films, crystallization was not observed and no crystallization time was measured. The 20 nm thickness limit on the crystallization suppression was approximately twice the thickness of the adsorbed layer. It had been known previously that crystallization was strongly suppressed in ultrathin films [202], but there is nevertheless a mechanism for the formation of crystallized structures in two-dimensional confinement [203, 204]. In these examples, a monolayer-thick film of PEG can dewet from its substrate, forming crystalline structures as it does so. Another route to highly confined crystallized structures was demonstrated with the synthesis of polyethylene nanoparticles [205]. These semi-crystalline layers comprised a mere fourteen polymer chains, and in this case were not found on the surface, but were formed sandwiched between amorphous layers.

Much of polymer crystallization research has been dedicated to semiconducting polymers. Semiconducting polymers are generally rather rigid, with a long persistence length, which means that they have a smaller entropic cost in forming lamellae than more loosely bound polymers. Formally, semiconducting polymers behave as "worm-like chains", whereas more flexible polymers can often be considered as "freely-jointed chains" (see section 2.1.4) [9]. Furthermore, the ability to form semicrystalline phases has advantages in terms of the charge transfer of these polymers. Semiconducting polymers are often conjugated, which means that they display alternating single and double bonds, along which charges can move. Movement of charges along a conjugated backbone is impeded by "traps", which are more likely near a kink. Certainly, there is experimental evidence linking the size of crystalline domains and charge transport phenomena [206]. It has also been shown that changing the nature of the material substrate will change the way that the film forms, affecting its crystallization. Polymers are known to align on structures that have a direction associated with them; these are often called alignment layers, and grazing incidence X-ray techniques have been used to determine the behaviour of polymers on these surfaces [207, 208].

The role of crystallization and its impact on charge transport is an underdeveloped subject, however, because there is evidence of charge transport remaining good, even though interfaces may be rough, or amorphous materials have been added that would normally be expected to limit polymer performance [209, 210]. Similar results have been shown to be the case in mixtures of small molecule semiconductors with polymeric additives (binders). The addition of polymers to small-molecule semiconductors is important because polymeric additives can allow greater control of the solution viscosity and the creation of good quality films from a variety of different coating methods, such as dip-coating, and particularly processing routes appropriate for real-world applications, such as ink-jet printing [211]. The first demonstration concerned the addition of different polymers to an important small-molecule semiconductor, 6,13-bis(triisopropylsilylethynyl) pentacene (TIPS-pentacene) with different polymeric

additives [212], which was followed by further work using the same semiconductor [213, 214, 215, 216, 217, 218, 219]. In all of these, some effort was made to understand the location of the different components with XPS used to locate the polymer and small molecule near the surface [212]; time-of-flight SIMS [214] (in three dimensions, Figure 20); neutron reflectometry [213]; optical absorption and X-ray diffraction coupled with solvent etching [216]; Raman spectroscopy [217]; electron microscopy [218]; and profilometry [219]. As an aside, it is worth noting that similar effects have been observed with a range of small molecules blended with TIPS-pentacene rather than polymers [220], but it is clear that polymeric additives have better film-forming properties.

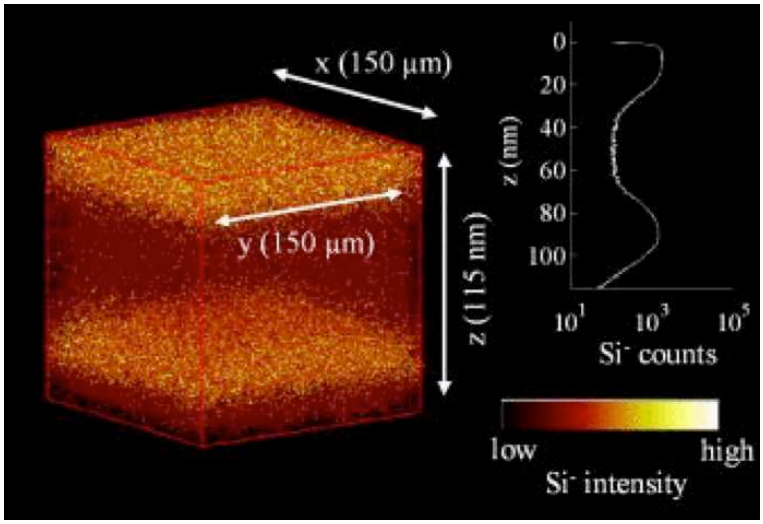

Figure 20. Time-of-flight SIMS has been used to map the location of silicon ions from a blend of TIPS-pentacene with poly(α-methylstyrene). There is clear TIPS-pentacene segregation to both interfaces. The technique is capable of scanning the film as a function of depth, and reveals no μm-scale lateral phase separation. Reprinted from Ohe *et al.* [214], with the permission of AIP Publishing

The TIPS-pentacene segregates strongly to only one interface (that of air) when cast from a blend with an amorphous polymer [212, 213], although this is a non-equilibrium structure and annealing ensures [213, 214] that TIPS-pentacene segregates from a blend with poly(α-methylstyrene) (PαMS) to both interfaces. (Large molar mass PαMS also segregates to both interfaces [213].) This is important because segregation of the TIPS-pentacene to the active interface ensures that there is good charge transport where it is needed. Importantly, however, the need for annealing can be removed by using a semi-crystalline polymer instead of PαMS (or atactic polystyrene [212]). It seems that the speed of crystallization (or structure formation in general) is an important parameter, and the use of crystallizable polymers such as isotactic polystyrene and poly(α-vinyl naphthalene) [212] means that the TIPS-pentacene can segregate to the surface forming crystals during spin-coating. A similar result was obtained by substantially increasing the molar mass of the amorphous material [213]. It is probable that the surface initiates the formation of TIPS-pentacene crystals. Of course, the lower surface energy phase

(including remaining solvent) is directed towards the surface. The surface energetics of phase containing crystalline and semi-crystalline materials is therefore of some interest. Isotactic polystyrene could be mixed to 90% of the film and the field-effect mobility of holes due to TIPS-pentacene (the other 10%) in a transistor created from the blend was shown to be as good as a transistor created with 90% TIPS-pentacene [212]. (Isotactic polystyrene is semi-crystalline, unlike its amorphous atactic counterpart.) The competition for surface crystallization is therefore critical for the creation of good quality devices. That TIPS-pentacene segregated to the (silicon oxide) substrate in a blend with isotactic polystyrene was determined by XPS measurements of the substrate-segregated side of the film, after it had been lifted from the substrate [221]. Other experiments show indirect evidence of TIPS-pentacene segregating to a photoresist interface [219].

3.4. Switchable surfaces

Understanding surface and interfacial properties is important for situations where appropriate surfaces are needed for a given purpose, but the ability of surfaces to actuate and interact with their environment conveys a form of *smart* behaviour that allows *ex situ* control of a device. Work on mixed brushes illustrated the possibility of switching their conformation [222]. In this early work, the environment was shown to be capable of switching the surface composition: a toluene environment would bring a polystyrene component to the surface, but in an acid environment, the poly(2-vinylpyridine) brush would coat the surface. This allowed control of the hydrophilicity of the surface. Such switchable properties (hydrophilic to hydrophobic and *vice versa* were later shown to be capable of being actuated by electric fields for smaller molecules [223]. Temperature responsive brushes were also developed starting with poly(*N*-isopropyl acrylamide) (PNIPAm) [224], a model temperature responsive polymer.

An environmentally switchable surface is one which requires no user interaction to make the surface change behaviour. Some reports have claimed switchable behaviour, but simply reported environment-dependent behaviour rather than demonstrating true switching [225, 226, 227]. Two components may not *attach* in a certain environment, but it does not follow that they will necessarily *detach* under those same conditions. An early and rather clever AFM-based experiment to measure *in situ* reversible behaviour involved the attachment of poly(methacryloyl ethylene phosphate) brushes to an AFM cantilever that was inserted into a liquid flow cell, through which pH or salt concentration could be altered [228]. Environment-induced conformational changes forced a change in the deflection of the AFM cantilever, which was therefore a signature of the environment. In essence, these experiments provided a prototype for how a nanotechnological "nose" might operate as a chemical sensor.

Currently, research into switchable behaviour is dominated by wettability and adhesion. These two properties are closely related, since the latter is in part a consequence of the former. Switchable wettability is not as intrinsically interesting as switchable adhesion, because it is hard to imagine how a switchable surface would

not exhibit a change in contact angle. Nevertheless, there has been substantial interest in switchable wettability with a number of review articles published [229, 230, 231, 232, 233, 234]. Surface control is usually achieved by using polymer brushes in different geometries [224, 235, 236, 237, 238, 239, 240, 241, 242, 243, 244]. Experimental work has also been augmented by a growing body of theoretical studies [245, 246, 247].

There are other means to control solubility and thus brush conformation which have been investigated, such as passing gases through the solution [248]. Nevertheless, the main route to switching polymer brushes is to use environmental factors such as pH and temperature. It is however sometimes desirable to use external electric fields to switch conformation, and there has been some experimental success demonstrating this [249, 250, 251] but the absence of a substantial body of work reflects the very real difficulty in producing reliably repeatable experiments. There has however been significant interest in the theory of polyelectrolyte brushes in electric fields [252, 253, 254, 255, 256, 257]. There are other possibilities, with different advantages.

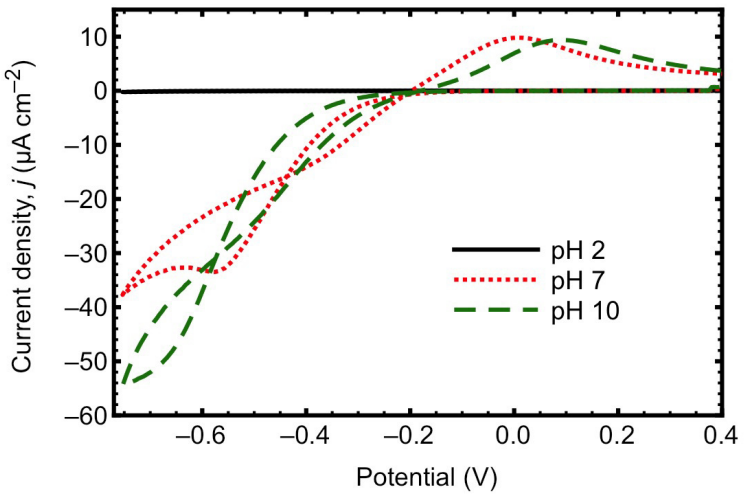

Figure 21. Cyclic voltammetry data for a 14 nm-thick PMAA brush layer as a function of pH in the presence of 3 mM ruthenium(III) hexamine redox probe relative to a saturated calomel reference electrode [258]. The data obtained at pH 2 show no response because the brush is fully protonated. The same null response is exhibited in the absence of the redox probe demonstrated that the brush is not contributing to the electrochemistry, but rather is gating it

Actuation is a rather vague application for what is simply a conformational switch, but there are nonetheless many possible uses for brushes that undergo such changes, whether environmentally triggered or otherwise. The use of hydrogels for pH-control of fluid flow has long since been demonstrated [259], but the pH-switchable nature of polyelectrolyte brushes can be used for electrochemical logic gates. Electrochemistry is, in its most basic form, integral to the switchable nature of polyelectrolyte brushes because it is charge that controls their conformational behaviour [236, 237, 239, 250, 260]. However, for the control of electrochemical reactions not explicitly involving the brush,

a mechanism has been shown that involves polyanionic brushes (polycations can also be used in the appropriate circumstances) attracting redox probes to the brush, which in turn allows electron transfer to take place at the substrate surface. If the pH is adjusted (lowered for polyanions), the polyelectrolyte loses its charge and the function is turned off (Figure 21). Electrochemical switching was seen to work well using standard silicon substrates [258], eliminating the need for the metal surfaces used in earlier work [260]. It is probable that the ability to replace standard metallic electrodes with silicon is likely to be of greater importance than the switchability aspect, and to this extent polyelectrolytes are not necessary [261].

The control of adhesion by environmental change remains a particularly appealing use of switchable surfaces. The demonstration of environmentally switchable adhesion using polymer brush layers has been achieved by a number of groups [117, 262, 263, 264, 265]. The simplest example is that where pH controls the adhesion, and here a polyelectrolyte brush has been shown to have its adhesion with hydrogels switched off when the pH is changed in aqueous solution. The hydrogel used need not itself be a polyelectrolyte [263], but oppositely charged polyelectrolytes are certainly very effective [117, 265]. Switchable adhesion between oppositely charged polyelectrolyte brushes has also been demonstrated [262], although in this case the "switch" was not pH, but rather the ionic strength of the medium. Adding NaCl was observed to cause the adhesion to fail. Since the adhesion was due to the electrostatic interaction between the two brushes, the salt was able to shield these charges and interfere with adhesion. This phenomenon is interesting, because it affects materials that are already adhering, which is important because it presents another means of controlling adhesion. However, it also demonstrates the challenge of applying such switchable adhesion in biological systems, which have considerable salt present. Bonding between two identical brush layers has also been demonstrated, in which polyzwitterions were shown to adhere due to long-range forces between the components [264]. However, in this case a change in temperature caused the brushes to swell, terminating the adhesion. Despite these efforts, application development is still not forthcoming. This is perhaps surprising because there are a number of areas where reversible glues could be useful, with a headline example being in wound dressing; removing dressings from a wound has risks of infection and numerous therapeutic challenges [266]. Recycling is another area because separating parts without damaging individual components decreases waste [267], with perhaps the automotive industry leading the way in separation technologies [268]. Despite these and many other needs, it is an open question as to whether brushes are robust enough to withstand the wear to which they may be subjected, and there is also the problem of ease of use because "one-pot" reversible adhesives of this nature are currently lacking. Nevertheless, these problems are related to development and it is inconceivable that there are no uses for what is likely to be a relatively inexpensive and versatile technology.

That surface switchability is exhibited more often than not in aqueous environments and that many water soluble polymers are biocompatible leaves open the possibility of engineering switchable surfaces with biological applications. An early example of this is

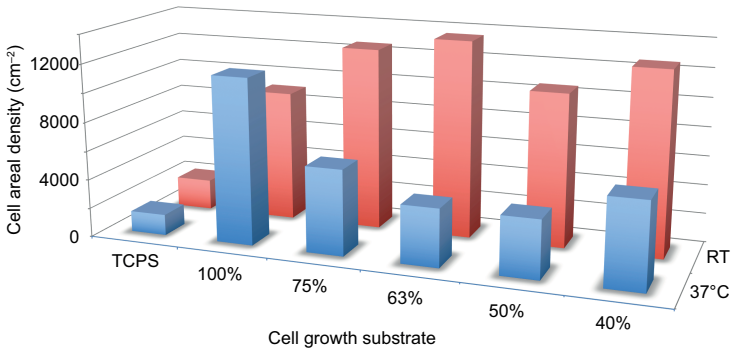

Figure 22. Chondrocytes grown at 37°C were released at room temperature (RT). The data show the areal density of cells in the medium (i.e. unattached to the substrate) for different compositions of hydrogel (e.g. 40% means that the substrate is composed of a graft copolymer containing 60% PNIPAm brush, and 40% by mass hydrogel) [269]. The data can be compared with a standard substrate for cell culture, tissue culture polystyrene (TCPS). The hydrogel does not allow cells to grow on it, whereas the TCPS cannot release cells with a change in temperature. The best sample is that which contains 37% grafted PNIPAm

in the cultivation of eukaryotic cells at surfaces. The idea that cells could be grown on a surface and then ejected on demand is appealing because cells need harvesting when they are to be used. In particular, growing cells on surfaces means that once a monolayer of cells has formed, no more area can be covered and although cells can divide, they cannot *expand* under their turgor (internal) pressure. Ejecting cells from the surface gives them the freedom to expand. The use of a conformational switch to eject cells has the additional advantage of removing the requirement for enzymes to detach them from tissue culture plates as is used in standard protocols. This has been demonstrated using a PNIPAm brush attached to a hydrogel of poly(2,3 propanediol-1-methacrylate) [269]. The hydrogel allows nutrients to circulate in the culture medium. Above its lower critical solution temperature (LCST) of 32°C PNIPAm adopts a collapsed conformation caused by intra-chain hydrogen bonding. It is solvated at lower temperatures, which makes it ideal for cell culture. In this particular case chondrocytes were cultured at 37°C, but when the temperature was allowed to relax to room temperature, the PNIPAm brush expanded and the cells consequently detached (Figure 22). This research was quickly followed by experiments showing that another temperature responsive brush, this time a copolymer of oligo(ethylene glycol) methacrylate and 2-(2-methoxyethoxy)ethyl methacrylate is shown to be resistant to L929 mouse [270] and 3T3 fibroblasts [271] below its LCST, which allowed the harvesting of cells cultured at higher temperatures. A different example comprises a biocidal polymer brush on which bacteria are killed, but which can be converted to a non-fouling surface by a simple hydrolysis procedure [272]. This ejects dead bacteria and leaves a bio-inert surface behind. Such a protocol involves an irreversible chemical change, and so is not fully switchable. Another irreversible

route involves converting a PEG brush-coated surface, which inhibits cellular adhesion to an adhesive substrate by the removal of the brush layer, achieved by ultraviolet light which acts on a photo-cleavable group connecting the brush to a glass substrate [273].

The ability to create "smart" surfaces that interact with cells is a considerable advance, and similar work has also been done on switchable adsorption of proteins [274, 275]. Specific interactions of biopolymers and cells with surfaces needs to be treated separately, and this is highlighted in Section 4 below.

4. Interactions of biopolymers with surfaces

If a macromolecule enters into close proximity with any surface and it is energetically favourable to interact with the surface rather than the surrounding liquid or gaseous environment, the molecule will attach to that surface. Such an attachment can be classified either as specific or non-specific, depending on the characteristics of both molecule and surface. The non-specific attachment of macromolecules to surfaces is well illustrated with the data shown in Figure 10. In biological systems, there are specific linkages involving proteins or lipids, whereby the polymer can recognize a particular receptor, triggering an interaction between two components. Bacteria, for example, may bind to particular proteins because these proteins may provide a signal that the bacteria are in an environment that can be colonized. Such a process requires the presence of adhesins on the bacterium to recognize macromolecules on the host surface. Specific interactions between proteins and other molecules are crucial throughout biological systems as they mediate a vast quantity of cellular processes such as adhesion, uptake of molecules, and information processing. Proteins, in selected environmental conditions, have exposed reactive sites that bind to a given part of a "partner" molecule due to the combination of closely fitting interfacial structure and exposed adhesive complexes within the interfacial binding area [276, 277]. Changes in structure due to modifications in the environmental conditions or oxidative state of the molecule can prevent or reverse this binding by either modifying the adhesive complexes or changing the shape of the "docking" area to prevent access to the adhesive complexes [278, 279, 280]. The identification of protein structures, their modification by exposure to different stimuli, and their interaction with different partner molecules are all important for our understanding of the multitude of processes occurring within any given biosystem, be it the mediation of interactions within a single cell or throughout a complex multicellular organism.

Most of the known structural information about proteins (and other biomolecules) was discovered through the application of X-ray crystallography to crystallized proteins. However, this technique has some limitations: in the case of complex or membrane proteins (including ion channels and receptors), the relevant molecules need to be extracted in relatively large quantities which can be challenging since overexpression of the majority of membrane proteins causes cell toxicity [281]. In addition, crystals made using these complex proteins are generally inhomogeneous, leading to widely

varying diffraction quality within a single sample and causing difficulties in terms of data interpretation [282].

X-ray crystallography cannot image proteins *in vivo* or probe the strength of bonds between a protein and itself or external partner molecules. Many proteins undergo physical modifications as part of their biological role, so it is useful to be able to track changes to their structure. Isolating and crystallizing proteins at these defined stages is challenging given the short timescales of the movement; folding and unfolding events generally occur in the range of microseconds to tens of seconds [283], except in the case of ultrafast folding proteins which can undergo folding in timescales from 10 μs down to several hundred nanoseconds [284, 285]. There have been advances in time-resolved X-ray crystallography that enable changes in structure to be tracked, e.g. the carboxy to deoxy state modifications of a L29F myoglobin mutant [286] and structural relaxation and ligand migration in the L29W myoglobin mutant following photodissociation of carbon monoxide from the heme (porphyrin encapsulated) iron [287].

There are several competing techniques which have been suggested to either enhance or replace X-ray crystallography data. Methodologies that are able to provide information about protein folding include vibrational and optical spectroscopy techniques such as fluorescence resonance energy transfer and infrared spectroscopy [288], and single molecule force spectroscopy (see Section 2.1.4).

The discussion is limited to force spectroscopy and QCM-D (see Section 2.1.5). Force spectroscopy enables quantitative information to be obtained, offering a versatile approach to understanding molecular interactions and the forces and structures which govern these interactions on nano- to micro-scales. QCM-D is then discussed as a method of understanding molecular binding on a macroscopic scale, using a population of molecules to examine binding trends over time and in different environmental conditions; research that has importance in understanding biofouling and also in the development of sensor technology [98].

4.1. Force mapping of cells

A challenging aspect of research of polymers at surfaces is involved in understanding the behaviour of complex biopolymers which are integrated into the outer wall of eukaryotic and prokaryotic cells. More generally, the interactions of biomacromolecules with living organisms, a means of testing molecular recognition, is a rapidly growing area of research, which is benefitting from the use of the SMFS-based techniques [289, 290, 291, 292]. Various forms of force mapping evolved simultaneously, with experiments performed using unmodified AFM tips [293, 294], chemically modified probes [295] (i.e. probes functionalized with a self-assembled monolayer), and probes functionalized with biopolymers [296]. The use of SMFS has revolutionalized the determination of cellular adhesion forces; previously micro-mechanical techniques were used [297], which were crude and did not allow mapping. An additional benefit of SMFS or SFM is that force-distance curves contain much information about the interaction

between the tip and the surface; whilst adhesive and repulsive forces are related to the portion of the force-distance curve that is in solution, the portion of the curve where the tip is in contact with and pressing into the sample surface contains information about the mechanical properties of the sample, and thus, with a well characterized probe [298], the viscoelastic properties of the sample can also be profiled. This technique has been applied to a wide range of samples including lipid bilayers [299], polymers and films [300, 301, 302, 303, 304], and whole cells [305, 306, 307, 308, 309, 310, 311, 312].

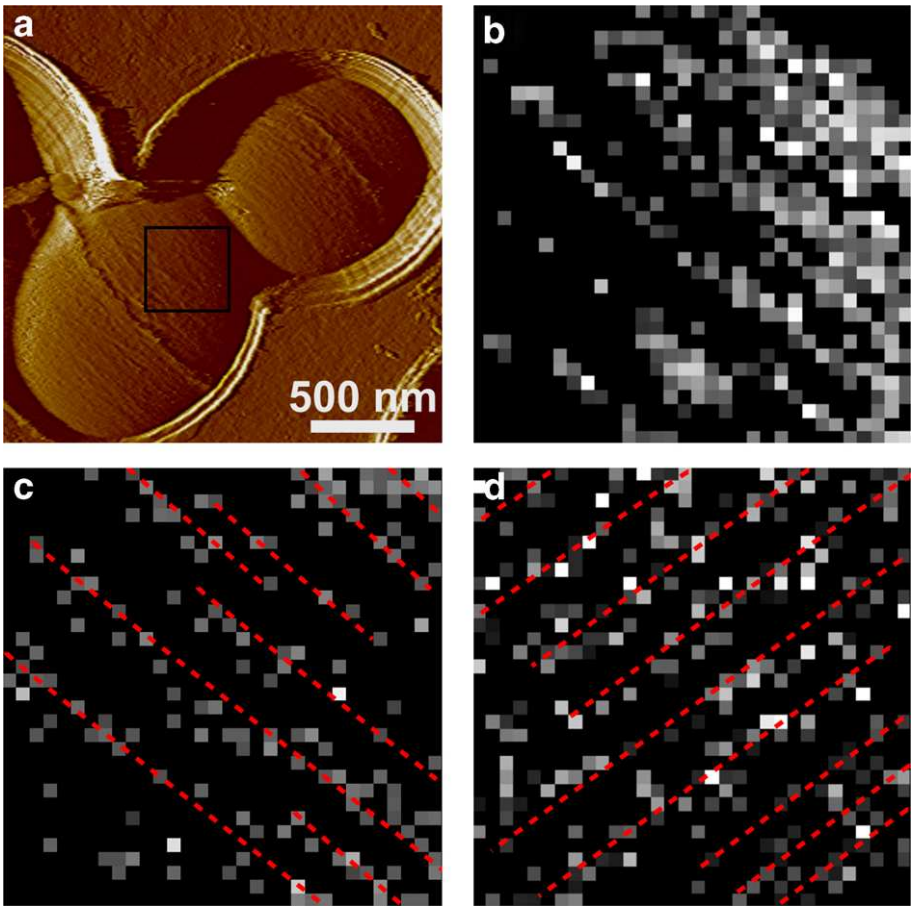

Figure 23. (a) Deflection image taken under a buffer solution of a dividing mutant *Lactococcus lactis* bacterium lacking its exopolysaccharides. (b) Adhesion force map (400×400 nm^2) recorded in the area denoted by the square in (a). (c, d) Adhesion force maps (500×500 nm^2) of another cell, taken of the same area but with the cell rotated by 90° between the two measurements. Bright pixels represent a positive interaction, i.e. adhesion. Dashed red lines are to guide the eye and lie parallel to the short cell axis. All force maps were obtained using a lysin-modified tip and a peak applied force of 250 pN. Reprinted with permission by Macmillan Publishers Ltd: *Nature Communications* from Andre *et al.* [313], copyright 2010

To exemplify the use of AFM tips modified with a biopolymer to explore the location of adhesive moieties on a living cell, work examining a mutant strain of *Lactococcus lactis* bacteria can be considered [313]. This strain lacks the exopolysaccharides that normally coat the wild type of this Gram-positive bacterium and so SFM images and

corresponding force maps were obtained using tips modified with a selectively binding peptidoglycan lysin motif: a recombinant AcmA protein cell wall-binding domain [314]. Using this chemically modified tip, localized distributions of peptidoglycan molecules (which give bacteria structural integrity and are a substantial component of the mass of lactococci) in lines parallel to the septum of the dividing bacterium were identified (Figure 23). The lines were still visible upon rotation of the cell by 90°, illustrating that the lines are a feature of the cell and not caused by imaging artefacts. Selectivity of adhesion was confirmed by adding unbound peptidoglycan to the imaging media and taking another force map, which revealed few adhesion events. Similar specific force mapping has recently been applied in studies of a wide range of substrates with biological relevance, including the presence of microRNA in neuron cells [315], the orientation and arrangement of P1 adhesin on *Streptococcus mutans* [316], biofilm-forming properties in genetic mutants of *Candida albicans* [317], clustering of adhesins on pathogenic bacterium *Bordetella pertussis* [318], and collagen-binding activity on *Staphylococcus epidermidis* [319].

While force mapping provides a wealth of spatially resolved information about the adhesion between the probe and the sample, it is important to consider that the magnitude and distance from the sample surface at which binding events occur is dependent on the selected experimental conditions (including the applied force, and probe speed and spring constant) [320, 321], so they must be selected with care and caution should be used in any direct comparisons of force spectroscopy data.

4.2. Dynamic force spectroscopy

Dynamic force spectroscopy [323, 324] offers a a means of exploring molecular binding without spatial resolution, but with an appreciation of the impact that the probe settings have upon the binding energetics of the system: measuring molecular interactions as a function of *loading rate* [325, 326]. This allows a measurement of the strength of molecular interactions and a determination of binding constants. To exemplify the utility of dynamic force spectroscopy, the interaction of mucins with molecules from a bacterial surface will be used. Mucins are glycoproteins with different biological functions involving the immune system, where they attach to pathogens, or in the lubrication of epithelial cells [327]. Their presence can also be used in cancer diagnosis [328]. The important question that follows is with which molecules on the cell surface are the mucins interacting, and what components in the mucin participate in that interaction. Much is known about what molecules are contained on the cell surface, and it is possible to harvest many of these to coat a surface, or an AFM tip, as in the example presented here. In Figure 24 data describing the interaction of a mucin with soybean agglutinin (SBA), a carbohydrate-binding protein (lectin) are presented [322]. In this case, the mucin, which will be referred to herein by the authors' abbreviation of TnPSM (which abbreviates a modified porcine submaxillary mucin, which is secreted from the salivary glands of pigs), was attached to an AFM tip and the SBA attached to

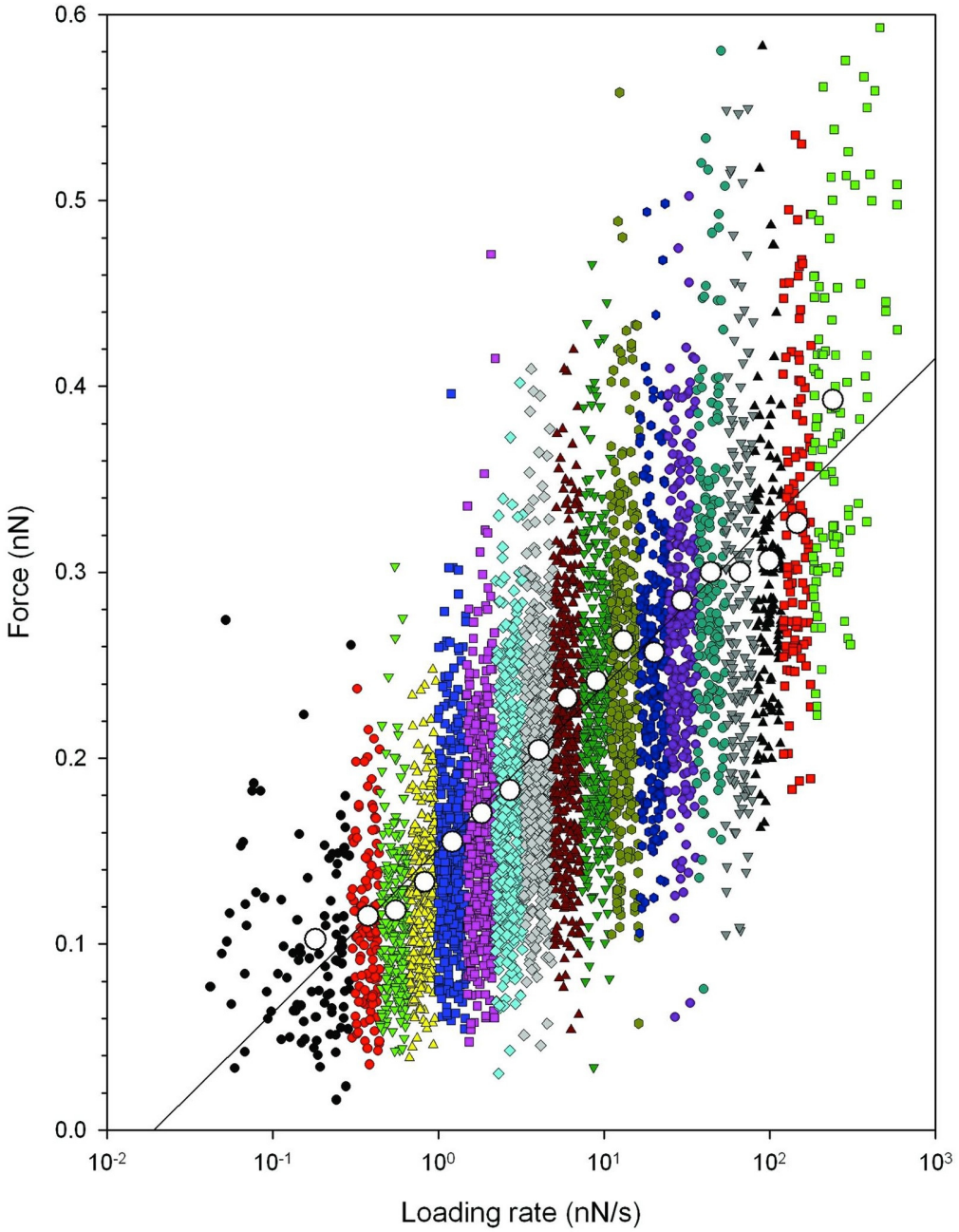

Figure 24. Dynamic force spectroscopy data for the unbinding of a mucin with soybean agglutinin. The large circles along the fit to the data (solid line) represent the most probable binding force, which is deduced from fitting to the statistical data. Reprinted with permission from Sletmoen *et al.* [322]. Copyright (2009) John Wiley and Sons

a mica surface. As the mucin was pulled away from the SBA, multiple binding events were observed over the length of the mucin chain, which supported an earlier model that proposed such "binding and jumping" events for this system [329].

The AFM can pull the polymer at different loading rates, and the force required

to break these bonds (i.e. to unbind) is very much dependent upon the speed of the tip [330], since slower speeds correlate with a smaller loading rate. Slower loading rates allow the polymer to explore a broader energy landscape and so there is more chance of the polymer unbinding. Correspondingly, faster loading rates require a larger force to unbind. Dynamic force spectroscopy allows the calculation of thermodynamic energies of binding, and also the size (in nm) of the potential barrier over which the binding takes place.

Analysis of dynamic force spectroscopy data is typically based upon a modified Bell-Evans model [331, 332, 333], with the theory described in detail elsewhere [324, 320, 334, 335, 336, 337]. In brief, an unbinding force, F, is applied to the bond, reducing the energy of the potential barrier, E by Fx_b, where x_b is the distance between the potential minimum and the potential barrier, along the direction of the applied force. The lifetime of the bond is dependent on the potential barrier height [333], and therefore the probability of the bond breaking under the applied unbinding force is dependent on the size of the applied force (as the barrier energy effectively becomes smaller when larger forces are applied). In the Bell-Evans model, at a constant loading rate, the probability distribution of the unbinding force, P, is described as

$$P = P_\mathrm{n} \exp\left(\frac{(F - F^*)x_\mathrm{b}}{k_\mathrm{B}T}\right) \exp\left[1 - \exp\left(\frac{(F - F^*)x_\mathrm{b}}{k_\mathrm{B}T}\right)\right], \tag{11}$$

where F^* is the most frequent rupture force and P_n is a normalization constant. F^* can be obtained from the histogram of measured unbinding forces obtained at a given loading rate, and is linearly dependent on the logarithm of the loading rate, $\mathrm{d}F/\mathrm{d}t$ by

$$F^* = \frac{k_\mathrm{B}T}{x_\mathrm{b}}\left[\ln\frac{\mathrm{d}F}{\mathrm{d}t} + \ln\left(\frac{\tau_\mathrm{b}x_\mathrm{b}}{k_\mathrm{B}T}\right)\right], \tag{12}$$

where τ_b is the lifetime of the molecular bond [324, 335, 337]. Following from Equation 12, the width of the potential barrier can be obtained from the gradient of the relationship between F^* and $\ln\dot{F}$, since the slope is proportional to x_b^{-1}. In the example shown in Figure 24, the potential energy barrier is of width 0.1 nm, which is quite small, and the lifetime of the interaction between the mucin and the SBA was determined to be more than 1 s, which is long. It was concluded in this case that the SBA was able to move along the TnPSM some distance before detaching. Clearly therefore, dynamic force spectroscopy reveals quite sophisticated biological information from a relatively simple experiment, and has been used in a wide range of biologially-relevant fields, including work with yeast [338], embryonic zebrafish cells [339], lipid bilayers [340] and proteins [341, 342]. The technique is also finding utility in synthetic polymer systems [22, 343, 344, 345] and can be undertaken in parallel with other high sensitivity force-measuring tools such as optical tweezers [346].

4.3. Protein adsorption to surfaces

Whereas force mapping and dynamic force spectroscopy are employed to understand and characterize molecular binding in detail, the use of the QCM-D to interrogate

molecular binding is appropriate in cases where the specifics of bond formation are not required, but where adsorption rates of different molecules are of importance, or where the viscoelastic or conformational properties of molecules forming an adsorbed layer are of interest.

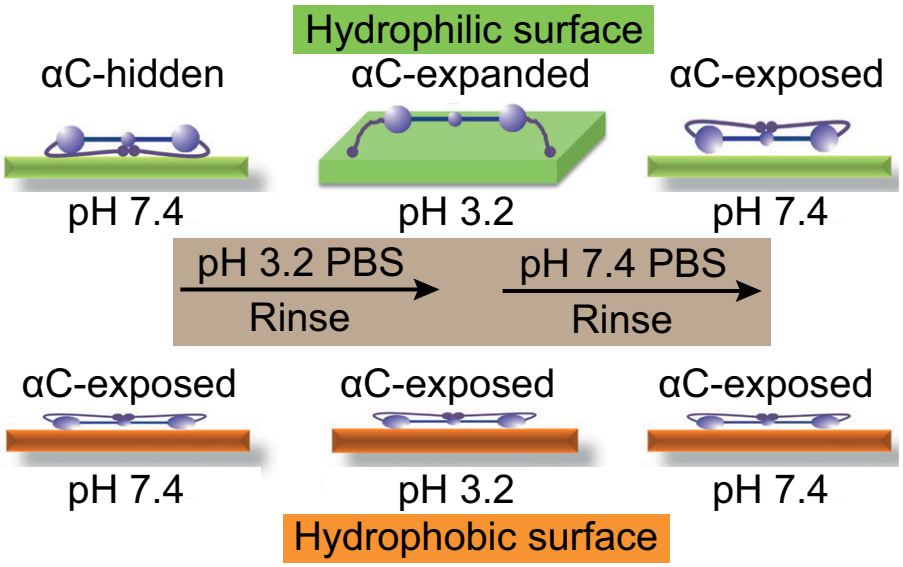

Figure 25. Differing conformation of adsorbed fibrinogen on hydrophilic (top) and hydrophobic (bottom) surfaces as a result of pH cycling, showing the transformation to an αC-exposed conformation for fibrinogen adsorbed to a hydrophilic surface following a wash at pH 3.2. Note the more collapsed conformation of fibrinogen on the hydrophobic surface, where the positively-charged αC domains remain exposed to the buffer solution (PBS) irrespective of pH. Adapted with permission from Hu *et al.* [347]. Copyright (2016) American Chemical Society

4.3.1. The effect of environmental conditions on adsorbed protein layers. By probing a population of like molecules, the QCM-D can be applied to intricate scientific questions, such as the effect of pH on the orientation of adsorbed molecules. Fibrinogen has been shown to alter its conformation on hydrophilic but not hydrophobic surfaces as a result of cycling the pH of the buffer solution flowed over the sensor (Figure 25) [347]. αC domains are largely globular regions of fibrinogen, of which there are two in each protein [348]. The terminus of the molecule is positively charged at physiological pH (7.4), resulting in a "folded"-type conformation where they interact with a negatively-charged central region (E domain). On a negatively-charged hydrophilic silica test surface, when adsorbed at pH 7.4, fibrinogen presents an "αC-hidden" orientation due to a combination of the positive charge of the αC domain at pH 7.4 and its hydrophilic nature relative to the other domains on the fibrinogen. In platelet adhesion experiments on this fibrinogen-coated surface, few platelets were found adhered to the surface, and those that were adsorbed had a non-activated appearance. By adsorbing fibrinogen at pH 7.4 then cycling the buffer pH down to 3.2 and back to 7.4, its conformation was

modified, becoming "αC-exposed" (Figure 25). Platelet adhesion experiments on this surface showed increased platelet adherence and activation. This conformation change is due to the charge of the E domain at lower pH: it holds a positive charge at pH 3.2 and therefore electrostatic repulsion occurs between it and the two αC domains. The fibrinogen molecule therefore unfolds, adopting an extended conformation which leads to an increase in the rigidity of the adsorbed layer. When the pH is returned to pH 7.4, the E domain regains a negative charge and attracts the αC domains, re-folding the fibrinogen. However, the side nearest the surface is no longer accessible due to the associated unfavourable entropic cost, and so the αC domains re-bind on top of the molecule, resulting in the αC-exposed conformation.

On the hydrophobic surface, the fibrinogen tends to adsorb with the αC domains uppermost due to the substantially more hydrophobic nature of the other domains on the molecule, meaning that it is αC-exposed even at pH 7.4. The combined hydrophobic interactions along the molecule are so strong that the fibrinogen forms a very thin layer (1.3 nm compared to 3.3 nm for the layer adsorbed to the hydrophilic surface), suggesting that it might have become denatured as a result of the strong interactions [347]. This type of experiment illustrates that QCM-D can play a role in the interrogation of biomolecule-surface interactions beyond simple mass adsorption, with the mass, thickness and viscoelasticity of the adsorbed material bringing new insights to the understanding of molecule–surface interactions and the effect of environment on the behaviour of adsorbed molecules.

Similarly, detailed QCM-D analysis can be used to explore the interaction of water with molecules at the test surface, and the influence of molecular architecture upon that interaction, such as in the case of synthetic hydrophilic random and block copolymers on different nanocellulose fibril-coated surfaces, which explored the possibility of water expulsion from the interface as a result of copolymer deposition and the driving forces behind that interaction (in this case, predicted to be of an electrostatic nature) [349]. In some cases this too can be linked to pH responsivity, such as in the case of mycolic acid monolayers [109].

4.3.2. Preventing protein adsorption. Protein adsorption is significant in large part due to the formation of largely unwanted biofilms which can lead to health issues. These areas include sanitation i.e. biofilm formation in water delivery systems; and medicine and dentistry, such as infection caused by bacterial colony formation on the teeth and post-surgical implant-related complications. Interface engineering can help prevent protein adsorption, either by making it energetically unfavourable or by out-competing the unwanted protein with a less damaging alternative. Water-soluble polymers are the basis for protein-resistant surfaces because they can remain solvated, which makes it more difficult for proteins to adsorb. This field is large and there are already substantial reviews [350, 351, 352, 353]. Here, examples are limited to those that exemplify the use of the QCM-D.

The fouling of surfaces is of much more than academic interest, and QCM-D can

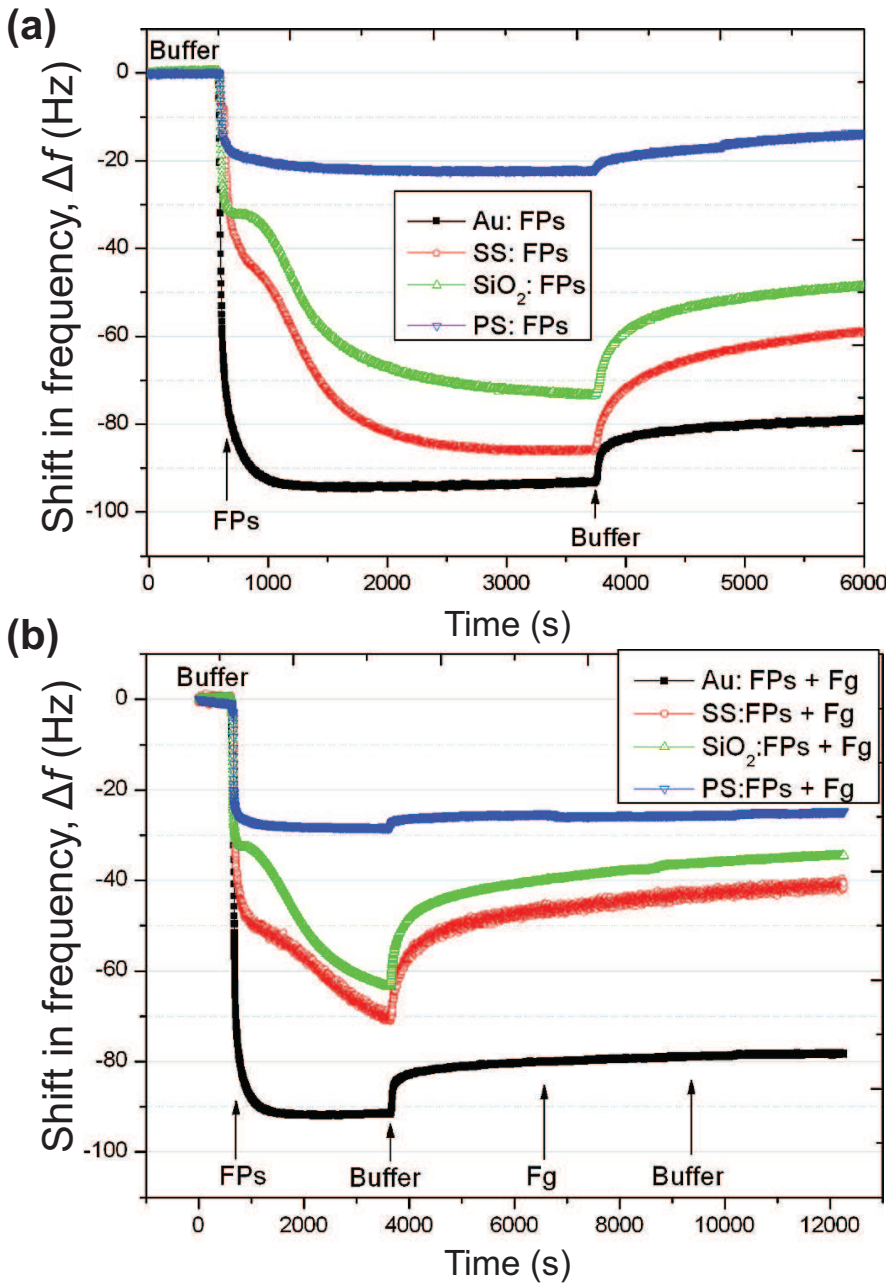

Figure 26. (a) QCM-D adsorption profiles for fish protein extract on four different surfaces. Reduced frequency is associated with increased mass adsorbed (see Section 2.1.5). (b) QCM-D adsorption profiles for fibrinogen (Fg) on different surfaces after preadsorption of fish protein extract. Reprinted with permission from Pillai *et al.* [354]. Copyright (2009) American Chemical Society

be used to assess unwanted tissue growth on implants or other medical devices. For example, in the assessment of the use of an aqueous fish protein extract (FPE) to prevent non-specific fibrinogen adhesion to a range of surfaces [354]. Experiments were performed both by preadsorbing FPE to the substrates then adding a test protein (Figure 26b), and adding FPE after the adsorption of test proteins to check for its

ability to out-compete previously attached molecules. Of the four substrates used (gold (Au), stainless steel (SS), silicone dioxide (SiO_2) and polystyrene (PS)), FPE was shown to adsorb most effectively to gold, while polystyrene exhibited the least FPE adsorption (Figure 26a). These surfaces are different and it is difficult to fully explain the adsorption behaviour. For example, the limited adsorption on polystyrene is likely to be due to a combination of the smoothness of the polystyrene compared to the other surfaces, and its hydrophobicity. Increased surface hydrophobicity means that the adsorbed proteins may have a smaller, more collapsed, conformation; the entropic penalty of water being close to the sample surface results in the proteins being less hydrated. (This depends on the relative balance of interactions between polymer, fluid, and surface.) In contrast, more hydrophilic silicon oxide, gold, and stainless steel surfaces encourage protein swelling, enabling a more elongated polymer conformation and allowing easier diffusion towards the surface.

Adsorbed FPE was effective at preventing fibrinogen adsorption (Figure 26b), but less so human serum albumin (HSA). HSA is comparatively small, which may allow it to exploit any gaps in the adsorbed FPE layer (there is also a lower entropic cost to stretch a small chain towards a surface compared to a long one e.g. HSA compared to fibrinogen) [354]. It was also shown that the orientation of FPE in the adsorbed layer did not affect the repellant properties, irrespective of test protein. This independence of adsorption blocking and molecular arrangement in the layer indicates that steric repulsion is the main contributor to the repulsion and so is independent of substrate. The post-fibrinogen/HSA FPE addition experiments showed that FPE is able to replace pre-adsorbed HSA and fibrinogen, indicating that the interfacial energy is comparatively lower for an FPE coating than for fibrinogen or HSA.

Of the four substrates tested, the three hydrophilic surfaces showed more FPE loss upon rinsing (Figure 26a), suggesting that the more hydrated proteins are less strongly bound than those on the polystyrene. Consideration of the dissipation confirmed this by suggesting that the protein on the hydrophilic surfaces exhibited more viscoelastic (hydrated) behaviour. The observed differences in levels of FPE on the contrasting surfaces could be at least partly explained by the amount of water close to the surface and involved in protein swelling [354]. Here, however, is an example of the compromises involved in such experiments. The higher energy hydrophilic surfaces are not expected to have many contact points with the proteins, but where they exist, it is quite possible that they are very adhesive. The hydrophobic surfaces are unlikely to have strong contacts, but the number of these contacts ensures that the proteins remain bound to the surface. In the case of these experiments, the hydrophobic surfaces retained more protein than the hydrophilic ones after rinsing, but a true test of how strongly the proteins are bound would require direct measurements using, for example, SMFS. The benefit of this combined approach is becoming more widely appreciated, with SMFS being employed increasingly in partnership with QCM-D measurements. This enables bulk behaviour to be linked to the adhesion strength of individual molecules and individual binding sites along the length of a single molecule [355, 356, 357]. An example of this is the

interaction of 16 amino acid-long random coil peptides with different inorganic surfaces, where a positive trend was observed between the total mass uptake as measured with QCM-D and the single molecule adhesion force on the same test substrate [358].

The creation of protein-resistant surfaces is directed towards retarding adsorption rather than stopping it; ultimately resistance is futile and surfaces will be coated. QCM-D remains an attractive technique for the study of the growth of biofilms in order to help address the mechanism of formation. The formation of biofilms is ubiquitous but different processes occur as the bacteria attach to the surface from an initial deposition to a final virtually immovable film. The early stages of this process are notoriously complex and can be followed in real time using QCM-D [359]. Considerable effort is devoted to the preparation of hydrophilic protein-resistant surfaces [351, 360, 361, 362], and it is also possible to convey protein resistance to hydrophobic polymers, by decorating them with hydrophilic side chains [363, 364].

5. Conclusions

The importance of polymers at surfaces and interfaces has developed over the past thirty years from fundamental concepts to being applied in different technologies for coatings, lubrication, and electronics amongst others. The state-of-the-art has developed to include non-uniform structured surfaces and, particularly, biomaterials. Despite impressive developments, many areas of polymer surface science still remain unclear. The role of surfaces in crystallization is still the subject of much research, as is the effect of aging on thin films. However, whereas twenty years ago, much of our understanding of polymer films was achieved by the use of depth profiling techniques, today it is atomic force microscopy-based techniques that provide much of our information. In this review the use of force spectroscopy in particular has been highlighted. Here, polymers in inaccessible environments can be interrogated. This is of great utility in our understanding of living cells. The ability to quantify specific interactions, and measure their strength in media that work as a proxy for real-world environments is particularly important.

The outlook is difficult to predict given the rapid progress made in biopolymers at surfaces as well as polymer electronics over the past twenty years. However, controlling the behaviour of polymers at surfaces will receive substantial attention, with significant effort dedicated to specific interactions. This is not limited to biological materials, because it is also important in patterning technologies. The solution to the longstanding problems of crystallization and other areas such as the polymer glass transition [365] may be closer in the coming years, but it is very likely that a paradigm shift in understanding would be required, after which case future developments will arrive at a very rapid pace.

Acknowledgement

ARH is grateful to the Engineering and Physical Sciences Research Council for the provision of a doctoral studentship. Simone Napolitano, Guido Panzarasa, and Günter Reiter are acknowledged for the provision of data.

References

[1] M Geoghegan and G Krausch. Wetting at polymer surfaces and interfaces. *Prog. Polym. Sci.*, 28:261–302, 2003.

[2] G Krausch. Surface induced self assembly in thin polymer films. *Mater. Sci. Eng. R*, 14:1–94, 1995.

[3] C J van Oss, R J Good, and M K Chaudhury. The role of van der Waals forces and hydrogen bonds in "hydrophobic interactions" between biopolymers and low energy surfaces. *J. Colloid Interface Sci.*, 111:378–390, 1986.

[4] R R Netz and D Andelman. Neutral and charged polymers at interfaces. *Phys. Rep.*, 380:1–95, 2003.

[5] S Reich and Y Cohen. Phase separation of polymer blends in thin films. *J. Polym. Sci.: Polym. Phys. Ed.*, 19:1255–1267, 1981.

[6] Q S Bhatia, D H Pan, and J T Koberstein. Preferential surface adsorption in miscible blends of polystyrene and poly(vinyl methyl ether). *Macromolecules*, 21:2166–2175, 1988.

[7] P J Flory. *Principles of Polymer Chemistry*. Cornell University Press, Ithaca, 1953.

[8] P-G de Gennes. *Scaling Concepts in Polymer Physics*. Cornell University Press, Ithaca, 1979.

[9] M Rubinstein and R H Colby. *Polymer Physics*. Oxford University Press, Oxford, 2003.

[10] J W Cahn. Critical point wetting. *J. Chem. Phys.*, 66:3667–3672, 1977.

[11] I Schmidt and K Binder. Model calculations for wetting transitions in polymer mixtures. *J. Physique*, 46:1631–1644, 1985.

[12] R A L Jones, E J Kramer, M H Rafailovich, J Sokolov, and S A Schwarz. Surface enrichment in an isotopic polymer blend film. *Phys. Rev. Lett.*, 62:280–283, 1989.

[13] P C Jukes, S Y Heriot, J S Sharp, and R A L Jones. Time-resolved light scattering studies of phase separation in thin film semiconducting polymer blends during spin-coating. *Macromolecules*, 38:2030–2032, 2005.

[14] S Y Heriot and R A L Jones. An interfacial instability in a transient wetting layer leads to lateral phase separation in thin spin-cast polymer-blend films. *Nature Mater.*, 4:782–786, 2005.

[15] M Souche and N Clarke. Interfacial instability in bilayer films due to solvent evaporation. *Eur. Phys. J. E*, 28:47–55, 2009.

[16] P Mokarian-Tabari, M Geoghegan, J R Howse, S Y Heriot, R L Thompson, and R A L Jones. Quantitative evaluation of evaporation rate during spin-coating of polymer blend films: Control of structure through defined-atmosphere solvent-casting. *Eur. Phys. J. E*, 33:1829–1839, 2010.

[17] S Ebbens, R Hodgkinson, A J Parnell, A Dunbar, S J Martin, P D Topham, N Clarke, and J R Howse. *In situ* imaging and height reconstruction of phase separation processes in polymer blends during spin coating. *ACS Nano*, 5:5124–5131, 2011.

[18] Y Mouhamad, P Mokarian-Tabari, N Clarke, R A L Jones, and M Geoghegan. Dynamics of polymer film formation during spin coating. *J. Appl. Phys.*, 116:123513, 2014.

[19] M Mears, D S Tarmey, and M Geoghegan. Single macromolecule diffusion in confined environments. *Macromol. Rapid Commun.*, 32:1411–1418, 2011.

[20] S A Sukhishvili, Y Chen, J D Mï£¡ller, E Gratton, K S Schweizer, and S Granick. Diffusion of a polymer 'pancake'. *Nature*, 406:146, 2000.

[21] J Zhao and S Granick. Polymer lateral diffusion at the solid liquid interface. *J. Am. Chem. Soc.*, 126:6242–6243, 2004.

[22] P Burgos, Z Zhang, R Golestanian, G J Leggett, and M Geoghegan. Directed single molecule diffusion triggered by surface energy gradients. *ACS Nano*, 3:3235–3243, 2009.

[23] G E Khalil, A M Adawi, A M Fox, A Iraqi, and D G Lidzey. Single molecule spectroscopy of red- and green-emitting fluorene-based copolymers. *J. Chem. Phys.*, 130:044903, 2009.

[24] M J Rust, M Bates, and X Zhuang. Sub-diffraction-limit imaging by stochastic optical reconstruction microscopy (STORM). *Nature Meth.*, 3:793–796, 2006.

[25] N Mullin and J K Hobbs. Direct imaging of polyethylene films at single-chain resolution with torsional tapping atomic force microscopy. *Phys. Rev. Lett.*, 107:197801, 2011.

[26] N Kalashnyk, J T Nielsen, E H Nielsen, T Skrydstrup, D E Otzen, E Lgsgaard, C Wang, F Besenbacher, N C Nielsen, and T R Linderoth. Scanning tunneling microscopy reveals single-molecule insights into the self-assembly of amyloid fibrils. *ACS Nano*, 6:6882–6889, 2012.

[27] L Gross, F Mohn, N Moll, P Liljeroth, and G Meyer. The chemical structure of a molecule resolved by atomic force microscopy. *Science*, 325:1110–1114, 2009.

[28] A D L Humphris, M J Miles, and J K Hobbs. A mechanical microscope: High-speed atomic force microscopy. *Appl. Phys. Lett.*, 86:034106, 2005.

[29] N Kodera, D Yamamoto, R Ishikawa, and T Ando. Video imaging of walking myosin V by high-speed atomic force microscopy. *Nature*, 468:72–76, 2010.

[30] I Raguzin, G Stoychev, M Stamm, and L Ionov. Single molecule investigation of complexes of oppositely charged bottle brushes. *Soft Matter*, 9:359–364, 2013.

[31] X Michalet and S Weiss. Single-molecule spectroscopy and microscopy. *C. R. Phys.*, 3:619–644, 2002.

[32] D A Smith, D J Brockwell, R C Zinober, A W Blake, G S Beddard, P D Olmsted, and S E Radford. Unfolding dynamics of proteins under applied force. *Phil. Trans. R. Soc. London A*, 361:713–730, 2003.

[33] M Hughes and L Dougan. The physics of pulling polyproteins: a review of single molecule force spectroscopy using the AFM to study protein unfolding. *Rep. Prog. Phys.*, 79:076601, 2016.

[34] Y F Dufrêne. Using nanotechniques to explore microbial surfaces. *Nature Rev. Microbiol.*, 2:451–460, 2004.

[35] P F van Hutten, V V Krasnikov, and G Hadziioannou. Role of interfaces in semiconducting polymer optoelectronic devices. In W R Salaneck, K Seki, A Kahn, and J-J Pireaux, editors, *Conjugated Polymer and Molecular Interfaces*, pages 113–152. Marcel Dekker, New York, 2001.

[36] M Grell. Electronic and electro-optic molecular materials and devices. In R W Kelsall, I W Hamley, and M Geoghegan, editors, *Nanoscale Science and Technology*, pages 282–342. Wiley, Chichester, 2005.

[37] M Geoghegan and G Hadziioannou. *Polymer Electronics*. Oxford University Press, Oxford, 2013.

[38] C Groves. Simulating charge transport in organic semiconductors and devices: a review. *Rep. Prog. Phys.*, 80:026502, 2017.

[39] D S Goodsell and A J Olson. Structural symmetry and protein function. *Annu. Rev. Biophys. Biomol. Struct.*, 29:105–153, 2000.

[40] D Lee, O Redfern, and C Orengo. Predicting protein function from sequence and structure. *Nature Rev. Mol. Cell Biol.*, 8:995–1005, 2007.

[41] J N Israelachvili. *Intermolecular and Surface Forces 3rd ed.* Academic Press, Massachusetts, 2011.

[42] W M Dunne. Bacterial adhesion: Seen any good biofilms lately? *Clin. Microbiol. Rev.*, 15:155–166, 2002.

[43] J R Banavar and A Maritan. Physics of proteins. *Annu. Rev. Biophys. Biomol. Struct.*, 36:261–280, 2007.

[44] M Tsutsumi and J M Otaki. Parallel and antiparallel β-strands differ in amino acid composition and availability of short constituent sequences. *J. Chem. Inf. Model.*, 51:1457–1464, 2011.

[45] J R Banavar, T X Hoang, F Seno, A Trovato, and A Maritan. Protein sequence and structure:

Is one more fundamental than the other? *J. Stat. Phys.*, 148:637–646, 2012.

[46] J C Vickerman. *Surface Analysis — The Principal Techniques*. Wiley, Chichester, 1997.

[47] A B Rodríguez, M M Voigt, S J Martin, T J Whittle, R M Dalgliesh, R L Thompson, D G Lidzey, and M Geoghegan. Structure of films of poly(3,4-ethylene dioxythiophene)-poly(styrene sulfonate) crosslinked with glycerol. *J. Mater. Chem.*, 21:19324–19330, 2011.

[48] T Nyberg. An alternative method to build organic photodiodes. *Synth. Met.*, 140:281–286, 2004.

[49] F Zhang, M Johansson, M R Andersson, J C Hummelen, and O Inganäs. Polymer photovoltaic cells with conducting polymer anodes. *Adv. Mater.*, 14:662–665, 2002.

[50] G Greczynski, T Kugler, and W R Salaneck. Characterization of the pedot-pss system by means of x-ray and ultraviolet photoelectron spectroscopy. *Thin Solid Films*, 354:129–135, 1999.

[51] P C Jukes, S J Martin, A M Higgins, M Geoghegan, R A L Jones, S Langridge, A Wehrum, and S Kirchmeyer. Controlling the surface composition of poly(3,4-ethylene dioxythiophene)-poly(styrene sulfonate) blends by heat treatment. *Adv. Mater.*, 16:807–811, 2004.

[52] J Y Lim, J C Hansen, C A Siedlecki, R W Hengstebeck, J Cheng, N Winograd, and H J Donahue. Osteoblast adhesion on poly(L-lactic acid)/polystyrene demixed thin film blends: effect of nanotopography, surface chemistry, and wettability. *Biomacromolecules*, 6:3319–3327, 2005.

[53] R G Harrison. The reaction of embryonic cells to solid structures. *J. Expt. Zool.*, 17:521–544, 1914.

[54] H N Kim, A Jiao, N S Hwang, M S Kim, D H Kang, D H Kim, and K-Y Suh. Nanotopography-guided tissue engineering and regenerative medicine. *Adv. Drug Deliv. Rev.*, 65:536–558, 2013.

[55] S N Magonov and D H Reneker. Characterization of polymer surfaces with atomic force microscopy. *Annu. Rev. Mater. Sci.*, 27:175–222, 1997.

[56] A Knoll, R Magerle, and G Krausch. Tapping mode atomic force microscopy on polymers: Where is the true sample surface? *Macromolecules*, 34:4159–4165, 2001.

[57] G Amontons. De la resistance causée dans les machines. *Hist. Acad. R. Sci.*, pages 206–227, 1699.

[58] G J Leggett, N J Brewer, and K S L Chong. Friction force microscopy: towards quantitative analysis of molecular organisation with nanometre spatial resolution. *Phys. Chem. Chem. Phys.*, 7:1107–1120, 2005.

[59] T Kajiyama, K Tanaka, N Satomi, and A Takahara. Surface relaxation process of monodisperse polystyrene film based on lateral force microscopic measurements. *Macromolecules*, 31:5150–5151, 1998.

[60] M Raftari, Z J Zhang, S R Carter, G J Leggett, and M Geoghegan. Nanoscale contact mechanics between two grafted polyelectrolyte surfaces. *Macromolecules*, 48:6272–6279, 2015.

[61] A Cadby, G Khalil, A M Fox, and D G Lidzey. Mapping exciton quenching in photovoltaic-applicable polymer blends using time-resolved scanning near-field optical microscopy. *J. Appl. Phys.*, 103:093715, 2008.

[62] P Vettiger, M Despont, U Drechsler, U Durig, W Haberle, MI Lutwyche, H E Rothuizen, R Stutz, R Widmer, and G K Binnig. The "millipede" — more than one thousand tips for future AFM data storage. *IBM J. Res. Dev.*, 44:323–340, 2000.

[63] E ul Haq, Z Liu, Y Zhang, S A Alang Ahmad, L-S Wong, S P Armes, J K Hobbs, G J Leggett, J Micklefield, C J Roberts, and J M R Weaver. Parallel scanning near-field photolithography: The Snomipede. *Nano Lett.*, 10:4375–4380, 2010.

[64] F Huo, G Zheng, X Liao, L R Giam, J Chai, X Chen, W Shim, and C A Mirkin. Beam pen lithography. *Nature Nanotech.*, 5:637–640, 2010.

[65] Z Zhang, M R Tomlinson, R Golestanian, and M Geoghegan. The interfacial behaviour of single poly(*N*,*N*-dimethylacrylamide) chains as a function of pH. *Nanotechnology*, 19:035505, 2008.

[66] W Zhang and X Zhang. Single molecule mechanochemistry of macromolecules. *Prog. Polym. Sci.*, 28:1271–1295, 2003.

[67] S Minko and Y Roiter. AFM single molecule studies of adsorbed polyelectrolytes. *Curr. Opin. Colloid Interface Sci.*, 10:9–15, 2005.

[68] R Merkel. Force spectroscopy on single passive biomolecules and single biomolecular bonds. *Phys. Rep.*, 346:343–385, 2001.

[69] M I Giannotti and G J Vancso. Interrogation of single synthetic polymer chains and polysaccharides by AFM-based force spectroscopy. *ChemPhysChem*, 8:2290–2307, 2007.

[70] T A Camesano, Y Liu, and M Datta. Measuring bacterial adhesion at environmental interfaces with single-cell and single-molecule techniques. *Adv. Water Resour.*, 30:1470–1491, 2007.

[71] M Hermansson. The dlvo theory in microbial adhesion. *Colloids Surf. B*, 14:105–119, 1999.

[72] T A Camesano and B E Logan. Probing bacterial electrosteric interactions using atomic force microscopy. *Environ. Sci. Technol.*, 34:3354–3362, 2000.

[73] N I Abu-Lail and T A Camesano. Role of ionic strength on the relationship of biopolymer conformation, DLVO contributions, and steric interactions to bioadhesion of *Pseudomonas putida* KT2442. *Biomacromolecules*, 4:1000–1012, 2003.

[74] L S Dorobantu, S Bhattacharjee, Julia M Foght, and M R Gray. Analysis of force interactions between afm tips and hydrophobic bacteria using dlvo theory. *Langmuir*, 25:6968–6976, 2009.

[75] J M Thwala, M Li, M C Y Wong, S Kang, E M V Hoek, and B B Mamba. Bacteria–polymeric membrane interactions: Atomic force microscopy and XDLVO predictions. *Langmuir*, 29:13773–13782, 2013.

[76] G Francius, R Henry, J F L Duval, E Bruneau, J Merlin, A Fahs, and N Leblond-Bourget. Thermo-regulated adhesion of the *Streptococcus thermophilus δrgg0182* strain. *Langmuir*, 29:4847–4856, 2013.

[77] Y Chen, H J Busscher, H C van der Mei, and W Norde. Statistical analysis of long- and short-range forces involved in bacterial adhesion to substratum surfaces measured using afm. *Appl. Environ. Microbiol.*, 77:5065–5070, 2011.

[78] J Ubbink and P Schär-Zammaretti. Probing bacterial interactions: integrated approaches combining atomic force microscopy, electron microscopy and biophysical techniques. *Micron*, 36:293–320, 2005.

[79] P Polyakov, C Soussen, J Duan, J F L Duval, D Brie, and G Francius. Automated force volume image processing for biological samples. *PLoS One*, 6:e18887, 2011.

[80] T A Camesano and N I Abu-Lail. Heterogeneity in bacterial surface polysaccharides, probed on a single-molecule basis. *Biomacromolecules*, 3:661–667, 2002.

[81] M Castelain, E Koutris, M Andersson, K Wiklund, O Björnham, S Schedin, and O Axner. Characterization of the biomechanical properties of T4 pili expressed by *Streptococcus pneumoniae*—a comparison between helix-like and open coil-like pili. *ChemPhysChem*, 10:1533–1540, 2009.

[82] C Bustamante, J F Marko, E D Siggia, and S Smith. Entropic elasticity of λ-phage DNA. *Science*, 265:1599–1600, 1994.

[83] Y Muroga, T Yoshida, and S Kawaguchi. Conformation of poly(methacrylic acid) in acidic aqueous solution studied by small angle X-ray scattering. *Biophys. Chem.*, 81:45–57, 1999.

[84] A J Parnell, S J Martin, C C Dang, M Geoghegan, R A L Jones, C J Crook, J R Howse, and A J Ryan. Synthesis, characterization and swelling behaviour of poly(methacrylic acid) brushes synthesized using atom transfer radical polymerization. *Polymer*, 50:1005–1014, 2009.

[85] N I Abu-Lail and T A Camesano. Elasticity of *Pseudomonas putida* kt2442 surface polymers probed with single-molecule force microscopy. *Langmuir*, 18:4071–4081, 2002.

[86] B H Lower, R Yongsunthon, F P Vallano III, and S K Lower. Simultaneous force and fluorescence measurements of a protein that forms a bond between a living bacterium and a solid surface. *J. Bacteriol.*, 187:2127–2137, 2005.

[87] M Diao, E Taran, S Mahler, T A H Nguyen, and A V Nguyen. Quantifying adhesion of acidophilic bioleaching bacteria to silica and pyrite by atomic force microscopy with a bacterial probe. *Colloids Surf. B*, 115:229–236, 2013.

[88] Y Hu, J Ulstrup, J Zhang, S Molin, and V Dupres. Adhesive properties of *Staphylococcus epidermidis* probed by atomic force microscopy. *Phys. Chem. Chem. Phys.*, 13:9995–10003,

2011.

[89] J Struckmeier, R Wahl, M Leuschner, J Nunes, H Janovjak, U Geisler, G Hofmann, T Jähnke, and D J Müller. Fully automated single-molecule force spectroscopy for screening applications. *Nanotechnology*, 19:384020, 2008.

[90] S Yamamoto, Y Tsujii, and T Fukuda. AFM study of stretching a single polymer chain in a polymer brush. *Macromolecules*, 33:5995–5998, 2000.

[91] S Al-Maawali, J E Bemis, B B Akhremitchev, R Leecharoen, B G Janesko, and G C Walker. Study of the polydispersity of grafted poly(dimethylsiloxane) surfaces using single-molecule atomic force microscopy. *J. Phys. Chem. B*, 105:3965–3971, 2001.

[92] D Goodman, J N Kizhakkedathu, and D E Brooks. Molecular weight and polydispersity estimation of adsorbing polymer brushes by atomic force microscopy. *Langmuir*, 20:3297–3303, 2004.

[93] D Goodman, J N Kizhakkedathu, and D E Brooks. Evaluation of an atomic force microscopy pull-off method for measuring molecular weight and polydispersity of polymer brushes: Effect of grafting density. *Langmuir*, 20:6238–6245, 2004.

[94] S Cuenot, S Gabriel, R Jérôme, C Jérôme, C-A Fustin, A M Jonas, and A-S Duwez. First insights into electrografted polymers by AFM-based force spectroscopy. *Macromolecules*, 39:8428–8433, 2006.

[95] A AL-Baradi, M R Tomlinson, Z J Zhang, and M Geoghegan. Determination of the molar mass of surface-grafted weak polyelectrolyte brushes using force spectroscopy. *Polymer*, 67:111–117, 2015.

[96] J D Willott, T J Murdoch, G B Webber, and E J Wanless. Nature of the specific anion response of a hydrophobic weak polyelectrolyte brush revealed by AFM force measurements. *Macromolecules*, 49:2327–2338, 2016.

[97] T Tischer, R Gralla-Koser, V Trouillet, L Barner, C Barner-Kowollik, and C Lee-Thedieck. Direct mapping of RAFT controlled macromolecular growth on surfaces via single molecule force spectroscopy. *ACS Macro Lett.*, 5:498–503, 2016.

[98] S Tadigadapa and K Mateti. Piezoelectric MEMS sensors: state-of-the-art and perspectives. *Meas. Sci. Technol.*, 20:092001, 2009.

[99] G Gautschi. Background of piezoelectric sensors. In *Piezoelectric Sensorics*, pages 5–11. Springer-Verlag, Berlin, 2002.

[100] K A Marx. Quartz crystal microbalance: A useful tool for studying thin polymer films and complex biomolecular systems at the solution-surface interface. *Biomacromolecules*, 4:1099–1120, 2003.

[101] F Höök, M Rodahl, P Brezezinski, and B Kasemo. Energy dissipation kinetics for protein and antibody - antigen adsorption under shear oscillation on a quartz crystal microbalance. *Langmuir*, 14:729–734, 1998.

[102] F Höök, B Kasemo, T Nylander, C Fant, K Sott, and H Elwing. Variations in coupled water, viscoelastic properties, and film thickness of a Mefp-1 protein film during adsorption and cross-linking: A quartz crystal microbalance with dissipation monitoring, ellipsometry, and surface plasmon resonance study. *Anal. Chem.*, 73:5796–5804, 2001.

[103] E F Irwin, J E Ho, S R Kane, and K E Healy. Analysis of interpenetrating polymer networks via quartz crystal microbalance with dissipation monitoring. *Langmuir*, 21:5529–5536, 2005.

[104] M Rodahl, F Höök, C Fredriksson, C A Keller, A Krozer, P Brzezinski, M Voinova, and B Kasemo. Simultaneous frequency and dissipation factor QCM measurements of biomolecular adsorption and cell adhesion. *Faraday Discuss.*, 107:229–246, 1997.

[105] M Edvardsson, S Svedhem, G Wang, R Richter, M Rodahl, and B Kasemo. QCM-D and reflectometry instrument: Applications to supported lipid structures and their biomolecular interactions. *Anal. Chem.*, 81:349–361, 2009.

[106] K K Kanazawa and J G Gordon. Frequency of a quartz microbalance in contact with liquid. *Anal. Chem.*, 57:1770–1771, 1985.

[107] S Geißler, A Barrantes, P Tengvall, P B Messersmith, and H Tiainen. Deposition kinetics of bioinspired phenolic coatings on titanium surfaces. *Langmuir*, 32:8050–8060, 2016.

[108] A R Ferhan, J A Jackman, and N-J Cho. Integration of quartz crystal microbalance-dissipation and reflection-mode localized surface plasmon resonance sensors for biomacromolecular interaction analysis. *Anal. Chem.*, 88:12524–12531, 2016.

[109] Z Zhang, Y Pen, R G J Edyvean, S A Banwart, R M Dalgliesh, and M Geoghegan. Adhesive and conformational behaviour of mycolic acid monolayers. *Biochim. Biophys. Acta*, 1798:1829–1839, 2010.

[110] J Penfold and R K Thomas. The application of the specular reflection of neutrons to the study of surfaces and interfaces. *J. Phys.: Condens. Matter*, 2:1369–1412, 1990.

[111] T P Russell. X-ray and neutron reflectivity for the investigation of polymers. *Mater. Sci. Rep.*, 5:171–271, 1990.

[112] G Reiter and M Geoghegan. Avantages de la réflectométrie des neutrons pour l'étude des polymères en couches minces. In A Brûlet and G Chaboussant, editors, *École Thématique Surfaces, Interfaces, Milieux Confinés par Diffusion de Neutrons*, volume 8 of *Collection de la Société Française de la Neutronique*, pages 103–113. EDP Sciences, Les Ulis, 2007.

[113] D G Bucknall and J S Higgins. Neutron reflection studies of polymer-polymer interfaces. In H Hommell, editor, *Polymer Surfaces and Interfaces - a Versatile Combination: Recent Research Developments in Polymer Science*, pages 161–199. Research Signpost, Trivandrum, India, 1998.

[114] A Liebmann-Vinson, L M Lander, M D Foster, W J Brittain, E A Vogler, C F Majkrzak, and S Satija. A neutron reflectometry study of human serum albumin adsorption *in situ*. *Langmuir*, 12:2256–2262, 1996.

[115] A Diethert and P Müller-Buschbaum. Probing the near-surface composition profile of pressure sensitive adhesive films with x-ray reflectivity. *J. Adhes.*, 87:1167–1190, 2011.

[116] R Schach, Y Tran, A Menelle, and C Creton. Role of chain interpenetration in the adhesion between immiscible polymer melts. *Macromolecules*, 40:6325–6332, 2007.

[117] R La Spina, M R Tomlinson, L Ruiz-Pérez, A Chiche, S Langridge, and M Geoghegan. Controlling network-brush interactions to achieve switchable adhesion. *Angew. Chem. Int. Ed.*, 46:6460–6463, 2007.

[118] G Sudre, D Hourdet, C Creton, F Cousin, and Y Tran. Probing pH-responsive interactions between polymer brushes and hydrogels by neutron reflectivity. *Langmuir*, 30:9700–9706, 2014.

[119] C White, K T Tan, D Hunston, K Steffens, D L Stanley, S K Satija, B Akgun, and B D Vogt. Mechanisms of criticality in environmental adhesion loss. *Soft Matter*, 11:3994–4001, 2015.

[120] L Alfhaid, R La Spina, M R Tomlinson, A R Hall, W D Seddon, Williams N H, F Cousin, S Gorb, and Geoghegan M. Adhesion between oppositely charged polyelectrolytes. *J. Adhes.*, 93:10.1080/00218464.2016.1265947, 2017.

[121] G Coulon, T P Russell, V R Deline, and P F Green. Surface-induced orientation of symmetric, diblock copolymers: A secondary ion mass spectrometry study. *Macromolecules*, 22:2581–2589, 1989.

[122] S A Schwarz, B J Wilkens, M A A Pudensi, M H Rafailovich, J Sokolov, X Zhao, W Zhao, X Zheng, T P Russell, and R A L Jones. Studies of surface and interface segregation in polymer blends by secondary ion mass spectrometry. *Mol. Phys.*, 76:937–950, 1992.

[123] M Geoghegan. MeV ion beam profiling of polymer surfaces and interfaces. In R W Richards and S K Peace, editors, *Polymer Surfaces and Interfaces III*, pages 43–73. Wiley, Chichester, 1999.

[124] R J Composto, R M Walters, and J Genzer. Application of ion scattering techniques to characterize polymer surfaces and interfaces. *Mater. Sci. Eng. R*, 38:107–180, 2002.

[125] H Geiger and E Marsden. On a diffuse reflection of the α-particles. *Proc. R. Soc. London A*, 82:495–500, 1909.

[126] J F Ziegler, J P Biersack, and U Littmark. *The Stopping Powers and Ranges of Ions in Solids.*

Pergamon Press, New York, 1985.

[127] E L Jablonski, R E Gorga, and B Narasimhan. Interdiffusion and phase behavior at homopolymer/random copolymer interfaces. *Polymer*, 44:729–741, 2003.

[128] P J Mills, C J Palmstrøm, and E J Kramer. Concentration profiles of non-Fickian diffusants in glassy polymers by Rutherford backscattering spectrometry. *J. Mater. Sci.*, 21:1479–1486, 1986.

[129] M S Kunz, K R Shull, and A J Kellock. Colloidal gold dispersions in polymeric matrices. *J. Colloid Interface Sci.*, 156:240–249, 1993.

[130] J Choi, M Cargnello, C B Murray, N Clarke, K I Winey, and R J Composto. Fast nanorod diffusion through entangled polymer melts. *ACS Macro Lett.*, 4:952–956, 2015.

[131] E J Kramer, P Green, and C J Palmstrøm. Interdiffusion and marker movements in concentrated polymer–polymer diffusion couples. *Polymer*, 25:473–480, 1984.

[132] M Geoghegan, R A L Jones, A S Clough, and J Penfold. The morphology of as-cast films of a polymer blend: Dependence on polymer molecular weight. *J. Polym. Sci. B: Polym. Phys.*, 33:1307–1311, 1995.

[133] U K Krieger, T Huthwelker, C Daniel, U Weers, T Peter, and W A Lanford. Rutherford backscattering to study the near-surface region of volatile liquids and solids. *Science*, 295:1048–1050, 2002.

[134] F Mathis, B Moignard, L Pichon, O Dubreuil, and J Salomon. Coupled PIXE and RBS using a 6 MeV $^4He^{2+}$ external beam: A new experimental device for particle detection and dose monitoring. *Nucl. Instr. Meth. B*, 240:532–538, 2005.

[135] T Young. An essay on the cohesion of fluids. *Phil. Trans. R. Soc. London*, 95:65–87, 1805.

[136] Y Xu, M Takai, and K Ishihara. Protein adsorption and cell adhesion on cationic, neutral, and anionic 2-methacryloyloxyethyl phosphorylcholine copolymer surfaces. *Biomaterials*, 30:4930–4938, 2009.

[137] S Farris, L Introzzi, P Biagioni, T Holz, A Schiraldi, and L Piergiovanni. Wetting of biopolymer coatings: Contact angle kinetics and image analysis investigation. *Langmuir*, 27:7563–7574, 2011.

[138] Y Xu, M Takai, and K Ishihara. Phospholipid polymer biointerfaces for lab-on-a-chip devices. *Ann. Biomed. Eng.*, 38:1938–1953, 2010.

[139] H Shahsavan, D Arunbabu, and B Zhao. Biomimetic modification of polymeric surfaces: A promising pathway for tuning of wetting and adhesion. *Macromol. Mater. Eng.*, 297:743–760, 2012.

[140] P G Gezer, S Brodsky, A Hsiao, G L Liu, and J L Kokini. Modification of the hydrophilic/hydrophobic characteristic of zein film surfaces by contact with oxygen plasma treated PDMS and oleic acid content. *Colloids Surf. B*, 135:433–440, 2015.

[141] A E Wiącek, K Terpiłowski, M Jurak, and M Worzakowska. Low-temperature air plasma modification of chitosan-coated PEEK biomaterials. *Polym. Test.*, 50:325–334, 2016.

[142] C-H Lin, Y-H Yeh, W-C Lin, and M-C Yang. Novel silicone hydrogel based on PDMS and PEGMA for contact lens application. *Colloids Surf. B*, 123:986–994, 2014.

[143] M Bianco, V Guarino, G Maruccio, G Galli, E Martinelli, G Montani, R Rinaldi, and V Arima. Non-biofouling fluorinated block copolymer coatings for contact lenses. *Sci. Adv. Mater.*, 7:1387–1394, 2015.

[144] W Cheng, C Yang, X Ding, A C Engler, J L Hedrick, and Y Y Yang. Broad-spectrum antimicrobial/antifouling soft material coatings using poly(ethylenimine) as a tailorable scaffold. *Biomacromolecules*, 16:1967–1977, 2015.

[145] S M Paterson, L Liu, M A Brook, and H Sheardown. Poly(ethylene glycol)-or silicone-modified hyaluronan for contact lens wetting agent applications. *J. Biomed. Mater. Res. A*, 103:2602–2610, 2015.

[146] X Hu and X Gong. A new route to fabricate biocompatible hydrogels with controlled drug delivery behavior. *J. Colloid Interface Sci.*, 470:62–70, 2016.

[147] F Lasowski and H Sheardown. Atropine and roscovitine release from model silicone hydrogels. *Optom. Vis. Sci.*, 93:404–411, 2016.

[148] A Milionis, R Ruffilli, and I S Bayer. Superhydrophobic nanocomposites from biodegradable thermoplastic starch composites (Mater-Bi®), hydrophobic nano-silica and lycopodium spores. *RSC Adv.*, 4:34395–34404, 2014.

[149] J P de Silva, M Geoghegan, A M Higgins, G Krausch, M-O David, and G Reiter. Switching layer stability in a polymer bilayer by thickness variation. *Phys. Rev. Lett.*, 98:267802, 2007.

[150] M Ilton, P Stasiak, M W Matsen, and K Dalnoki-Veress. Quantized contact angles in the dewetting of a structured liquid. *Phys. Rev. Lett.*, 112:068303, 2014.

[151] G Reiter, M Hamieh, P Damman, S Sclavons, S Gabriele, T Vilmin, and E Raphaël. Residual stresses in thin polymer films cause rupture and dominate early stages of dewetting. *Nature Mater.*, 4:754–758, 2005.

[152] A Silberberg. Distribution of conformations and chain ends near the surface of a melt of linear flexible macromolecules. *J. Colloid Interface Sci.*, 90:86–91, 1982.

[153] N Rehse, C Wang, M Hund, M Geoghegan, R Magerle, and G Krausch. Stability of thin polymer films on a corrugated substrate. *Eur. Phys. J. E*, 4:69–76, 2001.

[154] J-U Sommer. About the role of non-equilibrium effects for polymers at surfaces. *Eur. Phys. J. E*, 9:417–419, 2002.

[155] M Geoghegan, C Wang, N Rehse, R Magerle, and G Krausch. Thin polymer films on chemically patterned, corrugated substrates. *J. Phys.: Condens. Matter*, 17:S389–S402, 2005.

[156] R Mukherjee and A Sharma. Instability, self-organization and pattern formation in thin soft films. *Soft Matter*, 11:8717–8740, 2015.

[157] K M Ashley, D Raghavan, J F Douglas, and A Karim. Wetting-dewetting transition line in thin polymer films. *Langmuir*, 21:9518–9523, 2005.

[158] P Damman, S Gabriele, S Coppé, S Desprez, D Villers, T Vilmin, E Raphaël, M Hamieh, S Al Akhrass, and G Reiter. Relaxation of residual stress and reentanglement of polymers in spin-coated films. *Phys. Rev. Lett.*, 99:036101, 2007.

[159] S Al Akhrass, G Reiter, S Y Hou, M H Yang, Y L Chang, F C Chang, C F Wang, and A C-M Yang. Viscoelastic thin polymer films under transient residual stresses: Two stage dewetting on soft substrates. *Phys. Rev. Lett.*, 100:178301, 2008.

[160] P Lambooy, K C Phelan, O Haugg, and G Krausch. Dewetting at the liquid-liquid interface. *Phys. Rev. Lett.*, 76:1110–1113, 1996.

[161] F Brochard Wyart, P Martin, and C Redon. Liquid/liquid dewetting. *Langmuir*, 9:3682–3690, 1993.

[162] R Fetzer, K Jacobs, A Münch, B Wagner, and T P Witelski. New slip regimes and the shape of dewetting thin liquid films. *Phys. Rev. Lett.*, 95:127801, 2005.

[163] O Bäumchen, R Fetzer, M Klos, M Lessel, L Marquant, H Hähl, and K Jacobs. Slippage and nanorheology of thin liquid polymer films. *J. Phys.: Condens. Matter*, 24:325102, 2012.

[164] D Gentili, G Foschi, F Valle, M Cavallini, and F Biscarini. Applications of dewetting in micro and nanotechnology. *Chem. Soc. Rev.*, 41:4430–4443, 2012.

[165] H Sirringhaus, T Kawase, R H Friend, T Shimoda, M Inbasekaran, W Wu, and E P Woo. High-resolution inkjet printing of all-polymer transistor circuits. *Science*, 290:2123–2126, 2000.

[166] J Z Wang, Z H Zheng, H W Li, W T S Huck, and H Sirringhaus. Dewetting of conducting polymer inkjet droplets on patterned surfaces. *Nature Mater.*, 3:171–176, 2004.

[167] Y Xia and G M Whitesides. Soft lithography. *Angew. Chem. Int. Ed.*, 37:550–575, 1998.

[168] H-L Zhang, D G Bucknall, and A Dupuis. Uniform nanoscopic polystyrene patterns produced from a microscopic mold. *Nano Lett.*, 4:1513–1519, 2004.

[169] E Bystrenova, M Facchini, M Cavallini, M G Cacace, and F Biscarini. Multiple length-scale patterning of DNA by stamp-assisted deposition. *Angew. Chem. Int. Ed.*, 45:4779–4782, 2006.

[170] A Verma, S Sekhar, P Sachan, P D S Reddy, and A Sharma. Control of morphologies and length scales in intensified dewetting of electron beam modified polymer thin films under a liquid

solvent mixture. *Macromolecules*, 48:3318–3326, 2015.

[171] N Bhandaru, A Das, and R Mukherjee. Confinement induced ordering in dewetting of ultra-thin polymer bilayers on nanopatterned substrates. *Nanoscale*, 8:1073–1087, 2016.

[172] C K Chiang, C R Fincher Jr, Y W Park, A J Heeger, H Shirakawa, E J Louis, S C Gau, and A G MacDiarmid. Electrical conductivity in doped polyacetylene. *Phys. Rev. Lett.*, 39:1098–1101, 1977.

[173] L Groenendaal, F Jonas, D Freitag, H Pielartzik, and J R Reynolds. Poly(3,4-ethylenedioxythiophene) and its derivatives: past, present, and future. *Adv. Mater.*, 12:481–494, 2000.

[174] Y Xia, K Sun, and J Ouyang. Solution-processed metallic conducting polymer films as transparent electrode of optoelectronic devices. *Adv. Mater.*, 24:2436–2440, 2012.

[175] J Rivnay, R M Owens, and G G Malliaras. The rise of organic bioelectronics. *Chem. Mater.*, 26:679–685, 2014.

[176] D T Simon, E O Gabrielsson, K Tybrandt, and M Berggren. Organic bioelectronics: Bridging the signaling gap between biology and technology. *Chem. Rev.*, 116:13009–13041, 2016.

[177] F So, B Krummacher, M K Mathai, D Poplavskyy, S A Choulis, and V-E Choong. Recent progress in solution processable organic light emitting devices. *J. Appl. Phys.*, 102:091101, 2007.

[178] H Sirringhaus. Device physics of solution-processed organic field-effect transistors. *Adv. Mater.*, 17:2411–2425, 2005.

[179] A M Higgins, S J Martin, R L Thompson, J Chappell, M Voigt, D G Lidzey, R A L Jones, and M Geoghegan. Surface segregation and self-stratification in blends of spin-cast polyfluorene derivatives. *J. Phys.: Condens. Matter*, 17:1319–1328, 2005.

[180] J Morgado, E Moons, R H Friend, and F Cacialli. De-mixing of polyfluorene-based blends by contact with acetone: Electro- and photo-luminescence probes. *Adv. Mater.*, 13:810–814, 2001.

[181] M Voigt, J Chappell, T Rowson, A Cadby, M Geoghegan, R A L Jones, and D G Lidzey. The interplay between the optical and electronic properties of light-emitting-diode applicable conjugated polymer blends and their phase-separated morphology. *Org. Electron.*, 6:35–45, 2005.

[182] H W Ro, B Akgun, B T O'Connor, M Hammond, R J Kline, C R Snyder, S K Satija, A L Ayzner, M F Toney, C L Soles, and D M DeLongchamp. Poly(3-hexylthiophene) and [6,6]-phenyl-C-butyric acid methyl ester mixing in organic solar cells. *Macromolecules*, 45:6587–6599, 2012.

[183] D Deribew, E Pavlopoulou, G Fleury, C Nicolet, C Renaud, S-J Mougnier, L Vignau, E Cloutet, C Brochon, F Cousin, G Portale, M Geoghegan, and G Hadziioannou. Crystallization-driven enhancement in photovoltaic performance through block copolymer incorporation into P3HT:PCBM blends. *Macromolecules*, 46:3015–3024, 2013.

[184] M Brinkmann. Structure and morphology control in thin films of regioregular poly(3-hexylthiophene). *J. Polym. Sci. B: Polym. Phys.*, 49:1218–1233, 2011.

[185] J Balko, R H Lohwasser, M Sommer, M Thelakkat, and T Thurn-Albrecht. Determination of the crystallinity of semicrystalline poly(3-hexylthiophene) by means of wide-angle x-ray scattering. *Macromolecules*, 46:9642–9651, 2013.

[186] J Mei, K R Graham, R Stalder, and J R Reynolds. Synthesis of isoindigo-based oligothiophenes for molecular bulk heterojunction solar cells. *Org. Lett.*, 12:660–663, 2010.

[187] T Lei, Y Cao, Y Fan, C-J Liu, S-C Yuan, and J Pei. High-performance air-stable organic field-effect transistors: isoindigo-based conjugated polymers. *J. Am. Chem. Soc.*, 133:6099–6101, 2011.

[188] T Lei, J-Y Wang, and J Pei. Design, synthesis, and structure-property relationships of isoindigo-based conjugated polymers. *Acc. Chem. Res.*, 47:1117–1126, 2014.

[189] C Grand, S Baek, T-H Lai, N Deb, W Zajaczkowski, R Stalder, K Mï£¡llen, W Pisula, D G Bucknall, F So, and J R Reynolds. Structureï£¡property relationships directing transport and charge separation in isoindigo polymers. *Macromolecules*, 49:4008–4022, 2016.

[190] A Keller and S Z D Cheng. The role of metastability in polymer phase transitions. *Polymer*, 39:4461–4487, 1998.

[191] M Muthukumar. Nucleation in polymer crystallization. In S A Rice, editor, *Advances in Chemical Physics*, volume 128, chapter 1, pages 1–63. Wiley, Hoboken, NJ, 2003.

[192] G Strobl. Laws controlling crystallization and melting in bulk polymers. *Rev. Mod. Phys.*, 81:1287–1300, 2009.

[193] J K Hobbs, O E Farrance, and L Kailas. How atomic force microscopy has contributed to our understanding of polymer crystallization. *Polymer*, 50:4281–4292, 2009.

[194] P D Olmsted, W C K Poon, T C B McLeish, N J Terrill, and A J Ryan. Spinodal-assisted crystallization in polymer melts. *Phys. Rev. Lett.*, 81:373–376, 1998.

[195] M Durell, J E Macdonald, D Trolley, A Wehrum, P C Jukes, R A L Jones, C J Walker, and G Brown. The role of surface-induced ordering in the crystallisation of PET films. *Europhys. Lett.*, 58:844–850, 2002.

[196] P C Jukes, A Das, M Durell, D Trolley, A M Higgins, M Geoghegan, J E Macdonald, R A L Jones, S Brown, and P Thompson. The kinetics of surface crystallization in thin films of poly(ethylene terephthalate). *Macromolecules*, 38:2315–2320, 2005.

[197] K Shinotsuka, V N Bliznyuk, and H E Assender. Near-surface crystallization of PET. *Polymer*, 53:5554–5559, 2012.

[198] R M Michell, I Blaszczyk-Lezak, C Mijangos, and A J Müller. Confinement effects on polymer crystallization: From droplets toï£¡alumina nanopores. *Polymer*, 54:4059–4077, 2013.

[199] B Vanroy, M Wübbenhorst, and S Napolitano. Crystallization of thin polymer layers confined between two adsorbing walls. *ACS Macro Lett.*, 2:168–172, 2013.

[200] S Napolitano, D Prevosto, M Lucchesi, P Pingue, M D'Acunto, and P Rolla. Influence of a reduced mobility layer on the structural relaxation dynamics of aluminum capped ultrathin films of poly(ethylene terephthalate). *Langmuir*, 23:2103–2109, 2007.

[201] S Napolitano and M Wübbenhorst. Anomalous decoupling of translational and rotational motion under 1D confinement, evidences from crystallization and diffusion experiments. In F Kremer, editor, *Dynamics in Geometrical Confinement*, pages 279–306. Springer, Heidelberg, 2014.

[202] C W Frank, V Rao, M M Despotopoulou, R F W Pease, W D Hinsberg, R D Miller, and J F Rabolt. Structure in thin and ultrathin spin-cast polymer films. *Science*, 273:912–915, 1996.

[203] G Reiter and J-U Sommer. Crystallization of adsorbed polymer monolayers. *Phys. Rev. Lett.*, 80:3771–3774, 1998.

[204] G Reiter and J-U Sommer. Polymer crystallization in quasi-two dimensions. I. Experimental results. *J. Chem. Phys.*, 112:4376–4383, 2000.

[205] C H M Weber, A Chiche, G Krausch, S Rosenfeldt, M Ballauff, L Harnau, I Göttker-Schnetmann, Q Tong, and S Mecking. Single lamella nanoparticles of polyethylene. *Nano Lett.*, 7:2024–2029, 2007.

[206] L Kinder, J Kanicki, and P M Petroff. Structural ordering and enhanced carrier mobility in organic polymer thin film transistors. *Synth. Met.*, 146:181–185, 2004.

[207] S Kawana, M Durrell, J Lu, J E Macdonald, M Grell, D D C Bradley, P C Jukes, R A L Jones, and S L Bennett. X-ray diffraction study of the structure of thin polyfluorene films. *Polymer*, 43:1907–1913, 2002.

[208] A Bolognesi, C Botta, C Mercogliano, W Porzio, P C Jukes, M Geoghegan, M Grell, M Durell, D Trolley, A Das, and J E Macdonald. Structural features in aligned poly(3-alkylthiophene) films revealed by grazing incidence x-ray diffraction. *Polymer*, 45:4133–4138, 2004.

[209] G Lu, J Blakesley, S Himmelberger, P Pingel, J Frisch, I Lieberwirth, I Salzmann, M Oehzelt, R di Pietro, A Salleo, N Koch, and D Neher. Moderate doping leads to high performance of semiconductor/insulator polymer blend transistors. *Nature Commun.*, 4:1588, 2013.

[210] A B Rodríguez, M R Tomlinson, S Khodabakhsh, J-F Chang, F Cousin, D Lott, H Sirringhaus, W T S Huck, A M Higgins, and M Geoghegan. All-polymer field effect transistors using a brush gate dielectric. *J. Mater. Chem. C*, 1:7736–7741, 2013.

[211] M-B Madec, P J Smith, A Malandraki, N Wang, J G Korvink, and S G Yeates. Enhanced reproducibility of inkjet printed organic thin film transistors based on solution processable polymer-small molecule blends. *J. Mater. Chem.*, 20:9155–9160, 2010.

[212] M-B Madec, D Crouch, G Rincon Llorente, T J Whittle, M Geoghegan, and S G Yeates. Organic field effect transistors from ambient solution processed low molar mass semiconductor-insulator blends. *J. Mater. Chem.*, 18:3230–3236, 2008.

[213] J Kang, N Shin, D Y Jang, V M Prabhu, and D Y Yoon. Structure and properties of small molecule-polymer blend semiconductors for organic thin film transistors. *J. Am. Chem. Soc.*, 130:12273–12275, 2008.

[214] T Ohe, M Kuribayashi, R Yasuda, A Tsuboi, K Nomoto, K Satori, M Itabashi, and J Kasahara. Solution-processed organic thin-film transistors with vertical nanophase separation. *Appl. Phys. Lett.*, 93:053303, 2008.

[215] J-H Kwon, S-I Shin, K-H Kim, M J Cho, K N Kim, D H Choi, and B-K Ju. Organic thin film transistors using 6,13-bis(tri-isopropylsilylethynyl)pentacene embedded into polymer binders. *Appl. Phys. Lett.*, 94:013506, 2009.

[216] J H Park, K H Lee, S Mun, G Ko, S J Heo, J H Kim, E Kim, and S Im. Self-assembly of organic channel/polymer dielectric layer in solution process for low-voltage thin-film transistors. *Org. Electron.*, 11:1688–1692, 2010.

[217] D T James, B K Kjellander, W T T Smaal, G H Gelinck, C Combe, I McCulloch, R Wilson, J H Burroughes, D D C Bradley, and J-S Kim. Thin-film morphology of inkjet-printed single-droplet organic transistors using polarized raman spectroscopy: Effect of blending tips-pentacene with insulating polymer. *ACS Nano*, 5:9824–9835, 2011.

[218] Z He, D Li, D K Hensley, A J Rondinone, and J Chen. Switching phase separation mode by varying the hydrophobicity of polymer additives in solution-processed semiconducting small-molecule/polymer blends. *Appl. Phys. Lett.*, 103:113301, 2013.

[219] I Bose, K Tetzner, K Borner, and K Bock. Homogeneous crystallization of micro-dispensed tips-pentacene using a two-solvent system to enable printed inverters on foil substrates. *Electronics*, 4:565–581, 2015.

[220] Z He, J Chen, J K Keum, G Szulczewski, and D Li. Improving performance of tips pentacene-based organic thin film transistors with small-molecule additives. *Org. Electron.*, 15:150–155, 2014.

[221] M-B Madec, D J Crouch, G Rincon-Llorente, T J Whittle, M Geoghegan, and S G Yeates. Organic semiconductor-polymer insulator blends: a morphological study of the guest-host interaction. *e-J. Surf. Sci. Nanotechnol.*, 7:455–458, 2009.

[222] A Sidorenko, S Minko, K Schenk-Meuser, H Duschner, and M Stamm. Switching of polymer brushes. *Langmuir*, 15:8349–8355, 1999.

[223] J Lahann, S Mitragotri, T-N Tran, H Kaido, J Sundaram, I S Choi, S Hoffer, G A Somorjai, and R Langer. A reversibly switching surface. *Science*, 299:371–374, 2003.

[224] D M Jones, J R Smith, W T S Huck, and C Alexander. Variable adhesion of micropatterned thermoresponsive polymer brushes: AFM investigations of poly(N-isopropylacrylamide) brushes prepared by surface-initiated polymerization. *Adv. Mater.*, 14:1130–1134, 2003.

[225] H Retsos, G Gorodyska, A Kiriy, M Stamm, and C Creton. Adhesion between chemically heterogeneous switchable polymeric brushes and an elastomeric adhesive. *Langmuir*, 21:7722–7725, 2005.

[226] A Synytska, E Svetushkina, N Puretskiy, G Stoychev, S Berger, L Ionov, C Bellmann, K-J Eichhorn, and M Stamm. Biocompatible polymeric materials with switchable adhesion properties. *Soft Matter*, 6:5907–5914, 2010.

[227] E Svetushkina, N Puretskiy, L Ionov, M Stamm, and A Synytska. A comparative study on switchable adhesion between thermoresponsive polymer brushes on flat and rough surfaces. *Soft Matter*, 7:5691–5696, 2011.

[228] F Zhou, W Shu, M E Welland, and W T S Huck. Highly reversible and multi-stage cantilever

actuation driven by polyelectrolyte brushes. *J. Am. Chem. Soc.*, 128:5326–5327, 2006.

[229] I Luzinov, S Minko, and V V Tsukruk. Adaptive and responsive surfaces through controlled reorganization of interfacial polymer layers. *Prog. Polym. Sci.*, 29:635–698, 2004.

[230] I Luzinov, S Minko, and V V Tsukruk. Responsive brush layers: from tailored gradients to reversible assembled nanoparticles. *Soft Matter*, 4:714–725, 2008.

[231] A Sun and J Lahann. Dynamically switchable biointerfaces. *Soft Matter*, 5:1555–1561, 2009.

[232] M P Weir and A J Parnell. Water soluble responsive polymer brushes. *Polymers*, 3:2107–2132, 2011.

[233] X Liu, Y Liang, F Zhou, and W Liu. Extreme wettability and tunable adhesion: biomimicking beyond nature? *Soft Matter*, 8:2070–2086, 2012.

[234] S H Anastasiadis. Development of functional polymer surfaces with controlled wettability. *Langmuir*, 29:9277–9290, 2013.

[235] M C LeMieux, Y-H Lin, P D Cuong, H-S Ahn, E R Zubarev, and V V Tsukruk. Microtribological and nanomechanical properties of switchable Y-shaped amphiphilic polymer brushes. *Adv. Funct. Mater.*, 15:1529–1540, 2005.

[236] S Moya, O Azzaroni, T Farhan, V L Osborne, and W T S Huck. Locking and unlocking of polyelectrolyte brushes: Toward the fabrication of chemically controlled nanoactuators. *Ang. Chem. Int. Ed.*, 44:4578–4581, 2005.

[237] O Azzaroni, A A Brown, and W T S Huck. Tunable wettability by clicking counterions into polyelectrolyte brushes. *Adv. Mater.*, 19:151–154, 2007.

[238] M Motornov, R Sheparovych, R Lupitskyy, E MacWilliams, and S Minko. Superhydrophobic surfaces generated from water-borne dispersions of hierarchically assembled nanoparticles coated with a reversibly switchable shell. *Adv. Mater.*, 20:200–205, 2008.

[239] E Spruijt, E-Y Choi, and W T S Huck. Reversible electrochemical switching of polyelectrolyte brush surface energy using electroactive counterions. *Langmuir*, 24:11253–11260, 2008.

[240] K Hinrichs, D Aulich, L Ionov, N Esser, K-J Eichhorn, M Motornov, M Stamm, and S Minko. Chemical and structural changes in a pH-responsive mixed polyelectrolyte brush studied by infrared ellipsometry. *Langmuir*, 25:10987–10991, 2009.

[241] K Y Tan, J E Gautrot, and W T S Huck. Island brushes to control adhesion of water in oil droplets on planar surfaces. *Soft Matter*, 7:7013–7020, 2011.

[242] Z Hua, J Yang, T Wang, G Liu, and G Zhang. Transparent surface with reversibly switchable wettability between superhydrophobicity and superhydrophilicity. *Langmuir*, 29:10307–10312, 2013.

[243] J-J Li, Y-N Zhou, and Z-H Luo. Thermo-responsive brush copolymers with structure-tunable LCST and switchable surface wettability. *Polymer*, 55:6552–6560, 2014.

[244] M Raftari, Z Zhang, S R Carter, G J Leggett, and M Geoghegan. Frictional properties of a polycationic brush. *Soft Matter*, 10:2759–2766, 2014.

[245] H Merlitz, G-L He, J-U Sommer, and C-X Wu. Reversibly switchable polymer brushes with hydrophobic/hydrophilic behavior: A Langevin dynamics study. *Macromolecules*, 42:445–451, 2009.

[246] H Merlitz, G-L He, C-X Wu, and J-U Sommer. Nanoscale brushes: How to build a smart surface coating. *Phys. Rev. Lett.*, 102:115702, 2009.

[247] S de Beer. Switchable friction using contacts of stimulus-responsive and nonresponding swollen polymer brushes. *Langmuir*, 30:8085–8090, 2014.

[248] S Kumar, X Tong, Y L Dory, M Lepage, and Y Zhao. A CO_2-switchable polymer brush for reversible capture and release of proteins. *Chem. Commun.*, 49:90–92, 2013.

[249] M P Weir, S Y Heriot, S J Martin, A J Parnell, S A Holt, J R P Webster, and R A L Jones. Voltage-induced swelling and deswelling of weak polybase brushes. *Langmuir*, 27:11000–11007, 2011.

[250] G J Dunderdale and J P A Fairclough. Coupling pH-responsive polymer brushes to electricity: Switching thickness and creating waves of swelling or collapse. *Langmuir*, 29:3628–3635, 2013.

[251] H Zeng, Y Zhang, S Mao, H Nakajima, and K Uchiyama. A reversibly electro-controllable polymer brush for electro-switchable friction. *J. Mater. Chem. C*, 5:5877–5881, 2017.

[252] H Ouyang, Z Xia, and J Zhe. Static and dynamic responses of polyelectrolyte brushes under external electric field. *Nanotechnology*, 20:195703, 2009.

[253] T Yamamoto and P A Pincus. Collapse of polyelectrolyte brushes in electric fields. *EPL*, 95:48003, 2011.

[254] C Drummond. Electric-field-induced friction reduction and control. *Phys. Rev. Lett.*, 109:154302, 2012.

[255] Y-F Ho, T N Shendruk, G W Slater, and P-Y Hsiao. Structure of polyelectrolyte brushes subject to normal electric fields. *Langmuir*, 29:2359–2370, 2013.

[256] C Tong. Numerical self-consistent field theory study of the response of strong polyelectrolyte brushes to external electric fields. *J. Chem. Phys.*, 143:054903, 2015.

[257] F Zhang, H-D Ding, C Duan, S-L Zhao, and C-H Tong. Molecular dynamics simulation of the response of bi-disperse polyelectrolyte brushes to external electric fields. *Chin. Phys. B*, 26:088204, 2017.

[258] G Panzarasa, M Dübner, V Pifferi, G Soliveri, and C Padeste. ON/OFF switching of silicon wafer electrochemistry by pH-responsive polymer brushes. *J. Mater. Chem. C*, 4:6287–6294, 2016.

[259] D J Beebe, J S Moore, J M Bauer, Q Yu, R H Liu, C Devadoss, and B-H Jo. Functional hydrogel structures for autonomous flow control inside microfluidic channels. *Nature*, 404:588–590, 2000.

[260] E Katz, V M Fernández, and M Pita. Switchable bioelectrocatalysis controlled by pH changes. *Electroanalysis*, 27:2063–2073, 2015.

[261] G Panzarasa, M Dübner, V Pifferi, G Soliveri, and C Padeste. Tuning the electrochemical properties of silicon wafer by grafted-from micropatterned polymer brushes. *J. Mater. Chem. C*, 4:340–347, 2016.

[262] M Kobayashi, M Terada, and A Takahara. Reversible adhesive-free nanoscale adhesion utilizing oppositely charged polyelectrolyte brushes. *Soft Matter*, 7:5717–5722, 2011.

[263] G Sudre, L Olanier, Y Tran, D Hourdet, and C Creton. Reversible adhesion between a hydrogel and a polymer brush. *Soft Matter*, 8:8184–8193, 2012.

[264] M Kobayashi and A Takahara. Environmentally friendly repeatable adhesion using a sulfobetaine-type polyzwitterion brush. *Polym. Chem.*, 4:4987–4992, 2013.

[265] L Alfhaid, W D Seddon, N H Williams, and M Geoghegan. Double-network hydrogels improve pH-switchable adhesion. *Soft Matter*, 12:5022–5028, 2016.

[266] J Boateng and O Catanzano. Advanced therapeutic dressings for effective wound healing—a review. *J. Pharm. Sci.*, 104:3653–3680, 2015.

[267] J M Garcia and M L Robertson. The future of plastics recycling. *Science*, 358:870–872, 2017.

[268] Y Lu, J Broughton, and P Winfield. A review of innovations in disbonding techniques for repair and recycling of automotive vehicles. *Int. J. Adhes. Adhes.*, 50:119–127, 2014.

[269] J Collett, A Crawford, P V Hatton, M Geoghegan, and S Rimmer. Thermally responsive polymeric hydrogel brushes: synthesis, physical properties and use for the culture of chondrocytes. *J. R. Soc. Interface*, 4:117–126, 2007.

[270] E Wischerhoff, K Uhlig, A Lankenau, H G Börner, A Laschewsky, C Duschl, and J-F Lutz. Controlled cell adhesion on PEG-based switchable surfaces. *Angew. Chem. Int. Ed.*, 47:5666–5668, 2008.

[271] S Desseaux and H-A Klok. Temperature-controlled masking/unmasking of cell-adhesive cues with poly(ethylene glycol) methacrylate based brushes. *Biomacromolecules*, 15:3859–3865, 2014.

[272] G Cheng, H Xue, Z Zhang, S Chen, and S Jiang. A switchable biocompatible polymer surface with self-sterilizing and nonfouling capabilities. *Angew. Chem. Int. Ed.*, 47:8831–8834, 2008.

[273] C G Rolli, H Nakayama, K Yamaguchi, J P Spatz, R Kemkemer, and J Nakanishi. Switchable adhesive substrates: revealing geometry dependence in collective cell behavior. *Biomaterials*, 33:2409–2418, 2012.

[274] J Hyun, W-K Lee, N Nath, A Chilkoti, and S Zauscher. Capture and release of proteins on the nanoscale by stimuli-responsive elastin-like polypeptide "switches". *J. Am. Chem. Soc.*, 126:7330–7335, 2004.

[275] S Burkert, E Bittrich, M Kuntzsch, M Müller, K-J Eichhorn, C Bellmann, P Uhlmann, and M Stamm. Protein resistance of PNIPAAm brushes: Application to switchable protein adsorption. *Langmuir*, 26:1786–1795, 2010.

[276] N Malod-Dognin, A Bansal, and F Cazals. Characterizing the morphology of protein binding patches. *Proteins*, 80:2652–2665, 2012.

[277] Y Watanabe, T Kobayashi, H Yamamoto, H Hoshida, R Akada, F Inagaki, Y Ohsumi, and N N Noda. Structure-based analyses reveal distinct binding sites for Atg2 and phosphoinositides in Atg18. *J. Biol. Chem.*, 287:31681–31690, 2012.

[278] R Kumar and E B Thompson. Folding of the glucocorticoid receptor N-terminal transactivation function: Dynamics and regulation. *Mol. Cell. Endocrinol.*, 348:450–456, 2012.

[279] B Zhang, J C Crack, S Subramanian, J Green, A J Thomson, N E Le Brun, and M K Johnson. Reversible cycling between cysteine persulfide-ligated [2Fe-2S] and cysteine-ligated [4Fe-4S] clusters in the fnr regulatory protein. *Proc. Natl Acad. Sci. USA*, 109:15734–15739, 2012.

[280] J M Berrisford and L A Sazanov. Structural basis for the mechanism of respiratory complex I. *J. Biol. Chem.*, 284:29773–29783, 2009.

[281] T A Nguyen, S S Lieu, and G Chang. An *Escherichia coli*-based cell-free system for large-scale production of functional mammalian membrane proteins suitable for X-ray crystallography. *J. Mol. Microbiol. Biotechnol.*, 18:85–91, 2010.

[282] G Evans, D Axford, and R L Owen. The design of macromolecular crystallography diffraction experiments. *Acta Crystallogr. D: Biol. Crystallogr.*, 67:261–270, 2011.

[283] S Piana, K Lindorff-Larsen, and D E Shaw. Protein folding kinetics and thermodynamics from atomistic simulation. *Proc. Natl Acad. Sci. USA*, 109:17845–17850, 2012.

[284] J Kubelka, J Hofrichter, and W A Eaton. The protein folding 'speed limit'. *Curr. Opin. Struct. Biol.*, 14:76–88, 2004.

[285] J Kubelka, T K Chiu, D R Davies, W A Eaton, and J Hofrichter. Sub-microsecond protein folding. *J. Mol. Biol.*, 359:546–553, 2006.

[286] F Schotte, M Lim, T A Jackson, A V Smirnov, J Soman, J S Olson, G N Phillips Jr, M Wulff, and P A Anfinrud. Watching a protein as it functions with 150-ps time-resolved X-ray crystallography. *Science*, 300:1944–1947, 2003.

[287] M Schmidt, K Nienhaus, R Pahl, A Krasselt, S Anderson, F Parak, G U Nienhaus, and V Šrajer. Ligand migration pathway and protein dynamics in myoglobin: A time-resolved crystallographic study on l29w MbCO. *Proc. Natl Acad. Sci. USA*, 102:11704–11709, 2005.

[288] A L Serrano, M M Waegele, and F Gai. Spectroscopic studies of protein folding: Linear and nonlinear methods. *Protein Sci.*, 21:157–170, 2012.

[289] C-K Lee, Y-M Wang, L-S Huang, and S Lin. Atomic force microscopy: determination of unbinding force, off rate and energy barrier for protein-ligand interaction. *Micron*, 38:446–461, 2007.

[290] D P Allison, N P Mortensen, C J Sullivan, and M J Doktycz. Atomic force microscopy of biological samples. *Wiley Interdisc. Rev. Nanomed. Nanobiotechnol.*, 2:618–34, 2010.

[291] S Senapati and S Lindsay. Recent progress in molecular recognition imaging using atomic force microscopy. *Acc. Chem. Res.*, 49:503–510, 2016.

[292] U Maver, T Velnar, M Gaberšček, O Planinšek, and M Finšgar. Recent progressive use of atomic force microscopy in biomedical applications. *Trends Anal. Chem.*, 80:96–111, 2016.

[293] E A-Hassan, W F Heinz, M D Antonik, N P D'Costa, S Nageswaran, C-A Schoenenberger, and J H Hoh. Relative microelastic mapping of living cells by atomic force microscopy. *Biophys. J.*, 74:1564–1578, 1998.

[294] A Touhami, B Nysten, and Y F Dufrêne. Nanoscale mapping of the elasticity of microbial cells by atomic force microscopy. *Langmuir*, 19:4539–4543, 2003.

[295] Y F Dufrêne. Direct characterization of the physicochemical properties of fungal spores using functionalized AFM probes. *Biophys. J.*, 78:3286–3291, 2000.

[296] M Gad, A Itoh, and A Ikai. Mapping cell wall polysaccharides of living microbial cells using atomic force microscopy. *Cell Biol. Int.*, 21:697–706, 1997.

[297] E Evans, D Berk, and A Leung. Detachment of agglutinin-bonded red blood cells. I. Forces to rupture molecular-point attachments. *Biophys. J.*, 59:838–848, 1991.

[298] H K Nguyen, S Fujinami, and K Nakajima. Elastic modulus of ultrathin polymer films characterized by atomic force microscopy: The role of probe radius. *Polymer*, 87:114–122, 2016.

[299] J K Li, R M A Sullan, and S Zou. Atomic force microscopy force mapping in the study of supported lipid bilayers. *Langmuir*, 27:1308–1313, 2011.

[300] M Keshavarz, H Engelkamp, J Xu, E Braeken, M B J Otten, H Uji-i, E Schwartz, M Koepf, A Vananroye, J Vermant, R J M Nolte, F De Schryver, J C Maan, J Hofkens, P C M Christianen, and A E Rowan. Nanoscale study of polymer dynamics. *ACS Nano*, 10:1–13, 2016.

[301] P C Chung, E Glynos, G Sakellariou, and P F Green. Elastic mechanical response of thin supported star-shaped polymer films. *ACS Macro Lett.*, 5:439–443, 2016.

[302] A K Denisin and B L Pruitt. Tuning the range of polyacrylamide gel stiffness for mechanobiology applications. *ACS Appl. Mater. Interfaces*, 8:21893–21902, 2016.

[303] I A Morozov. Structural-mechanical AFM study of surface defects in natural rubber vulcanizates. *Macromolecules*, 49:5985–5992, 2016.

[304] Y-Y Kim, M Semsarilar, J D Carloni, K R Cho, A N Kulak, I Polishchuk, C T Hendley, P J M Smeets, L A Fielding, B Pokroy, C C Tang, L A Estroff, S P Baker, S P Armes, and F C Meldrum. Structure and properties of nanocomposites formed by the occlusion of block copolymer worms and vesicles within calcite crystals. *Adv. Funct. Mater.*, 26:1382–1392, 2016.

[305] F M Hecht, J Rheinlaender, N Schierbaum, W H Goldmann, B Fabry, and T E Schäffer. Imaging viscoelastic properties of live cells by AFM: power-law rheology on the nanoscale. *Soft Matter*, 11:4584–4591, 2015.

[306] Y Pen, Z J Zhang, A L Morales-García, M Mears, D S Tarmey, R G Edyvean, S A Banwart, and M Geoghegan. Effect of extracellular polymeric substances on the mechanical properties of *Rhodococcus*. *Biochim. Biophys. Acta.*, 1848:518–526, 2015.

[307] X Wang, R Bleher, M E Brown, J G N Garcia, S M Dudek, G S Shekhawat, and V P Dravid. Nano-biomechanical study of spatio-temporal cytoskeleton rearrangements that determine subcellular mechanical properties and endothelial permeability. *Sci. Rep.*, 5:11097, 2015.

[308] A X Cartagena-Rivera, W-H Wang, R L Geahlen, and A Raman. Fast, multi-frequency, and quantitative nanomechanical mapping of live cells using the atomic force microscope. *Sci. Rep.*, 5:11692, 2015.

[309] A Rigato, F Rico, F Eghiaian, M Piel, and S Scheuring. Atomic force microscopy mechanical mapping of micropatterned cells shows adhesion geometry-dependent mechanical response on local and global scales. *ACS Nano*, 9:5846–5856, 2015.

[310] A X Cartagena-Rivera, J S Logue, C M Waterman, and R S Chadwick. Actomyosin cortical mechanical properties in nonadherent cells determined by atomic force microscopy. *Biophys. J.*, 110:2528–2539, 2016.

[311] G Smolyakov, C Formosa-Dague, C Severac, R E Duval, and E Dague. High speed indentation measures by FV, QI and QNM introduce a new understanding of bionanomechanical experiments. *Micron*, 85:8–14, 2016.

[312] N Gavara and R S Chadwick. Relationship between cell stiffness and stress fiber amount, assessed by simultaneous atomic force microscopy and live-cell fluorescence imaging. *Biomech. Model. Mechanobiol.*, 15:511–523, 2016.

[313] G Andre, S Kulakauskas, M-P Chapot-Chartier, B Navet, M Deghorain, E Bernard, P Hols, and

Y F Dufrêne. Imaging the nanoscale organization of peptidoglycan in living *Lactococcus lactis* cells. *Nature Commun.*, 1:27, 2010.

[314] G Buist, A Steen, J Kok, and O P Kuipers. LysM, a widely distributed protein motif for binding to (peptido)glycans. *Mol. Microbiol.*, 68:838–847, 2008.

[315] H Koo, I Park, Y Lee, H J Kim, J H Jung, J H Lee, Y Kim, J-H Kim, and J W Park. Visualization and quantification of microRNA in a single cell using atomic force microscopy. *J. Am. Chem. Soc.*, 138:11664–11671, 2016.

[316] K P Heim, R M A Sullan, P J Crowley, S El-Kirat-Chatel, A Beaussart, W Tang, R Besingi, Y F Dufrene, and L J Brady. Identification of a supramolecular functional architecture of *Streptococcus mutans* adhesin p1 on the bacterial cell surface. *J. Biol. Chem.*, 290:9002–9019, 2015.

[317] V Cabral, S Znaidi, L A Walker, H Martin-Yken, E Dague, M Legrand, K Lee, M Chauvel, A Firon, T Rossignol, M L Richard, C A Munro, S Bachellier-Bassi, and C D'Enfert. Targeted changes of the cell wall proteome influence *Candida albicans* ability to form single- and multi-strain biofilms. *PLoS Pathog.*, 10:e1004542, 2014.

[318] L Arnal, G Longo, P Stupar, M F Castez, N Cattelan, R C Salvarezza, O M Yantorno, S Kasas, and M E Vela. Localization of adhesins on the surface of a pathogenic bacterial envelope through atomic force microscopy. *Nanoscale*, 7:17563–17572, 2015.

[319] P Herman-Bausier and Y F Dufrêne. Atomic force microscopy reveals a dual collagen-binding activity for the staphylococcal surface protein SdrF. *Mol. Microbiol.*, 99:611–621, 2016.

[320] A Noy. Chemical force microscopy of chemical and biological interactions. *Surf. Interface Anal.*, 38:1429–1441, 2006.

[321] A Ptak, H Gojzewski, M Kappl, and H-J Butt. Influence of humidity on the nanoadhesion between a hydrophobic and a hydrophilic surface. *Chem. Phys. Lett.*, 503:66–70, 2011.

[322] M Sletmoen, T K Dam, T A Gerken, B T Stokke, and C F Brewer. Single-molecule pair studies of the interactions of the α-GalNAc (Tn-antigen) form of porcine submaxillary mucin with soybean agglutinin. *Biopolymers*, 91:719–728, 2009.

[323] E Evans. Probing the relation between force–lifetime–and chemistry in single molecular bonds. *Annu. Rev. Biophys. Biomol. Struct.*, 30:105–128, 2001.

[324] C Friedsam, A K Wehle, F Kühner, and H E Gaub. Dynamic single-molecule force spectroscopy: bond rupture analysis with variable spacer length. *J. Phys.: Condens. Matter*, 15:S1709–S1723, 2003.

[325] R W Friddle. Theoretical models in force spectroscopy. In A R Bizzarri and S Cannistraro, editors, *Dynamic Force Spectroscopy and Biomolecular Recognition*, pages 51–91. CRC press, Boca Raton, 2012.

[326] J T Bullerjahn, S Sturm, and K Kroy. Theory of rapid force spectroscopy. *Nat. Commun.*, 5:4463, 2014.

[327] R Bansil and B S Turner. Mucin structure, aggregation, physiological functions and biomedical application. *Curr. Opin. Colloid Interface Sci.*, 11:164–170, 2006.

[328] S Rachagani, M P Torres, N Moniaux, and S K Batra. Current status of mucins in the diagnosis and therapy of cancer. *Biofactors*, 35:509–527, 2009.

[329] T K Dam, T A Gerken, B S Cavada, K S Nascimento, T R Moura, and C F Brewer. Binding studies of α-GalNAc-specific lectins to the α-GalNAc (Tn-antigen) form of porcine submaxillary mucin and its smaller fragments. *J. Biol. Chem.*, 282:28256–28263, 2007.

[330] E Evans and K Ritchie. Dynamic strength of molecular adhesion bonds. *Biophys. J.*, 72:1541–1555, 1997.

[331] G I Bell. Models for the specific adhesion of cells to cells. *Sci.*, 200:618 – 627, 1978.

[332] E Evans. Energy landscapes of biomolecular adhesion and receptor anchoring at interfaces explored with dynamic force spectroscopy. *Faraday Discuss.*, 111:1–16, 1998.

[333] R Merkel, P Nassoy, a Leung, K Ritchie, and E Evans. Energy landscapes of receptor-ligand bonds explored with dynamic force spectroscopy. *Nature*, 397:50–53, 1999.

[334] F Hanke and H. J. Kreuzer. Breaking bonds in the atomic force microscope: Theory and analysis. *Phys. Rev. E*, 74:031909, 2006.

[335] A Taninaka, Y Hirano, O Takeuchi, and H Shigekawa. Force measurement enabling precise analysis by dynamic force spectroscopy. *Int. J. Mol. Sci.*, 13:453–465, 2012.

[336] A R Bizzarri. Biological applications of dynamic force spectroscopy. In A R Bizzarri and S Cannistraro, editors, *Dynamic Force Spectroscopy and Biomolecular Recognition*, pages 193–241. CRC press, Boca Raton, 2012.

[337] S Getfert and P Reimann. Hidden multiple bond effects in dynamic force spectroscopy. *Biophys. J.*, 102:1184–1193, 2012.

[338] J te Riet, I Reinieren-Beeren, C G Figdor, and A Cambi. AFM force spectroscopy reveals how subtle structural differences affect the interaction strength between *Candida albicans* and DC-SIGN. *J. Mol. Recognit.*, 28:687–698, 2015.

[339] V Vásquez, M Krieg, D Lockhead, and M B Goodman. Phospholipids that contain polyunsaturated fatty acids enhance neuronal cell mechanics and touch sensation. *Cell Rep.*, 6:70–80, 2014.

[340] A Alessandrini and P Facci. Nanoscale mechanical properties of lipid bilayers and their relevance in biomembrane organization and function. *Micron*, 43:1212–1223, 2012.

[341] M Ritzefeld, V Walhorn, D Anselmetti, and N Sewald. Analysis of DNA interactions using single-molecule force spectroscopy. *Amino Acids*, 44:1457–1475, 2013.

[342] J Tao, K C Battle, H Pan, E A Salter, Y-C Chien, A Wierzbicki, and J J De Yoreo. Energetic basis for the molecular-scale organization of bone. *Proc. Natl. Acad. Sci. USA*, 112:326–331, 2015.

[343] B Eslami, E A López-Guerra, M Raftari, and S D Solares. Evolution of nano-rheological properties of Nafion® thin films during pH modification by strong base treatment: a static and dynamic force spectroscopy study. *J. Appl. Phys.*, 119:165301, 2016.

[344] E Spruijt, M A Cohen Stuart, and J van der Gucht. Dynamic force spectroscopy of oppositely charged polyelectrolyte brushes. *Macromolecules*, 43:1543–1550, 2010.

[345] L Sonnenberg, J Parvole, F Kühner, L Billon, and H E Gaub. Choose sides: Differential polymer adhesion. *Langmuir*, 23:6660–6666, 2007.

[346] O Axner, M Andersson, O Bjoernham, M Castelain, J Klinth, E Koutris, and S Schedin. Assessing bacterial adhesion on an individual adhesin and single pili level using optical tweezers. In D Linke and A Goldman, editors, *Bacterial Adhesion: Chemistry, Biology and Physics*, volume 715 of *Advances in Experimental Medicine and Biology*, pages 301–313. Springer, Berlin, 2011.

[347] Y Hu, J Jin, H Liang, X Ji, J Yin, and W Jiang. pH dependence of adsorbed fibrinogen conformation and its effect on platelet adhesion. *Langmuir*, 32:4086–4094, 2016.

[348] J W Weisel and L Medved. The structure and function of the αC domains of fibrinogen. *Ann. N. Y. Acad. Sci.*, 936:312–327, 2001.

[349] M Vuoriluoto, H Orelma, L-S Johansson, B Zhu, M Poutanen, A Walther, J Laine, and O J Rojas. Effect of molecular architecture of PDMAEMA-POEGMA random and block copolymers on their adsorption on regenerated and anionic nanocelluloses and evidence of interfacial water expulsion. *J. Phys. Chem. B*, 119:15275–15286, 2015.

[350] A Hucknall, S Rangarajan, and A Chilkoti. In pursuit of zero: Polymer brushes that resist the adsorption of proteins. *Adv. Mater.*, 21:2441–2446, 2009.

[351] S Chen, L Li, C Zhao, and J Zheng. Surface hydration: Principles and applications toward low-fouling/nonfouling biomaterials. *Polymer*, 51:5283–5293, 2010.

[352] M Krishnamoorthy, S Hakobyan, M Ramstedt, and J E Gautrot. Surface-initiated polymer brushes in the biomedical field: applications in membrane science, biosensing, cell culture, regenerative medicine and antibacterial coatings. *Chem. Rev.*, 114:10976–1026, 2014.

[353] J O Zoppe, N C Ataman, P Mocny, J Wang, J Moraes, and H-A Klok. Surface-initiated controlled radical polymerization: State-of-the-art, opportunities, and challenges in surface and interface engineering with polymer brushes. *Chem. Rev.*, 117:1105–1318, 2017.

[354] S Pillai, A Arpanaei, R L Meyer, V Birkedal, L Gram, F Besenbacher, and P Kingshott. Preventing protein adsorption from a range of surfaces using an aqueous fish protein extract. *Biomacromolecules*, 10:2759–2766, 2009.

[355] E Pensini, C M Yip, D O'Carroll, and B E Sleep. Carboxymethyl cellulose binding to mineral substrates: Characterization by atomic force microscopy-based Force spectroscopy and quartz-crystal microbalance with dissipation monitoring. *J. Colloid Interface Sci.*, 402:58–67, 2013.

[356] A Eleta-Lopez, J Etxebarria, N-C Reichardt, R Georgieva, H Bäumler, and J L Toca-Herrera. On the molecular interaction between albumin and ibuprofen: An AFM and QCM-D study. *Colloids Surfaces B Biointerfaces*, 134:355–362, 2015.

[357] C Gutiérrez Sánchez, Q Su, H Schönherr, M Grininger, and G Nöll. Multi-ligand-binding flavoprotein dodecin as a key element for reversible surface modification in nano-biotechnology. *ACS Nano*, 9:3491–3500, 2015.

[358] S-O Kim, J A Jackman, M Mochizuki, B K Yoon, T Hayashi, and N-J Cho. Correlating single-molecule and ensemble-average measurements of peptide adsorption onto different inorganic materials. *Phys. Chem. Chem. Phys.*, 18:14454–14459, 2016.

[359] I M Marcus, M Herzberg, S L Walker, and V Freger. *Pseudomonas aeruginosa* attachment on QCM-D sensors: The role of cell and surface hydrophobicities. *Langmuir*, 28:6396–6402, 2012.

[360] H Ma, D Li, X Sheng, B Zhao, and A Chilkoti. Protein-resistant polymer coatings on silicon oxide by surface-initiated atom transfer radical polymerization. *Langmuir*, 22:3751–3756, 2006.

[361] A M Alswieleh, N Cheng, I Canton, B Ustbas, X Xue, V Ladmiral, S Xia, R E Ducker, O El Zubir, M L Cartron, C N Hunter, G J Leggett, and S P Armes. Zwitterionic poly(amino acid methacrylate) brushes. *J. Am. Chem. Soc.*, 136:9404–9413, 2014.

[362] Y Teramura, K Kuroyama, and M Takai. Influence of molecular weight of PEG chain on interaction between streptavidin and biotin-PEG-conjugated phospholipids studied with QCM-D. *Acta Biomater.*, 30:135–143, 2016.

[363] J M Medley, E J Beane, S C Sundararaj, E Kaplan, D A Puleo, and T D Dziubla. Block copolymers for the rational design of self-forming postsurgical adhesion barriers. *Acta Biomater.*, 6:72–82, 2010.

[364] C Ma, H Zhou, B Wu, and G Zhang. Preparation of polyurethane with zwitterionic side chains and their protein resistance. *ACS Appl. Mater. Interfaces*, 3:455–461, 2011.

[365] S Napolitano, E Glynos, and N B Tito. Glass transition of polymers in bulk, confined geometries, and near interfaces. *Rep. Prog. Phys.*, 80:036602, 2017.